UCRL-TR-236978

LAWRENCE LIVERMORE NATIONAL LABORATORY

HIGHWAY INFRASTRUCTURE FOCUS AREA NEXT-GENERATION INFRASTRUCTURE MATERIALS VOLUME I - TECHNICAL PROPOSAL & MANAGEMENTENHANCEMENT OF TRANSPORTATION INFRASTRUCTURE WITH IRON-BASED AMORPHOUS-METAL AND CERAMIC COATINGS

J. C. Farmer

December 4, 2007

This work performed under the auspices of the U.S. Department of Energy by Lawrence Livermore National Laboratory under Contract DE-AC52-07NA27344.

PART A. TITLE PAGE

HIGHWAY INFRASTRUCTURE FOCUS AREA
NEXT-GENERATION INFRASTRUCTURE MATERIALS
VOLUME I – TECHNICAL PROPOSAL & MANAGEMENT

ENHANCEMENT OF TRANSPORTAITON INFRASTRUCTURE WITH IRON-BASED AMORPHOUS-METAL AND CERAMIC COATINGS

Prepared for:

Yash Paul Virmani – Program Manger
Reinforced and Prestressed Concrete and Cable-Stayed Corrosion
Office of Infrastructure Research and Development
Federal Highway Administration
Turner-Fairbank Highway Research Center
6300 Georgetown Pike
McClean, Virginia 22101-2296
Tel. 202-493-3052
Fax 202-493-3442
Email paul.virmani@fhwa.dot.gov

Prepared by:

Joseph Collin Farmer – Directorate Senior Scientist
Chemistry, Materials and Life Sciences Directorate
Lawrence Livermore National Laboratory
7000 East Avenue – Mail Stop L638
Livermore, California 94550
Tel. 925-423-6574
Email farmer4@llnl.gov

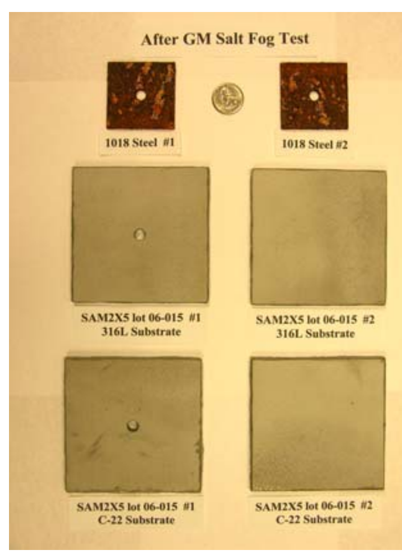

PART B. EXECUTIVE SUMMARY

The infrastructure for transportation in the United States allows for a high level of mobility and freight activity for the current population of 300 million residents, and several million business establishments. According to a Department of Transportation study, more than 230 million motor vehicles, ships, airplanes, and railroads cars were used on 6.4 million kilometers (4 million miles) of highways, railroads, airports, and waterways in 1998. Pipelines and storage tanks were considered to be part of this deteriorating infrastructure. The annual direct cost of corrosion in the infrastructure category was estimated to be approximately $22.6 billion in 1998.

There were 583,000 bridges in the United States in 1998. Of this total, 200,000 bridges were steel, 235,000 were conventional reinforced concrete, 108,000 bridges were constructed using pre-stressed concrete, and the balance was made using other materials of construction. Approximately 15 percent of the bridges accounted for at this point in time were structurally deficient, primarily due to corrosion of steel and steel reinforcement.

Iron-based amorphous metals, including SAM2X5 ($Fe_{49.7}Cr_{17.7}Mn_{1.9}Mo_{7.4}W_{1.6}B_{15.2}C_{3.8}Si_{2.4}$) and SAM1651 ($Fe_{48}Mo_{14}Cr_{15}Y_2C_{15}B_6$) have been developed, and have very good corrosion resistance. These materials have been prepared as a melt-spun ribbons, as well as gas atomized powders and thermal-spray coatings. During electrochemical testing in several environments, including seawater at 90°C, the passive film stabilities of these materials were found to be comparable to that of more expensive high-performance alloys, based on electrochemical measurements of the passive film breakdown potential and general corrosion rates. These materials also performed very well in standard salt fog tests. Chromium (Cr), molybdenum (Mo) and tungsten (W) provided corrosion resistance, and boron (B) enabled glass formation. The high boron content of this particular amorphous metal made it an effective neutron absorber, and suitable for criticality control applications. These amorphous alloys appear to maintain their corrosion resistance up to the glass transition temperature.

Visionary research is proposed to extend the application of corrosion-resistant iron-based amorphous metal coatings, and variants of these coatings, to protection of the Nation's transportation infrastructure. Specific objectives of the proposed work are: (1) fabrication of appropriate test samples for evaluation of concept; (2) collection of production and test data for coated steel reinforcement bars, enabling systematic comparison of various coating options, based upon performance and economic considerations; and (3) construction and testing of concrete structures with coated steel reinforcement bars, thereby demonstrating the value of amorphous-metal coatings. The benefits of ceramic coatings as thermal barriers will also be addressed.

PART C: INNOVATIVE CLAIMS

This proposal will explore several creative approaches to preventing the corrosion of steel reinforcement bars in concrete structures. Novel corrosion-resistant iron-based amorphous metal coatings will be applied to steel reinforcement bars, embedded in concrete, and exposed to seawater and other corrosive environments. Characterization of this steel reinforcement bar will be used to establish enhanced corrosion performance of these advanced steel-reinforced concrete structures. By minimizing the generation of metal-oxide corrosion products within the concrete, oxide wedging, and consequent concrete cracking will be minimized.

In addition to using SAM2X5 and SAM1651 formulations which have been shown to have very good corrosion resistance, compositions believed to have even better corrosion resistance will be explored. For example, samples of SAM6 survive for several months in concentrated hydrochloric acid, whereas nickel-based Alloy C-22 readily dissolves.

In addition to using gas-atomization and high-velocity oxy-fuel (HVOF) processes, other approaches that could be used for relatively small diameter reinforcement bars will also be explored. For example, cladding with a wire-fed arc system may be possible. Relatively thick coatings could also be applied on all sides of reinforcement bar by sputter deposition from planar magnetrons, with the steel bars passed between the magnetrons continuously. Laser ablation has also been considered, and would have the same economy of scale as laser welding processes.

Dip coating might ultimately be possible, if the bars could be withdrawn from an amorphous metal melt fast enough to maintain the critical cooling rate at the surface of the bar, wet with the molten amorphous metal. However, dip such dip coating is considered beyond the scope of this program.

This proposal will also explore combining the use of the novel amorphous-metal coatings with other approaches to mitigation, including epoxy coating and the use of sacrificial metals such as zinc. In addition to electrolytic deposition, zinc could be applied with cold spray. The synergistic benefits of simultaneous application of such multiple approaches could be dramatic.

The development of production processes for coating steel reinforcement bars with iron-based amorphous metals, as well as other amorphous alloys, could enable the production of other advanced materials. For example, an HVOF process could also be used to apply ceramic thermal barrier coatings to steel reinforcement bars, thereby making steel reinforced structures more resistant to fire. Such thermal barrier coatings might provide additional performance margin during accidents such as the one that recently caused collapse of a section of Interstate 880 in Oakland, California.

The application of ultrasonics and advanced radiographic techniques will be used to study the bonding of coatings to steel reinforcement bars, and to observe corrosion and oxide formation of coated steel reinforcement bars in concrete.

PART D: VISION

This visionary research will culminate in the development of advanced reinforcement bars, coated with corrosion-resistant amorphous metals and ceramics, for concrete structures. These new reinforcement bars will substantially enhance the life of the Nation's infrastructure by mitigating corrosion, and will enable application of thermal barrier coatings where needed.

PART E: TECHNICAL RATIONALE

Background

Deterioration of Nation's Infrastructure

The infrastructure for transportation in the United States allows for a high level of mobility and freight activity for the current population of 300 million residents, and several million business establishments. According to a Department of Transportation study, more than 230 million motor vehicles, ships, airplanes, and railroads cars were used on 6.4 million kilometers (4 million miles) of highways, railroads, airports, and waterways in 1998. Pipelines and storage tanks were considered to be part of this deteriorating infrastructure. The annual direct cost of corrosion in the infrastructure category was estimated to be approximately $22.6 billion in 1998 [1].

There were 583,000 bridges in the United States in 1998. Of this total, 200,000 bridges were steel, 235,000 were conventional reinforced concrete, 108,000 bridges were constructed using pre-stressed concrete, and the balance was made using other materials of construction. Approximately 15 percent of the bridges accounted for at this point in time were structurally deficient, primarily due to corrosion of steel and steel reinforcement (Figure 1). The annual direct cost of corrosion for highway bridges was estimated at $8.3 billion to replace structurally deficient bridges over a 10-year period of time, $2 billion for maintenance and cost of capital for concrete bridge decks, $2 billion for maintenance and cost of capital for concrete substructures, and $0.5 billion for maintenance of painting of steel bridges. Life-cycle analysis estimates indirect costs to the user due to traffic delays and lost productivity at more than 10 times the direct cost of corrosion maintenance, repair and rehabilitation [1].

In the early 1970's on epoxy-coated reinforcing steel (ECR) was qualified as an alternative to black bar to help address the problems associated with corrosion. For the past 30 years, ECR has been specified by several State Departments of Transportation for major decks and sub-structures exposed to chlorides. At the same time, ECR was augmented by use of low water-to-cement ratio (w/c) concrete, possibly with corrosion inhibitors. However, in Florida coastal waters, ECR has proven ineffective because of the combined effects of higher average temperature and more prolonged moist exposure [2].

The Innovative Bridge Research and Construction (IBRC) Program was authorized by Congress in the Transportation Equity Act for the 21st Century legislation initially as a 6-year effort (1998-2003), but was subsequently extended through May 2005. The majority of the funding was for actual repair, rehabilitation and replacement of existing structures, and for new construction with a lesser amount for research, both based upon innovative materials. Corrosion-resistant reinforcements constituted one component of the program. Reinforcement materials included black bar, epoxy-coated reinforcing steel (ECR), solid stainless steel (Types 316LN and 2205), clad stainless steel, galvanized steel and others [2].

Since the IBRC Program, new iron-based amorphous metals with good corrosion resistance have been developed, along with the technology necessary for applying these materials as coatings to large-area substrates, including steel reinforcing bars. It is believed that these coatings may be able to substantially enhance the corrosion resistance steel reinforcements in concrete structures. This proposal aims to evaluate these new advanced materials as a practical means of enhancing the performance of steel reinforcing bars.

Figure 1 – Photograph showing corrosion of steel reinforcement bar in concrete supporting highway bridge.

Corrosion-Resistant Amorphous-Metal Coatings

The outstanding corrosion resistance that may be possible with amorphous metals was recognized several years ago [3-5]. Compositions of several iron-based amorphous metals were published, including several with very good corrosion resistance. Examples include: thermally sprayed coatings of Fe-10Cr-10-Mo-(C,B), bulk Fe-Cr-Mo-C-B, and Fe-Cr-Mo-C-B-P [6-8]. The corrosion resistance of an iron-based amorphous alloy with yttrium, $Fe_{48}Mo_{14}Cr_{15}Y_2C_{15}B_6$, was also established [9-11]. Yttrium was added to this alloy to lower the critical cooling rate. In addition to iron-based materials, nickel-based amorphous metals have been developed that exhibit exceptional corrosion performance in acids. Very good nickel-based crystalline coatings were deposited with thermal spray, but appeared to have less corrosion resistance than amorphous-metal coatings [12].

Several additional iron-based amorphous alloys have been recently developed, characterized and tested. Many of these materials have demonstrated very good corrosion resistance [13-16]. Most of these alloys are based upon a common parent alloy, SAM40 ($Fe_{52.3}Mn_2Cr_{19}Mo_{2.5}W_{1.7}B_{16}C_4Si_{2.5}$), and can be applied as thermal spray coatings [17-18]. Promising alloys include SAM2X5 ($Fe_{49.7}Cr_{17.7}Mn_{1.9}Mo_{7.4}W_{1.6}B_{15.2}C_{3.8}Si_{2.4}$) and SAM1651 ($Fe_{48}Mo_{14}Cr_{15}Y_2C_{15}B_6$), which include chromium (Cr), molybdenum (Mo), and tungsten (W) for enhanced corrosion resistance, and boron (B) to enable glass formation and neutron absorption. The target compositions of this alloy, other amorphous alloys in the same families, and crystalline alloys such as Type 316L stainless steel (UNS # S31603) and nickel-based Alloy C-22 (UNS # N06022) are summarized in Table I.

Conclusions regarding the exceptional passive film stability and corrosion resistance of this iron-based amorphous alloy compared to crystalline reference materials were based on measurements of passive film breakdown potential and corrosion rate, as well as observed performance during salt fog testing. Such measurements enabled the corrosion performance of various iron-based amorphous alloys, carbon steel, iron-based stainless steels and nickel-based alloys to be directly compared.

Other Industrially Important Applications of New Materials

This alloy was recently discussed at a meeting of the Materials Research Society (MRS) in regard to its beneficial application to the safe storage of spent nuclear fuel [19]. The high boron content of (SAM2X5) $Fe_{49.7}Cr_{17.7}Mn_{1.9}Mo_{7.4}W_{1.6}B_{15.2}C_{3.8}Si_{2.4}$ makes it an effective neutron absorber, and suitable for criticality control applications. Average measured values of the neutron absorption cross section in transmission (Σ_t) for Type 316L stainless steel, Alloy C-22, borated stainless steel, a Ni-Cr-Mo-Gd alloy, and SAM2X5 have been determined to be approximately 1.1, 1.3, 2.3, 3.8 and 7.1, respectively, and are discussed in detail in the literature. The high boron content of this particular amorphous metal makes it an effective neutron absorber, and suitable for criticality control applications. This material and its parent alloy have been shown to maintain corrosion resistance up to the glass transition temperature, and to remain in the amorphous state after receiving relatively high neutron dose.

Table I – The melt-spinning process was used to perform a systematic study of various elemental compositions, each based on the Fe-based DAR40 composition, with 1, 3, 5, and 7 atomic percent additions of specific elements believed to be beneficial to glass formation or corrosion resistance. Elemental additions investigated included nickel (Ni), molybdenum (Mo), yttrium (Y), titanium (Ti), zirconium (Zr) and chromium (Cr). The two formulations of greatest interest at the present time, based upon corrosion resistance and ease of processing are SAM2X5 ($Fe_{49.7}Cr_{17.7}Mn_{1.9}Mo_{7.4}W_{1.6}B_{15.2}C_{3.8}Si_{2.4}$), which has a relatively high CCR, and yttrium-containing SAM1651 ($Fe_{48.0}Cr_{15.0}Mo_{14.0}B_{6.0}C_{15.0}Y_{2.0}$), which has a relatively low CCR.

Target Compositions in Atomic Percent - Used to Prepare Samples														
Alloy	Specification / Formula	Fe	Cr	Mn	Mo	W	B*	C*	Si	Y	Ni	P*	Co	Total
Type 316L	UNS S31603	68.0	18.0	1.5	1.5	0.0	0.0	0.0	1.0	0.0	10.0	0.0	0.0	100
Alloy C-22	UNS N06022	4.0	25.0	0.1	8.0	1.4	0.0	0.0	1.0	0.0	60.0	0.0	0.5	100
SAM40	$Fe_{52.3}Mn_2Cr_{19}Mo_{2.5}W_{1.7}B_{16}C_4Si_{2.5}$	52.3	19.0	2.0	2.5	1.7	16.0	4.0	2.5	0.0	0.0	0.0	0.0	100
SAM2X1	$(SAM40)_{99} + Mo_1$	51.8	18.8	2.0	3.5	1.7	15.8	4.0	2.5	0.0	0.0	0.0	0.0	100
SAM2X3	$(SAM40)_{97} + Mo_3$	50.7	18.4	1.9	5.4	1.6	15.5	3.9	2.4	0.0	0.0	0.0	0.0	100
SAM2X5	$(SAM40)_{95} + Mo_5$	49.7	18.1	1.9	7.4	1.6	15.2	3.8	2.4	0.0	0.0	0.0	0.0	100
SAM2X7	$(SAM40)_{93} + Mo_7$	48.6	17.7	1.9	9.3	1.6	14.9	3.7	2.3	0.0	0.0	0.0	0.0	100

Experimental Approach

Melt Spinning Process

Maximum cooling rates of one million Kelvin per second (10^6 K/s) have been achieved with melt spinning, which is an ideal process for producing amorphous metals over a very broad range of compositions. This process was used to synthesize completely amorphous, Fe-based, corrosion-resistant alloys with near theoretical density, and thereby enabled the effects of coating morphology on corrosion resistance to be separated from the effects of elemental composition. The melt-spun ribbon (MSR) samples prepared with this equipment were several meters long, several millimeters wide and approximately 150 microns thick.

Thermal Spray Process

The coatings discussed here were made with the high-velocity oxy-fuel (HVOF) process, which involves a combustion flame, and is characterized by gas and particle velocities that are three to four times the speed of sound (mach 3 to 4). This process is ideal for depositing metal and cermet coatings, which have typical bond strengths of 5,000 to 10,000 pounds per square inch (5-10 ksi), porosities of less than one percent (< 1%) and extreme hardness. The cooling rate that can be achieved in a typical thermal spray process such as HVOF are on the order of ten thousand Kelvin per second (10^4 K/s), and are high enough to enable many alloy compositions to be deposited above their respective critical cooling rate (CCR), thereby maintaining the vitreous state. However, the range of amorphous metal compositions that can be processed with HVOF is more restricted than those that can be prepared with melt spinning, due to the differences in achievable cooling rates. Both kerosene and hydrogen have been investigated as fuels in the HVOF process used to deposit SAM2X5. While the thickness of a typical coating ranges from 0.4 to 1.0 mm (nominally 15 to 40 mils), adherent coatings with thicknesses of 7.5 mm have been produced. Free-standing plates with thicknesses as great as 20 mm have also been produced.

Energy Dispersive Spectroscopy

Melt-spun ribbons were prepared by adding 1, 3, 5 and 7 atomic percent molybdenum (Mo) to SAM40 ($Fe_{52.3}Mn_2Cr_{19}Mo_{2.5}W_{1.7}B_{16}C_4Si_{2.5}$), and were designated SAM2X1, SAM2X3, SAM2X5 and SAM2X7, respectively. The SAM2X5 ($Fe_{49.7}Cr_{17.7}Mn_{1.9}Mo_{7.4}W_{1.6}B_{15.2}C_{3.8}Si_{2.4}$) provided adequate corrosion resistance, and was a formulation that could be processed with relative ease. The SAM2X7 composition had a higher calculated pitting-resistance equivalence number (PREN) than the alloys with less molybdenum, and slightly better corrosion resistance than SAM2X5, but was somewhat more difficult to make. The PREN is discussed in detail subsequently.

The target concentrations of heavier elements such as Cr, Mo and W were verified with Energy Dispersive Spectroscopy (EDS). Microanalysis of each sample was performed at three randomly selected locations at 10,000X magnification. Compositional analysis was performed on the smoother side of each melt-spun ribbon (MSR), as the rougher sides were found in some cases to be contaminated with trace amounts of copper, presumably from contact with the copper wheel during the melt spinning process. The concentrations of relatively light elements such as B and C could not be determined with EDS, and were therefore estimated with a simple difference calculation, so that the sum of concentrations for all elements totaled one hundred percent.

X-Ray Diffraction

The basic theory for X-ray diffraction (XRD) of amorphous materials is well developed and has been published in the literature [20-21]. In the case of amorphous materials, broad peaks are observed. During this study, XRD was done with CuK_α X-rays, a crystalline graphite analyzer, and a Philips vertical goniometer, using the Bragg-Bretano method. The X-ray optics were self-focusing, and the distance between the X-ray focal point to the sample position was equal to the distance between the sample position and the receiving slit for the reflection mode. Thus, the intensity and resolution were optimized. Parallel vertical slits were added to improve the scattering signal. Step scanning was performed from 20 to 90° (2θ) with a step size of 0.02° at 4 to 10 seconds per point, depending on the amount of sample. The samples were loaded into low-quartz holder since the expected intensity was very low, thus requiring that the background scattering be minimized.

Thermal Analysis

The thermal properties of these Fe-based amorphous metals have also been determined. Thermal analysis of these Fe-based amorphous metals, with differential scanning calorimetry (DSC) or differential thermal analysis (DTA), allowed determination of important thermal properties such as the glass transition temperature (T_g), crystallization temperature (T_x), and the melting point (T_m). Results from the thermal analysis of amorphous samples provided initial assessment of the glass forming ability of these materials through conventional metrics, such as the reduced glass transition temperature ($T_{rg} = T_g/T_L$).

Mechanical Properties

Hardness was also measured, since it determined wear resistance, as well as resistance to erosion-corrosion. Vickers micro-hardness (HV) was the standard approach used to assess the hardness of these thermal spray coatings. A 300-gram load was used since it was believed that this load and the affected area were large enough to sample across any existing macro-porosity, thereby producing a spatially averaged measurement. Micro-hardness measurements were also made with a 100-gram load since it was believed that this load and the affected area were small enough to accurately sample bulk material properties.

Cyclic Polarization

Cyclic polarization was used to determine the relative susceptibility of candidate amorphous metals to passive film breakdown and localized corrosion. The resistance to localized corrosion is quantified through measurement of the open-circuit corrosion potential (E_{corr}), the breakdown or critical potential ($E_{critical}$), and the repassivation potential (E_{rp}), which can all be determined from such measurements. The greater the difference between the open-circuit corrosion potential and the critical potential (ΔE), the more resistant a material is to modes of localized corrosion such a pitting and crevice corrosion. Spontaneous breakdown of the passive film and localized corrosion require that the open-circuit corrosion potential exceed the critical potential. General corrosion is assumed when E_{corr} is less than $E_{critical}$ ($E_{corr} < E_{critical}$), and localized corrosion is assumed when E_{corr} exceeds $E_{critical}$.[20] Measured values of the repassivation potential (E_{rp}) are sometimes used as conservative estimates of the critical potential ($E_{critical}$) [22].

In the published scientific literature, different bases exist for determining the critical potential from such electrochemical measurements [23]. The breakdown or critical potential has been defined as the potential where the passive current density increases to a level between 1 to 10 μA/cm^2 (10^{-6} to 10^{-5} A/cm^2) while increasing potential in the positive (anodic) direction during cyclic polarization or potential-step testing. The repassivation potential has been defined as the potential where the current density drops to a level indicative of passivity, which has been *assumed* to be between 0.1 to 1.0 μA/cm^2 (10^{-6} to 10^{-7} A/cm^2), while decreasing potential from the maximum level reached during cyclic polarization or potential-step testing. Alternatively, the repassivation potential has been defined as the potential during cyclic polarization where the forward and reverse scans intersect, a point where the measured current density during the reverse scan drops to a level *known* to be indicative of passivity. Details are discussed in the subsequent section.

Cyclic polarization (CP) measurements were based on a procedure similar to ASTM (American Society for Testing and Materials) G-5 and other similar standards with slight modification [24-27]. The ASTM G-5 standard calls for a 1N H_2SO_4 electrolyte, whereas synthetic bicarbonate, sulfate-chloride, chloride-nitrate, and chloride-nitrate solutions, with sodium, potassium and calcium cations, as well as natural seawater were used during this investigation. The natural seawater used in these tests was obtained directly from Half Moon Bay along the northern coast of California. Furthermore, the ASTM G-5 standard calls for the use of de-aerated solutions, whereas aerated and de-aerated solutions were used here.

Temperature-controlled borosilicate glass (Pyrex) electrochemical cells were used for cyclic polarization and other similar electrochemical measurements. This cell had three electrodes, a working electrode (test specimen), a reference electrode, and a counter electrode. A standard silver silver-chloride electrode, filled with near-saturation potassium chloride solution, was used as the reference, and communicated with the test solution via a Luggin probe placed in close proximity to the working electrode, which minimized Ohmic losses. The electrochemical cell was equipped with a water-cooled junction to maintain reference electrode at ambient temperature, which thereby maintained integrity of the potential measurement, and a water-cooled condenser, which prevented the loss of volatile species from the electrolyte.

To assess the sensitivity of these iron-based amorphous metals to devitrification, which can occur at elevated temperature, melt-spun ribbons of Fe-based amorphous metals were intentionally devitrified by heat treating them at various temperatures for one hour. After heat treatment, the samples were evaluated in high temperature seawater (90°C) with cyclic polarization, to determine the impact of the heat treatment on passive film stability and corrosion resistance. The temperatures used for the heat treatment were: 150, 300, 800 and 1000°C. In general, corrosion resistance was maintained below the crystallization temperature, and lost after prolonged aging at higher temperatures.

Potentiostatic Polarization

Potential step tests were used to determine the potential at which the passive film breaks down on $Fe_{49.7}Cr_{17.7}Mn_{1.9}Mo_{7.4}W_{1.6}B_{15.2}C_{3.8}Si_{2.4}$ (SAM2X5) and the reference material, nickel-based Alloy C-22. During prolonged periods of at a constant applied potential, which were typically 24 hours in duration, the current was monitored as a function of time. In cases where passivity was lost, the current increased, and the test sample was aggressively attacked. In cases where passivity was maintained, the current decayed to a relatively constant asymptotic level, consistent with the known passive current density. In these tests, periods of polarization were preceded by one hour at the open circuit corrosion potential (OCP), or rest potential. As a practical matter, increments of applied potential were controlled relative to the initial rest potential. To eliminate the need for surface roughness corrections in the conversion of measured current and electrode area to current density, the SAM2X5 coatings were polished to a 600-grit finish prior to testing. The constant potential denoted in the figures was applied after 1 hour at the OCP.

Linear Polarization

The linear polarization method was used as a method for determining the apparent corrosion rates of the various amorphous metal coatings. The procedure used for linear polarization testing consisted of the following steps: (1) holding the sample for ten seconds at the OCP; (2) beginning at a potential 20 mV below the OCP, increasing the potential linearly at a constant rate of 0.1667 mV per second to a potential 20 mV above the OCP; (3) recording the current being passed from the counter electrode to the working electrode as a function of potential relative to a standard Ag/AgCl reference electrode; and (4) determining the parameters in the cathodic Tafel line by performing linear regression on the voltage-current data, from 10 mV below the OCP, to 10 mV above the OCP. The slope of this line was the polarization resistance, *Rp* (ohms), and was defined in the published literature [28]. While no values for the Tafel parameter (*B*) of Fe-based amorphous metals have yet been developed, it was believed that a conservative value of approximately 25 mV was reasonable, based upon the range of published values for several Fe- and Ni-based alloys. The corrosion current density was then defined in terms of *B*, R_p and *A*, the actual exposed area of the sample being tested.

$$R_P = \left(\frac{\partial E}{\partial I} \right)_{E_{corr}} \tag{1}$$

The parameter (*B*) was defined in terms of the slopes of the anodic and cathodic branches of the Tafel line:

$$B = \frac{\beta_a \beta_c}{2.303(\beta_a + \beta_c)} \tag{2}$$

Values of B were published for a variety of iron-based alloys, and varied slightly from one alloy-environment combination to another. For example, values for carbon steel, as well as Type 304, 304L and 430 stainless steels, in a variety of electrolytes which include seawater, sodium chloride, and sulfuric acid, ranged from 19 to 25 mV. A value for nickel-based Alloy 600 in lithiated water at 288°C was given as approximately 24 mV. While no values have yet been developed for the Fe-based amorphous metals that are the subject of this investigation, it was believed that a conservative representative value of approximately 25 mV was appropriate for the conversion of polarization resistance to corrosion current. Given the value for Alloy 600, a value of 25 mV was also believed to be acceptable for converting the polarization resistance for nickel-based Alloy C-22 to corrosion current.

The general corrosion rate was calculated from the corrosion current density through application of Faraday's Law. The corrosion current, I_{corr} (A) was then defined as:

$$I_{corr} = \frac{B}{R_p} \tag{3}$$

where the parameter B was conservatively assumed to be approximately 25 mV. The corrosion current density, i_{corr} (A cm^{-2}), was defined as the corrosion current, normalized by electrode area, *A* (cm^2). The corrosion (or penetration) rates of the amorphous alloy and reference materials were calculated from the corrosion current densities with the following formula, which is similar to that given by Jones [29]:

$$\frac{dp}{dt} = \frac{i_{corr}}{\rho_{alloy} n_{alloy} F} \quad (4)$$

where p was the penetration depth, t was time, i_{corr} was the corrosion current density, ρ_{alloy} was the density of the alloy (g cm^{-3}), n_{alloy} was the number of gram equivalents per gram of alloy, and F was Faraday's constant. The value of n_{alloy} was calculated with the following formula:

$$n_{alloy} = \sum_j \left(\frac{f_j n_j}{a_j} \right) \quad (5)$$

where f_j was the mass fraction of the jth alloying element in the material, n_j was the number of electrons involved in the anodic dissolution process, which was assumed to be congruent, and a_j was the atomic weight of the jth alloying element. Congruent oxidation or dissolution was assumed, which meant that the dissolution rate of a given alloy element was assumed to be proportional to its concentration in the bulk alloy. These equations were used to calculate factors for the conversion of corrosion current density to the corrosion rate. The conversion factors for converting corrosion current density to corrosion rate are approximately: 6.38 to 10.7 μm cm^2 μA^{-1} yr^{-1} for Type 316L stainless steel; 5.57 to 9.89 μm cm^2 μA^{-1} yr^{-1} for Alloy C-22; and 5.39 to 7.89 μm cm^2 μA^{-1} yr^{-1} for SAM2X5, depending upon the exact composition of each alloy within the specified ranges.

Junction Potential Correction

It is important to understand the magnitude of the error in the potential measurements due to the junction potential. Consistent with the methods given by Bard and Faulkner, a correction was performed based upon the Henderson Equation [30]. The calculated junction potentials for several test solutions were estimated with ionic properties also taken from Bard and Faulkner. These corrections were not very large, with the largest being less than approximately 10 mV. It was therefore concluded that no significant error would result from neglecting the junction potential correction. Some uncertainty and error would have been introduced by using the correction.

Standard Test Solutions Used for Immersion Testing

In addition of natural seawater and 3.5-molal sodium chloride solutions, several standardized test solutions have been developed based upon the well J-13 water composition determined by Harrar et al. [31]. Relevant test environments are assumed to include simulated dilute water (SDW), simulated concentrated water (SCW), and simulated acidic water (SAW) at 30, 60, and 90°C. The compositions of all of the environments are given in Table II. The compositions of these test media are based upon the work of Gdowski et al. [32-34].

Salt Fog Testing

Salt fog tests were conducted according to the standard General Motors (GM) salt fog test, identified as GM9540P, or an abbreviation of that test. The protocol for this test is summarized in Table III. Reference samples included 1018 carbon steel, Type 316L stainless steel, nickel-based Alloy C-22, Ti Grade 7, and the 50:50 nickel-chromium binary.

Table II – A description of the standard GM9540P Salt Fog Test is summarized here. Note that the salt solution mists (denoted with asterisks) consisted of 1.25% solution containing 0.9% sodium chloride, 0.1% calcium chloride, and 0.25% sodium bicarbonate.

24-Hour Test Cycle for GM9540P Accelerated Corrosion Test		
Shift	Elapsed Time (hrs)	Event
Ambient Soak	0	Salt solution mist for 30 seconds, followed by ambient exposure at 13-28°C (55-82°F)
	1.5	Salt solution mist for 30 seconds, followed by ambient exposure at 13-28°C (55-82°F)
	3	Salt solution mist for 30 seconds, followed by ambient exposure at 13-28°C (55-82°F)
	4.5	Salt solution mist for 30 seconds, followed by ambient exposure at 13-28°C (55-82°F)
Wet Soak	8 to 16	High humidity exposure for 8 hours at 49 ± 0.5°C (120 ± 1°F) and 100% RH, including a 55-minute ramp to wet conditions
Dry Soak	16 to 24	Elevated dry exposure for 8 hours at 60 ± 0.5°C (140 ± 1°F) and less than 30% RH, including a 175-minute ramp to dry conditions

Table III – Composition of standard test media based upon 2ell J-13 water.

Ion	SDW	SCW	SAW
	(mg/L^{-1})	(mg/L^{-1})	(mg/L^{-1})
K^{+1}	34	3,400	3,400
Na^{+1}	409	40,900	40,900
Mg^{+2}	1	1	1,000
Ca^{+2}	1	1	1,000
F^{-1}	14	1,400	0
Cl^{-1}	67	6,700	6,700
NO_3^{-1}	64	6,400	6,400
SO_4^{-2}	167	16,700	16,700
HCO_3^{-1}	947	70,000	0
Si (60°C)	27	27	27
Si (90°C)	49	49	49
pH	8.1	8.1	2.7

Experimental Results

Amorphous Structure

Melt-spun ribbons prepared by The NanoSteel Company (TNC) were characterized with XRD. Diffraction patterns of melt-spun ribbons of Alloy C-22 and Type 316L stainless steel showed that these samples were indeed crystalline, and that the melt spinning process could not capture the meta-stable glassy state for these compositions. Figure 2 shows X-ray diffraction data for melt-spun ribbon (MSR) samples of iron-based amorphous metals identified as: (a) SAM40; (b) SAM2X1; (c) SAM2X3; (d) SAM2X5; (e) SAM2X7; (f) SAM6; (g) SAM7 or SAM1651; and SAM8. All ribbons were completely amorphous. These data were indicative of amorphous structure, and a complete lack of crystalline structure, which was attributed to the relatively high concentrations of boron, and a cooling rate above the critical cooling rate (CCR).

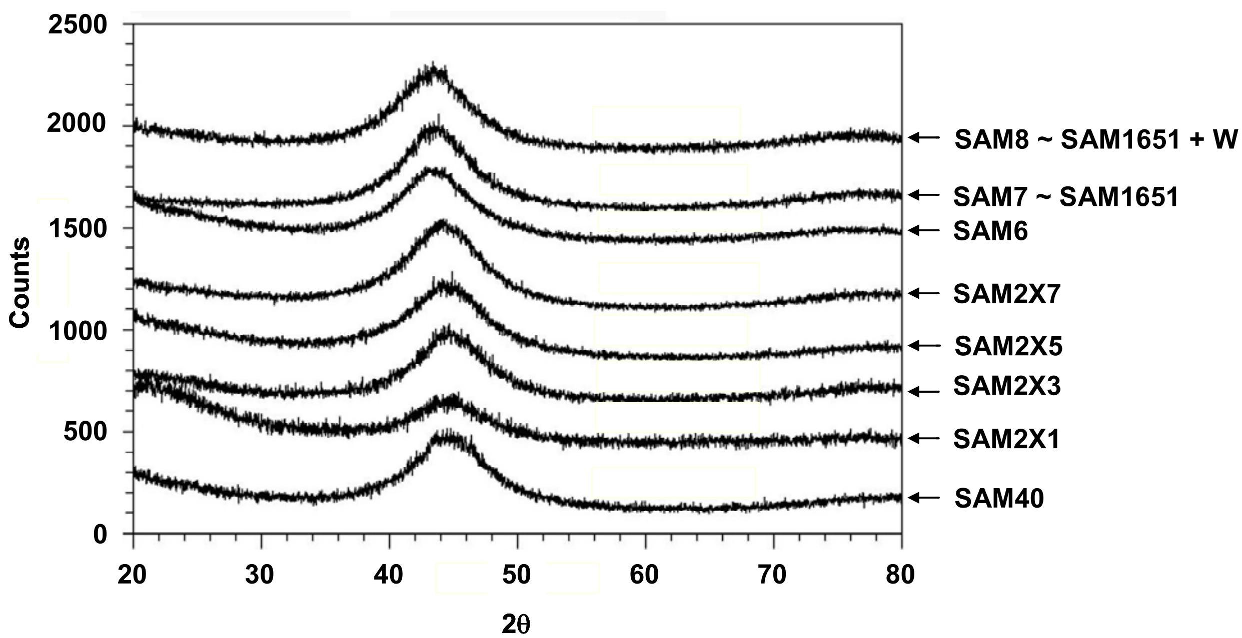

Figure 2 – This figure shows X-ray diffraction data for melt-spun ribbon (MSR) samples of iron-based amorphous metals identified as: (a) SAM40; (b) SAM2X1; (c) SAM2X3; (d) SAM2X5; (e) SAM2X7; (f) SAM6; (g) SAM7 or SAM1651; and SAM8. All ribbons were completely amorphous.

Gas Atomized Powders

The absence of crystalline structures was believed to be one factor that contributes to the corrosion resistance of amorphous alloys. Residual crystalline structure, mechanical properties, corrosion resistance were assumed to depend upon the distribution of particle sizes in feed powders. A portion of this investigation was directed towards the proof or disproof of this hypothesis. The crystalline structure of powders was found to vary with particle size, since different cooling rates were experienced by particles with different sizes. Particle size sensitivity was explored in regard to the residual crystalline phases present in powders and coatings, as well as in regard to the impact of those crystalline phases on the corrosion resistance of coatings. A correlation has been observed between the formation of substantial amounts of deleterious crystalline phases, such as bcc ferrite, in Fe-based amorphous metals, and the susceptibility to corrosion in chloride-containing environments.

Due to the relatively high critical cooling rate of $Fe_{49.7}Cr_{17.7}Mn_{1.9}Mo_{7.4}W_{1.6}B_{15.2}C_{3.8}Si_{2.4}$ (SAM2X5) in comparison to that of other alloys such as $Fe_{48}Mo_{14}Cr_{15}Y_{2}C_{15}B_{6}$ (SAM1651), technological challenges had to be overcome to produce completely amorphous powder with this high-boron Fe-based amorphous metal. It was found that particular care had to be paid to the control of raw materials and conditions within the atomization process. Through careful control of these variables, completely amorphous powders were produced with the SAM2X5 high-boron composition. The particle size distributions of powders typically used as feedstock for HVOF deposition processes usually lie between 15 and 53 microns (−53/+15 μm). To explore the impact of particle size on the residual crystalline content of coatings, as well as the corrosion resistance of these coatings, several particle size distributions were explored. This work therefore provides unique insight into the relationship between particle size, which determines the cooling rate along the radius of the amorphous metal particles, the presence of crystalline phases in the prepared coatings, and the corresponding corrosion resistance. In general, broad halos were observed at 2θ-angles of 44° and 78°, which indicated that SAM2X5 feed powders were predominately amorphous. However, relatively small sharp peaks were also observed, and were attributed primarily to four crystalline phases, including Cr_2B, WC, $M_{23}C_6$ and bcc ferrite.[32] These potentially deleterious precipitates deplete the amorphous matrix of those alloying elements, such as chromium, responsible for enhanced passivity. The largest amount of these crystalline phases was found in Lots # 04-265 (−53/+15 μm) and 04-200 (−53/+30 μm), with relatively little found in Lot # 04-199 (−30/+15 μm). These results are reflected in the XRD data for the coatings produced with each of these powders.

Thermal-Spray Coatings

Several generic types of thermal spray coatings were produced for characterization and testing, and are shown in Figure 3. XRD data for a HVOF coating of SAM2X5 on a nickel-based Alloy C-22 substrate, and deposited with with a JP5000™ thermal-spray gun (Praxair TAFA JP5000 System), is shown in Figure 4. This coating also had residual crystalline phases present, and was prepared with Lot # 04-265 powder, which had a broad range of particle sizes (−53/+15 μm).

XRD data for a HVOF coating of SAM2X5 on a Type 316L stainless steel substrate, deposited with the JK2000™ thermal spray gun (Deloro Stellite JetKote JK2000 System), is shown in Figure 5. This coating was prepared with Lot # 04-200 powder which had a particle size distribution typical of those used for HVOF processes (−53/+30 μm). XRD data for another HVOF coating of SAM2X5 on a Type 316L stainless steel substrate, deposited with JK2000 thermal spray gun is shown in Figure 6. The coatings with largest amount of Cr_2B, WC, $M_{23}C_6$ and bcc ferrite were prepared with Lots # 04-265 (−53/+15 μm) and 04-200 (−53/+30 μm), while the coating with the least amount of these three crystalline phases was prepared with Lot # 04-199 (−30/+15 μm).

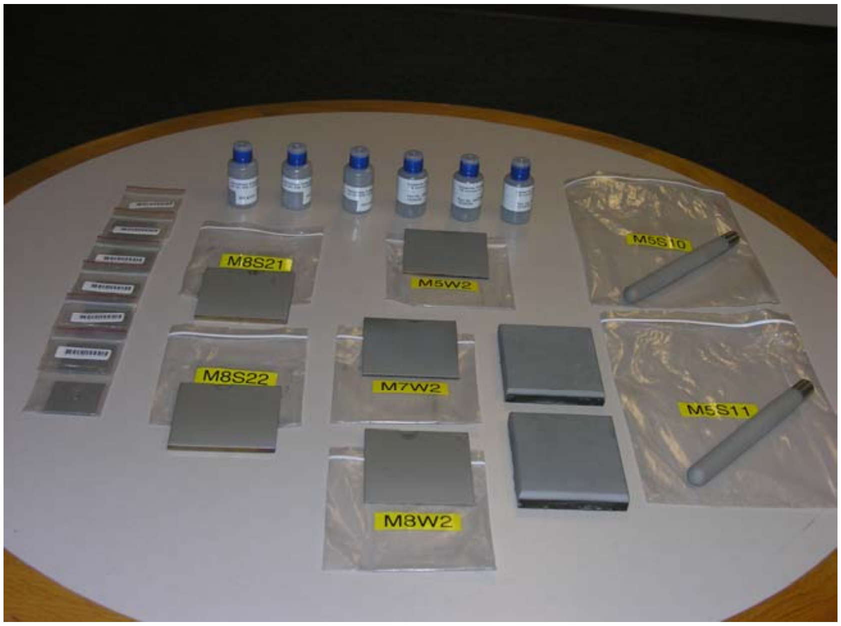

Figure 3 – Samples of amorphous-metal HVOF coatings used for long-term corrosion testing.

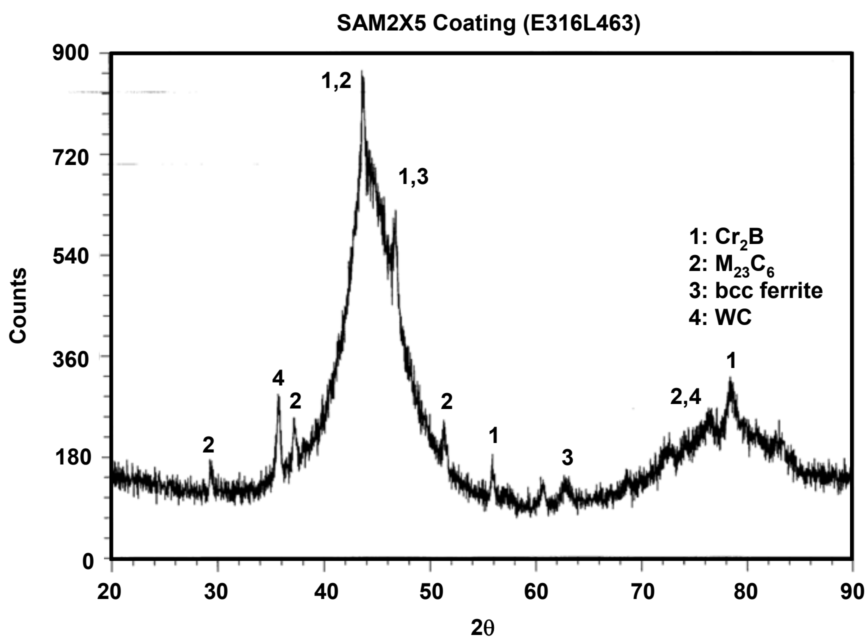

Figure 4 – XRD data (intensity vs. diffraction angle 2θ) for high-velocity oxy-fuel (HVOF) coating of $Fe_{49.7}Cr_{17.7}Mn_{1.9}Mo_{7.4}W_{1.6}B_{15.2}C_{3.8}Si_{2.4}$ (SAM2X5) on Type 316L stainless steel substrate prepared with JP5000 thermal spray gun. This coating, identified as E316L463, was prepared with Lot #04-265 powder, which had a broad range of particle sizes (–53/+15µm).

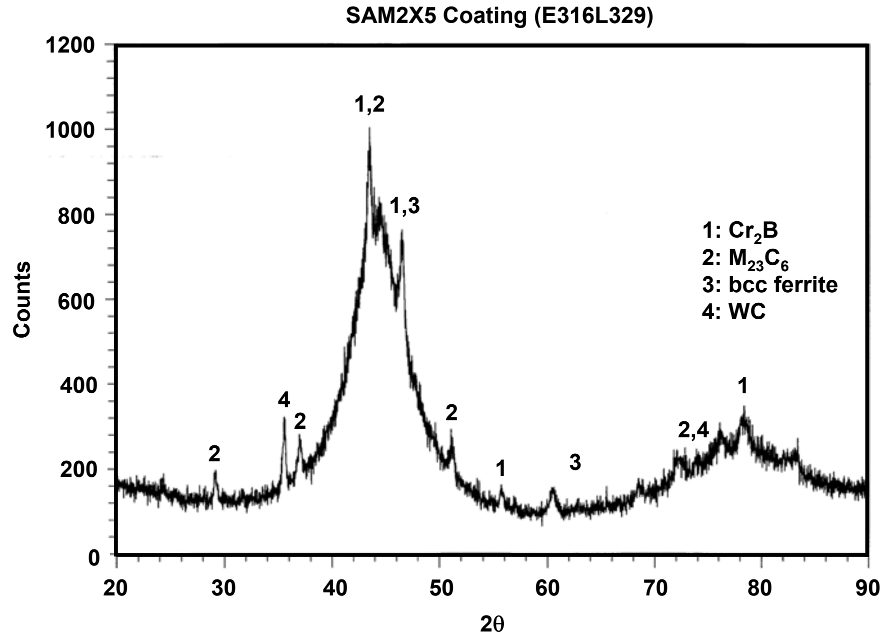

Figure 5 – XRD data (intensity vs. diffraction angle 2θ) for high-velocity oxy-fuel (HVOF) coating of $Fe_{49.7}Cr_{17.7}Mn_{1.9}Mo_{7.4}W_{1.6}B_{15.2}C_{3.8}Si_{2.4}$ (SAM2X5) on a Type 316L stainless steel substrate, and deposited with a JK2000 thermal-spray gun at Plasma Tech Incorporated (PTI). This coating, identified as E316L329, was prepared with Lot # 04-200 powder, which had a relatively coarse range of particle sizes (−53/+30µm).

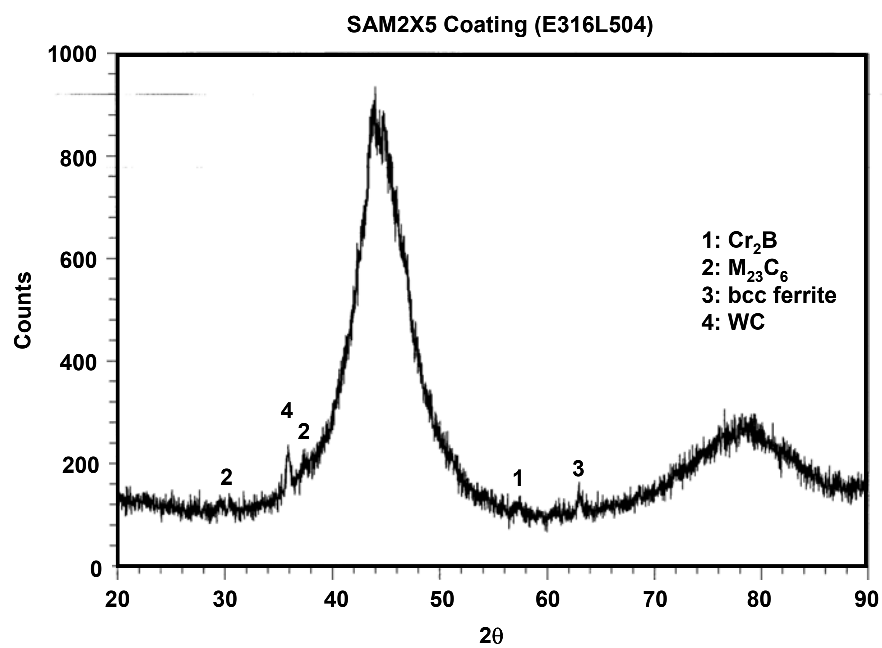

Figure 6 – XRD data (intensity vs. diffraction angle 2θ) for high-velocity oxy-fuel (HVOF) coating of SAM2X5 on a Type 316L stainless steel substrate, deposited with a JK2000 thermal-spray gun at Plasma Tech Incorporated (PTI). This coating, identified as E316L504, was prepared with Lot # 04-199 powder, which had a relatively fine range of particle sizes (−30/+15µm), and is a standard size distribution for HVOF applications.

Thermal Properties

The yttrium-containing SAM1651 formulation has a glass transition temperature of ~584°C, a crystallization temperature of ~653°C, a melting point of ~1121°C, and a reduced glass transition temperature of ~0.55. The critical cooling rate of SAM1651 has been determined to be ≤ 80 K per second, which is significantly less than other corrosion-resistant iron-based amorphous metals such as SAM2X5. Clearly, the yttrium additions in SAM1651 enhance glass-forming ability of these materials.

As an example, the thermal properties of for the SAM2X-series alloys are summarized in Table IV. SAM2X5 ($Fe_{49.7}Cr_{17.7}Mn_{1.9}Mo_{7.4}W_{1.6}B_{15.2}C_{3.8}Si_{2.4}$) had a glass transition temperature of ~579°C, a crystallization temperature of ~628°C, a melting point of ~1133°C, and a reduced glass transition temperature of ~0.57. SAM2X7 had a glass transition temperature of ~573°C, a crystallization temperature of ~630°C, a melting point of ~1137°C, and a reduced glass transition temperature of 0.57. As the Mo additions to SAM40 were increased from 1 to 7 atomic percent, the crystallization temperature increased from ~620 to ~630°C, and the melting point increased from 1110 to 1137°C. Other trends with composition were less obvious. The critical cooling rates for these alloys have been determined to be ~610 Kelvin per second.

Mechanical Properties

As previously discussed, hardness determines wear resistance, as well as resistance to erosion-corrosion. Vickers micro-hardness (HV) was the standard approach used to assess the hardness of these thermal spray coatings. A 300-gram load was used since it was believed that this load and the affected area were large enough to sample across any existing macro-porosity, thereby producing a spatially averaged measurement. Micro-hardness measurements were also made with a 100-gram load since it was believed that this load and the affected area were small enough to accurately sample bulk material properties. Micro-hardness measurements made with the 100-gram load were: 1050-1200 kg mm^{-2} (HVN) for as-sprayed HVOF coatings; and 1300-1500 kg mm^{-2} (HVN) for materials that were annealed 700°C for 10 minutes to induce devitrification. Micro-hardness measurements made with the 100-gram load were: 1050-1200 kg mm^{-2} (HVN) for as-sprayed HVOF coatings; and 1300-1500 kg mm^{-2} (HVN) for materials that were annealed 700°C for 10 minutes to induce devitrification. The increase in hardness with devitrification is attributed to the formation of crystalline precipitates.

Passive-Film Stability – SAM1651

Cyclic polarization data for three drop-cast ingots of SAM1651 Fe-based amorphous metal with yttrium in three different environments is shown in Figure 7: seawater at 90°C; 3.5 molal NaCl at 90°C; and 5M $CaCl_2$ at 105°C. All three cyclic polarization curves show outstanding passivity. Cyclic polarization data for a wrought prism of nickel-based Alloy C-22, a drop-cast ingot of Fe-based SAM1651 amorphous metal, and a melt-spun ribbon of SAM8 (SAM1651 + 3 atomic percent tungsten), all obtained with 5M $CaCl_2$ at 105°C is shown in Figure 8. Both the SAM1651 and SAM8 showed passive film stability comparable to (or better than) Alloy C-22. The addition of 3 atomic-percent tungsten to the SAM1651 enhanced the passive film stability, and also yielded more ductile and damage-tolerant amorphous metal ribbons.

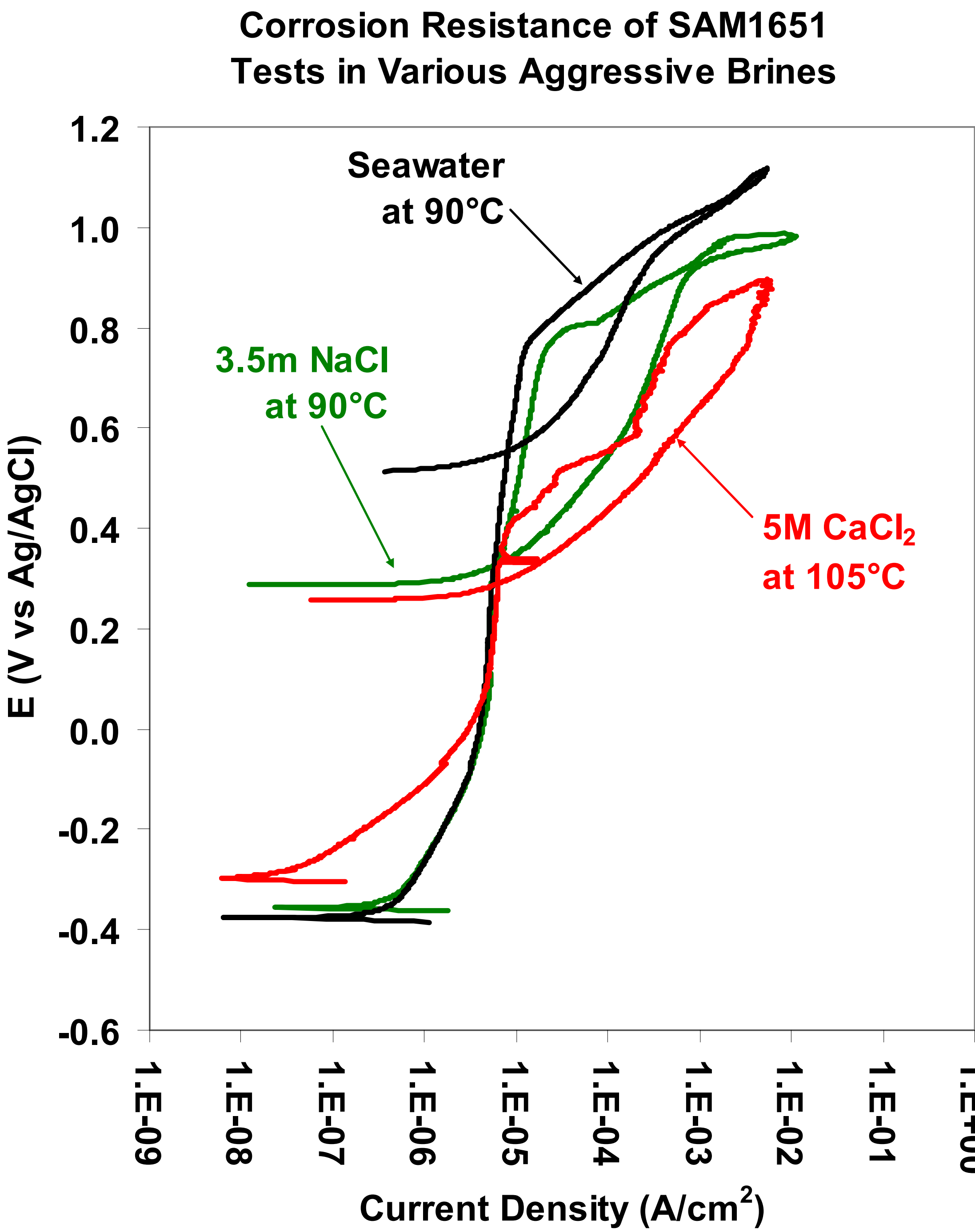

Figure 7 – Cyclic polarization data for three drop-cast ingots of SAM1651 (SAM7) Fe-based amorphous metal with yttrium in three different environments: seawater at 90°C; 3.5 molal NaCl at 90°C; and 5M $CaCl_2$ at 105°C.

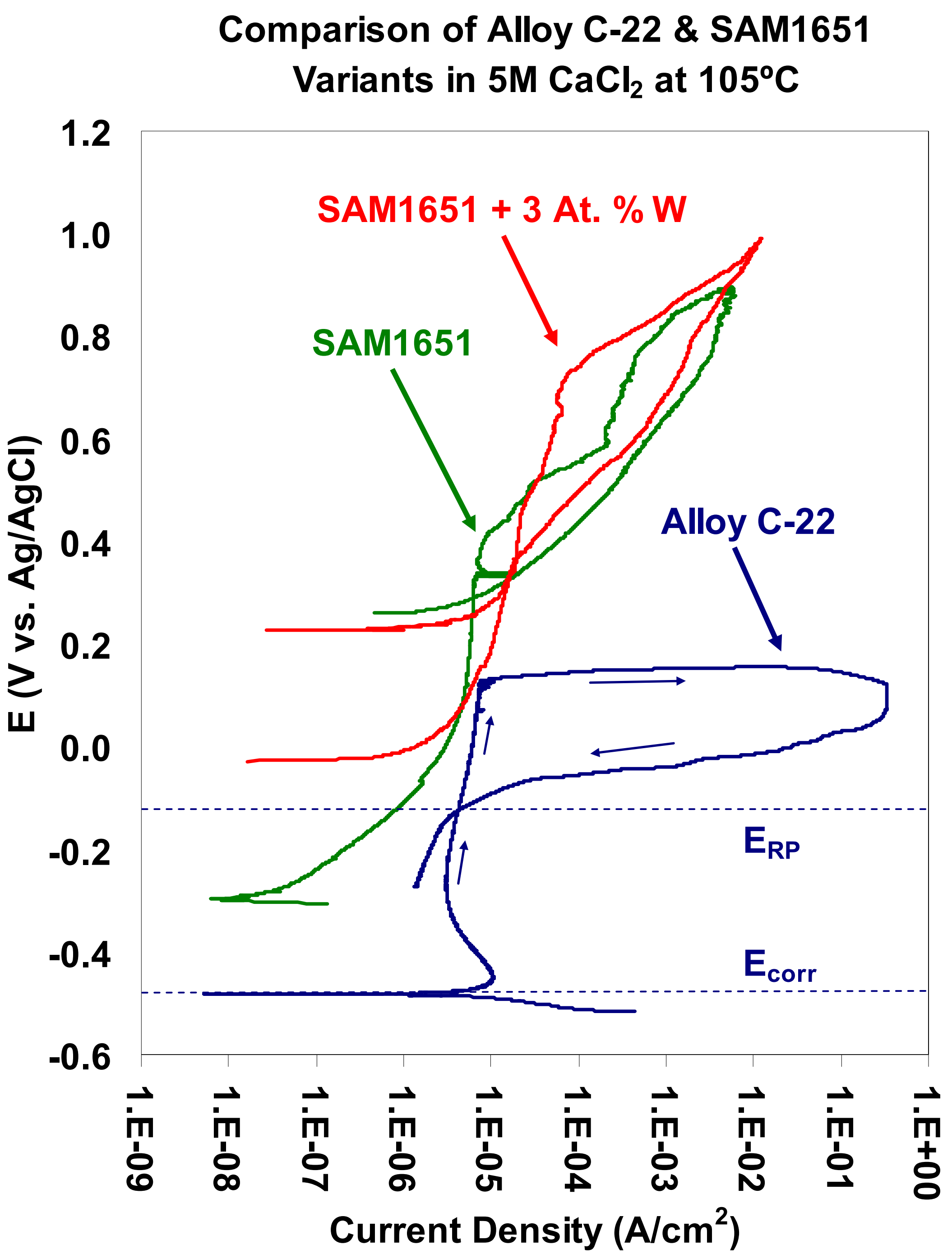

Figure 8 – Cyclic polarization data for a wrought prism of nickel-based Alloy C-22, a drop-cast ingot of iron-based SAM7 (SAM1651) amorphous metal, and a melt-spun ribbon of SAM8 (SAM1651 (SAM7) + 3 atomic percent tungsten), all obtained with 5M $CaCl_2$ at 105°C.

Passive-Film Stability – SAM2X5

Potential-step testing in natural seawater heated to 90° was done with: wrought Alloy C-22 (reference material); fully dense and completely amorphous melt spun ribbons of SAM2X5; optimized HVOF coatings prepared with coarse (−53/+30 μm) powders of SAM2X5; and optimized HVOF coatings prepared with relatively fine (−30/+15 μm) powders of SAM2X. These coatings were prepared with SAM2X5 powder supplied by The NanoSteel Company (TNC), and deposited by Plasma Tech Incorporated (PTI) in Torrance, California. Coatings prepared with finer powders were found to have a smaller volume fraction of crystalline precipitates than those prepared with coarser powders. To eliminate the need for surface roughness corrections in the conversion of measured current and electrode area to current density, the SAM2X5 coatings were polished to a 600-grit finish prior to testing.

Figures 9 and 10 show measured transients in current density at constant applied potentials of 1000 and 1200 mV vs. OCP (open circuit potential) for several different materials in natural seawater at 90°C. The materials compared in each figure include wrought Alloy C-22 (reference material), a fully dense and completely amorphous melt-spun ribbon (MSR) of SAM2X5, HVOF coatings prepared with coarse (−53/+30 μm) powders of SAM2X5, and HVOF coatings prepared with relatively fine (−30/+15 μm) powders of SAM2X5. The constant potential was applied after 1 hour at the OCP. The passive film on the MSR samples and HVOF coatings of SAM2X5 were more stable than that on wrought nickel-based Alloy C-22 under these conditions, which lead to the conclusion that this iron-based amorphous metal had superior corrosion resistance.

Transients in current density at a constant applied potential of 1000 mV are compared in Figure 9. Gradually increasing current density observed during testing of Alloy C-22 was indicative of passive film breakdown. The HVOF coating of SAM2X5 prepared with relatively fine (−30/+15 μm) powder had a temporary loss of passivity at 1×10^4 seconds, but underwent repassivation at 6×10^4 seconds. In contrast, the coating prepared with coarse (−53/+30 μm) powder appeared to be completely stable, as did the melt-spun ribbon. The differences in the corrosion resistance of the SAM2X5 coatings prepared with coarse (−53/+30 μm) and relatively fine (−30/+15 μm) powders are not completely understood. Since the coating prepared with the coarser powder had slightly more Cr_2B, WC, $M_{23}C_6$ and bcc ferrite than the coatings produced with the finer powder, the superior passive film stability found with these powders cannot be attributed to the formation of these potentially deleterious crystalline phases. Differences in the interfacial composition, structure and area of individual particles that comprise the coatings may be responsible. The passive film on the melt spun ribbon and HVOF coatings of SAM2X5 prepared with coarse (−53/+30 μm) powder were more stable than that on wrought nickel-based Alloy C-22 under similar conditions, which lead to the conclusion that this iron-based amorphous metal had superior corrosion resistance. In all cases with SAM2X5, melt-spun ribbons performed better than HVOF coatings.

As the applied potential was increased to 1200 mV, as shown in Figure 10, the Alloy C-22 samples lost all passivity, while the melt-spun ribbons and thermal spray coatings of SAM2X5 maintained passivity. The passivity of coatings prepared with the finer powder stabilized at this higher anodic potential.

Current density transients at 100 to 1500 mV were measured with a SAM2X5 thermal-spray coating prepared with relatively fine (−30/+15 μm) SAM2X5 powder in deaerated natural seawater at 90°C. Data for 100, 600, 700 and 1500 mV are shown in Figure 11. Complete passive film stability of this SAM2X5 sample was maintained at potentials up to 600 mV, with current density fluctuations observed at 700 mV which were indicative of the onset of passive film metastability. Similar current density fluctuations were observed at potentials up to 1400 mV. At an applied potential of 1500 mV, passivity was completely lost.

Current density transients at 100 to 1500 mV were measured with a SAM2X5 thermal-spray coating prepared with relatively coarse (−53/+30 μm) SAM2X5 powder in deaerated natural seawater at 90°C. Data for 100, 500, 800, 1400 and 1500 mV are shown in Figure 12. Complete passive film stability of this SAM2X5 sample was maintained at potentials up to 1400 mV. However, at an applied potential of 1500 mV, passivity was completely lost. Coatings produced with coarse powder exhibited less metastability than coatings produced with fine powder.

Figure 13 shows a comparison and summary of the data presented in Figures 8 through 11, as well as other supporting data. The asymptotic current density reached after 24 hours at each applied potential (each data point represents a 24 hour test) is plotted for wrought Alloy C-22; fully dense and completely amorphous melt spun ribbons of SAM2X5; HVOF coatings of SAM2X5 prepared with coarse (−53/+30 μm) powder; and HVOF coatings of SAM2X5 prepared with relatively fine (−30/+15 μm) powder. As a practical matter, all data in this figure was plotted as a function of potential relative to the Ag/AgCl reference electrode to enable comparison on a common scale, since each individual sample had its own unique OCP. From this plot of current density vs. potential, it appears that stability of the passive film on wrought Alloy C-22 was maintained at applied potentials below approximately 250 mV vs. Ag/AgCl, the point at which a dramatic change in slope was observed. Similarly, it was concluded that stabilities of passive films on SAM2X5 thermal spray coatings were maintained at applied potentials below approximately 900 mV vs. Ag/AgCl. The stability of the passive film on the SAM2X5 melt-spun ribbon was maintained at applied potentials below approximately 1200 mV vs. Ag/AgCl. Passive films on the SAM2X5 samples exhibited better stability than those on Alloy C-22. These data enabled a clear and unambiguous determination of the threshold potentials for passive film breakdown in a non-creviced condition.

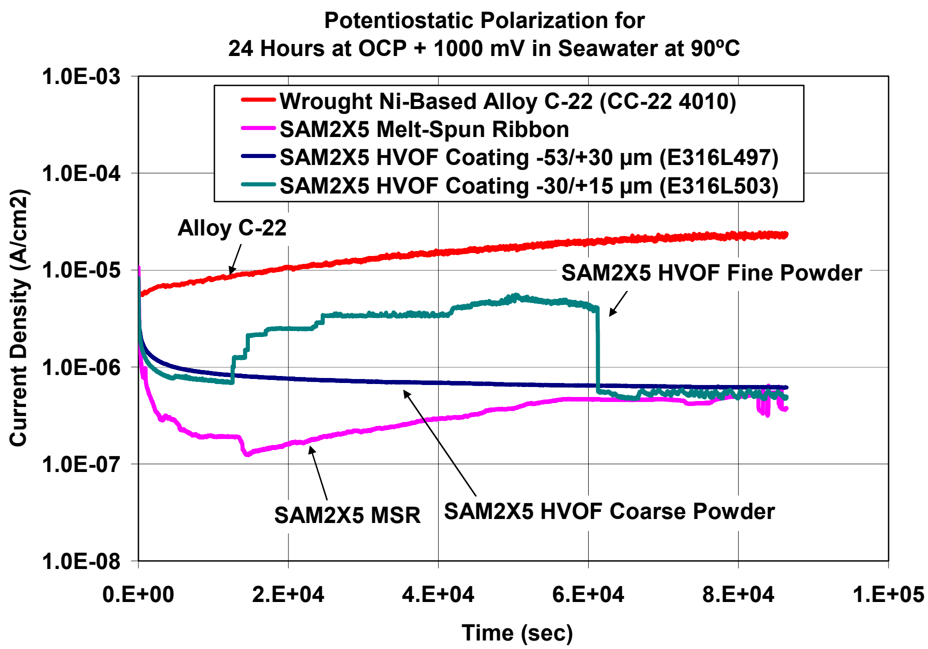

Figure 9 – Transients in current density at a constant applied potential of 1000 mV vs. OCP for wrought Alloy C-22 (reference material), a fully dense and completely amorphous melt spun ribbon (MSR) of SAM2X5, HVOF coatings prepared with −53/+30 micron powders of SAM2X5, and HVOF coatings prepared with −30/+15 micron powders of SAM2X5, all in natural seawater heated to 90°C, are compared.

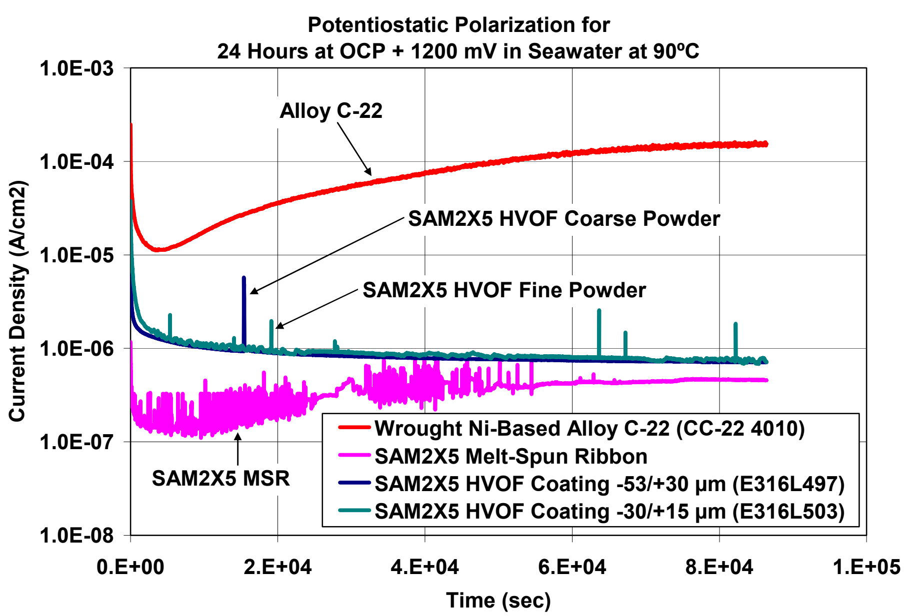

Figure 10 – Transients in current density at a constant applied potential of 1200 mV vs. OCP for wrought Alloy C-22 (reference material), a fully dense and completely amorphous melt spun ribbon (MSR) of SAM2X5, HVOF coatings prepared with −53/+30 micron powders of SAM2X5, and HVOF coatings prepared with −30/+15 micron powders of SAM2X5, all in natural seawater heated to 90°C, are compared.

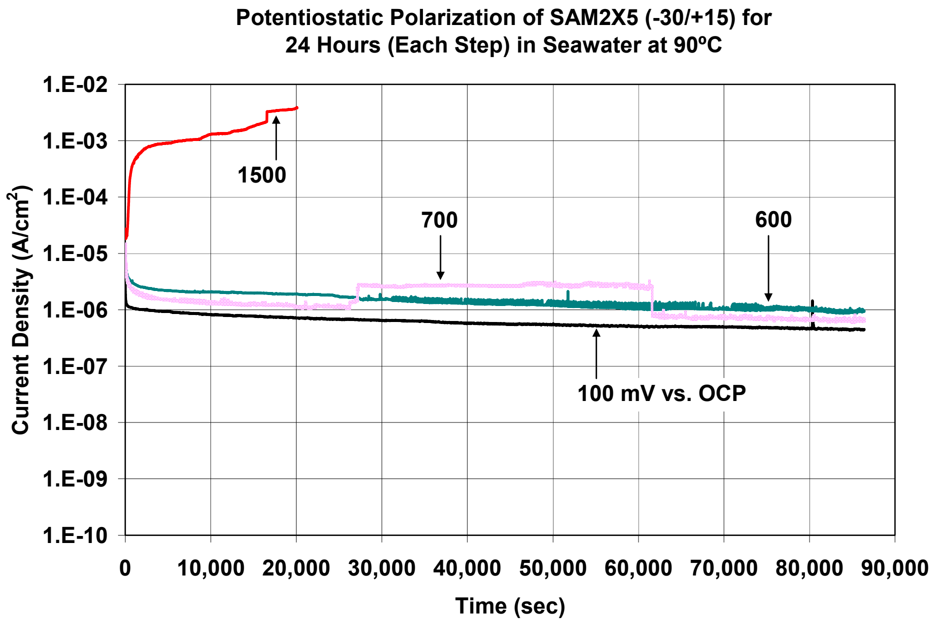

Figure 11 – Transients in current density at various levels of constant applied potential ranging from 100 to 1500 mV vs. OCP for a recently optimized SAM2X5 HVOF coating (–30/+15 micron powder) in deaerated natural seawater at 90°C are indicative of good passive film stability.

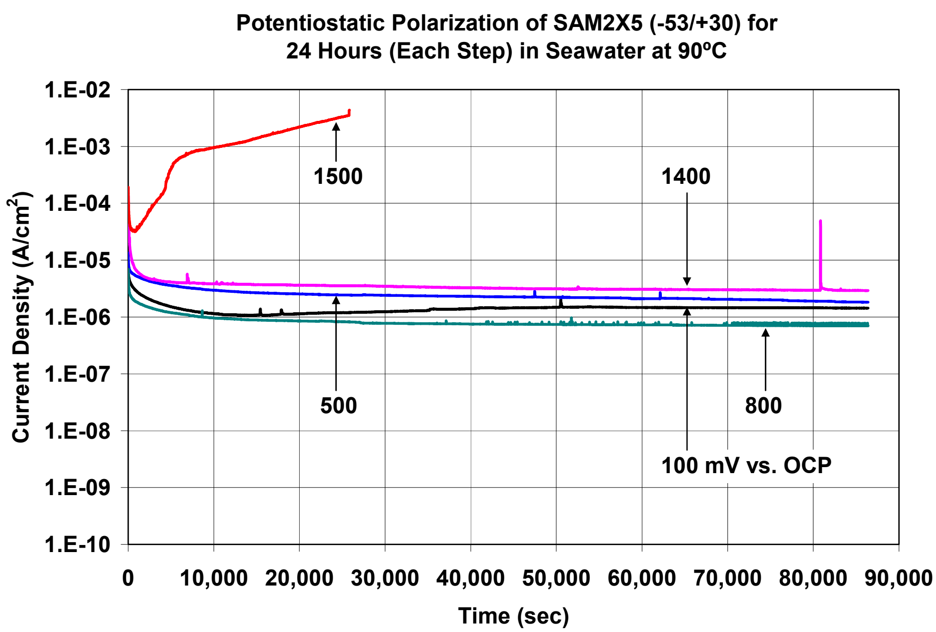

Figure 12 – Transients in current density at various levels of constant applied potential ranging from 100 to 1500 mV vs. OCP for a recently optimized SAM2X5 HVOF coating (–53/+30 micron powder) in natural seawater at 90°C are indicative of exceptional passive film stability.

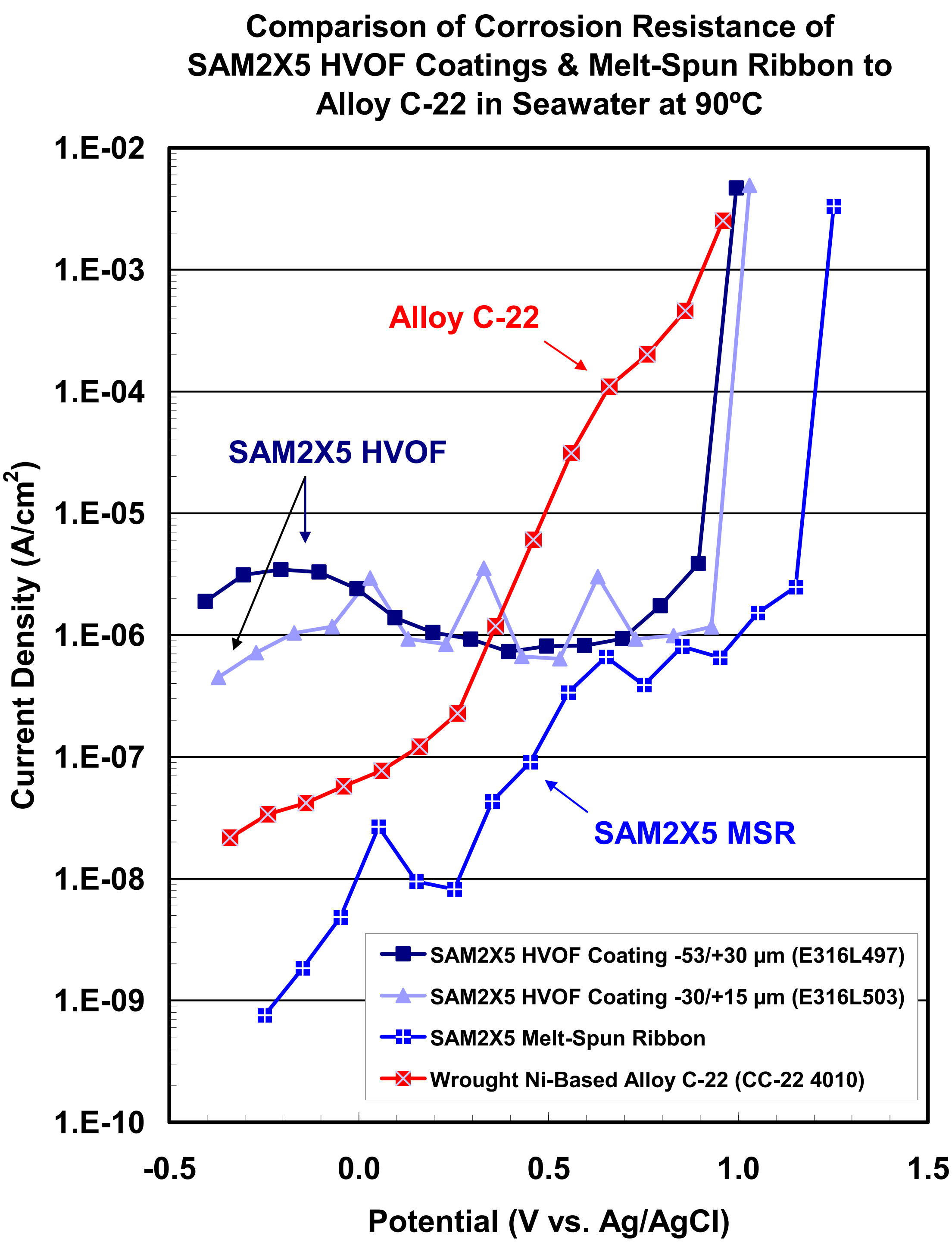

Figure 13 – Potential-step testing has been performed on wrought Alloy C-22 (reference material); fully dense and completely amorphous melt spun ribbons of SAM2X5; optimized HVOF coatings prepared with −53/+30 micron powders of SAM2X5; and optimized HVOF coatings prepared with −30/+15 micron powders of SAM2X5. All were tested in natural seawater heated to 90°C.

Thermal-Aging Effects on Corrosion

To assess the sensitivity of these iron-based amorphous metals to devitrification, which can occur at elevated temperature, melt-spun ribbon (MSR) samples of the parent alloy, SAM2X5 ($Fe_{52.3}Mn_2Cr_{19}Mo_{2.5}W_{1.7}B_{16}C_4Si_{2.5}$), were intentionally devitrified by annealing them at 150, 300, 800 and 1000°C for one hour. The full polarization curves for the samples annealed at 150 and 800°C are shown in Figure 14, while the forward scans for all samples are shown in Figure 15. These samples were then evaluated in natural seawater at 90°C with cyclic polarization, to determine the impact of annealing on passive film stability and corrosion resistance. Untreated (as received) ribbons were also tested, and provided insight into the baseline performance. The cyclic polarization curves for the as-received sample and the samples annealed at 150-300°C exhibited only slight hysteresis, with no obvious change in the formal repassivation potential with annealing temperature. However, samples annealed at 800-1000°C, well above the crystallization temperature of ~623°C (Table III), showed large hysteresis loops, and a dramatic lowering of the formal repassivation potential. Similar results were obtained with melt spun ribbons of $Fe_{49.7}Cr_{17.7}Mn_{1.9}Mo_{7.4}W_{1.6}B_{15.2}C_{3.8}Si_{2.4}$ (SAM2X5). The operational limit for these materials may be bounded by either the glass transition or crystallization temperature.

The anodic branches of cyclic polarization curves (forward scans) for a wrought sample of Alloy C-22, a MSR sample of SAM2X5, and an HVOF coating of SAM2X5, all tested in natural seawater at 90°C, are shown in Figure 16. In general, the measured current densities for iron-based amorphous-metal coatings in heated seawater were less than those measured for wrought samples of Alloy C-22, indicating better passivity of HVOF SAM2X5 coatings in this particular environment. The distinct anodic oxidation peaks for Alloy C-22 and the SAM2X5 MSR, and the faint peak for the SAM2X5 thermal spray coating, are all believed to be due to the oxidation of molybdenum (Mo).

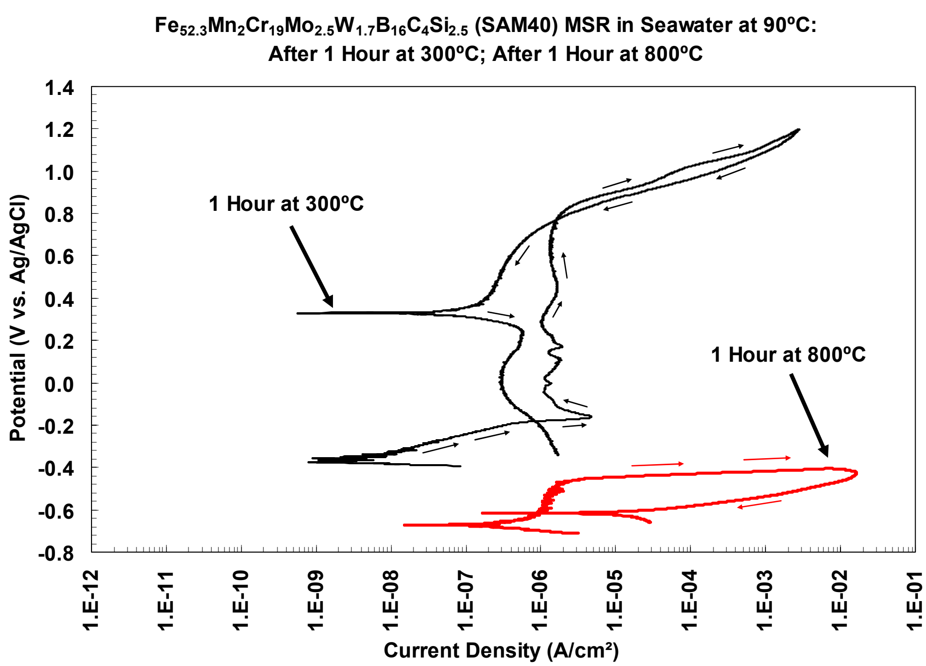

Figure 14 – Cyclic polarization of SAM40 ($Fe_{52.3}Mn_2Cr_{19}Mo_{2.5}W_{1.7}B_{16}C_4Si_{2.5}$) melt-spun ribbons in natural seawater at 90°C, after the ribbons were annealed at various temperatures for one hour. Annealing temperatures were 150, 300, 800 and 1000°C, with the curves for 300 and 800°C shown.

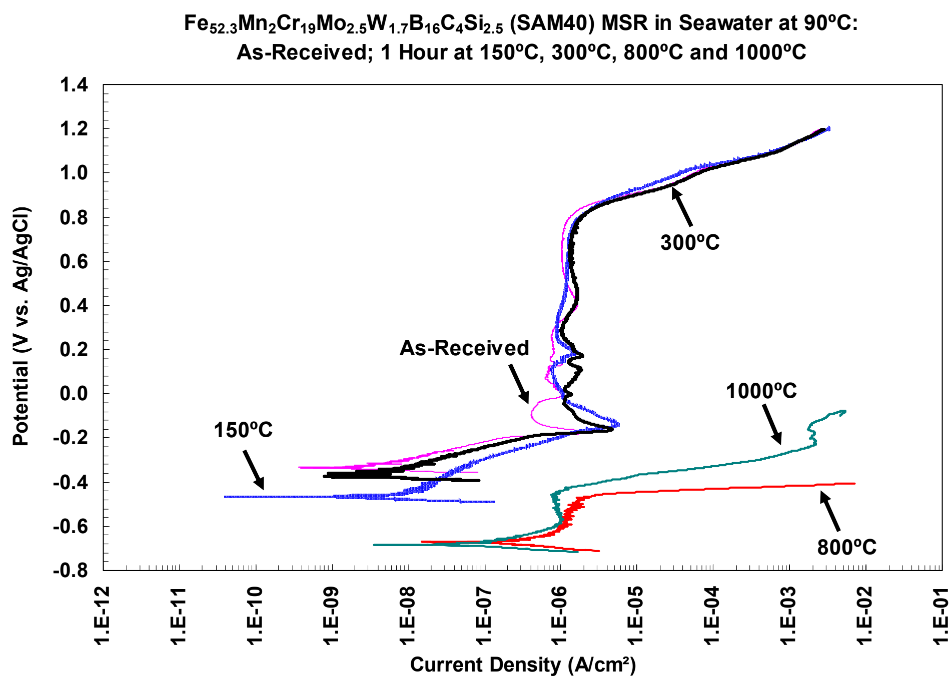

Figure 15 – Anodic branches (forward scans) of cyclic polarization curves for SAM40 ($Fe_{52.3}Mn_2Cr_{19}Mo_{2.5}W_{1.7}B_{16}C_4Si_{2.5}$) melt-spun ribbons in natural seawater at 90°C, after the ribbons were annealed at various temperatures for one hour. Annealing temperatures were 150, 300, 800 and 1000°C.

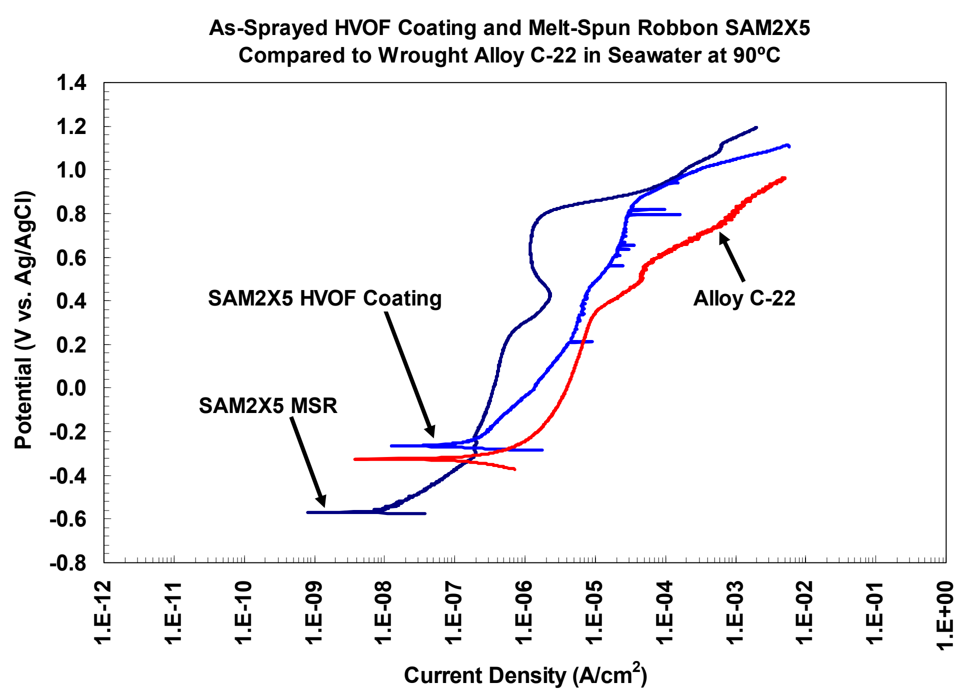

Figure 16 – This figure shows the anodic branches of cyclic polarization curves (forward scans) for a wrought sample of Alloy C-22, a MSR sample of SAM2X5, and an HVOF coating of SAM2X5 on Type 316L stainless steel, all tested in natural seawater at 90°C.

Solutions Used for Long-Term Immersion Tests

Ground water in the proposed repository at Yucca Mountain has been classified in three general categories, depending upon the terminal compositions that evolve during evaporative concentration: These categories include: calcium chloride; sulfate chloride; and bicarbonate. In general, the calcium choride brines are the most aggressive, and the bicarbonate brines are the least aggressive. As shown in Figure 17, compositions of groundwater samples taken from Yucca mountain fall into all categories. Standardized test solutions have therefore been developed which also fall into each ground water category. These synthetic brines were based upon concentrated J-13 well water, and are known as simulated dilute water (SDW), simulated concentrated water (SCW), and simulated acidic water (SAW) [23-27]. The natural seawater used in these tests was obtained directly from Half Moon Bay along the northern coast of California.

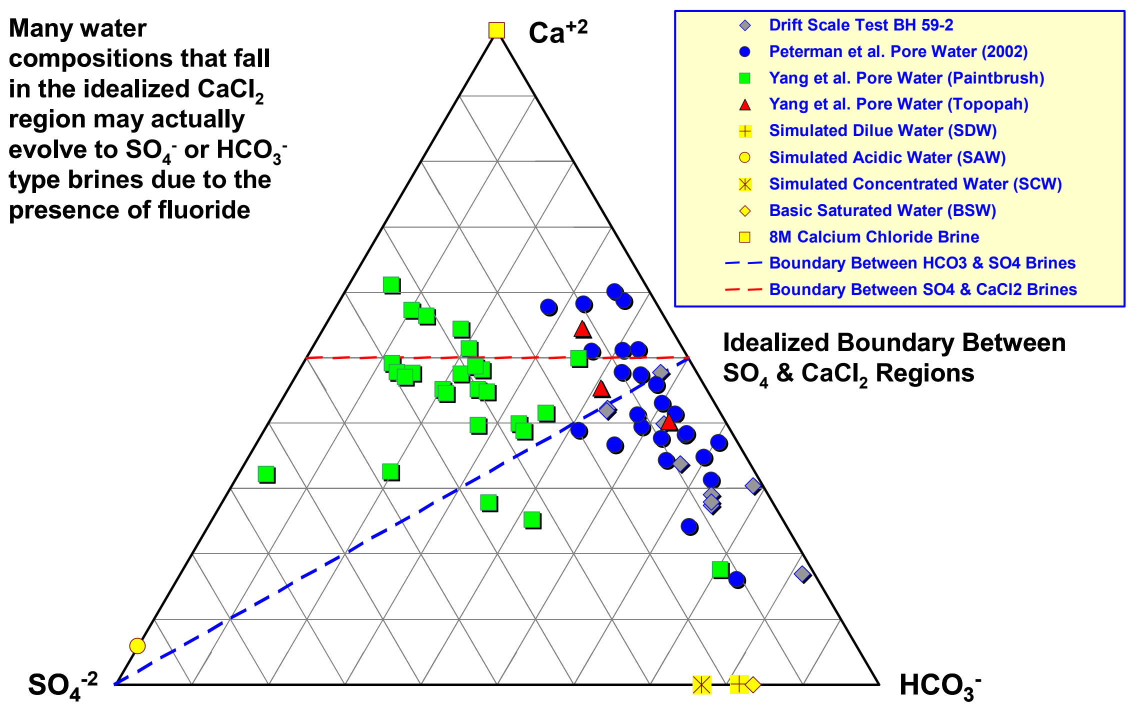

Figure 17 – Ground water in the proposed underground repository at Yucca Mountain has been classified as calcium chloride brine; sulfate-chloride brine, or bicarbonate brine.

Corrosion Rates – Linear Polarization Rates

Linear polarization was used to determine the approximate corrosion rates of the thermal spray coatings of amorphous metals of interest (HVOF SAM2X5 and other coatings) seven relevant environments including: seawater at 90°C; 3.5-molal NaCl solution at 30 and 90°C; 3.5-molal NaCl solution with 0.525-molal KNO_3 at 90°C; and SDW, SCW and SAW at 90°C. Figure 18 shows values of the linear-polarization corrosion rate (LPCR) values for SAM2X5 coating samples during immersion in seven different brines over period of approximately 135 days (the last linear polarization measurement made after 133 days). These samples were produced by depositing Lot #06-015 powder on Ni-based Alloy C-22 substrates with a hydrogen-fueled high-velocity oxy-fuel (HVOF) process. In the case of the LPCR and OCP measurements, the Alloy C-22 substrates were cylindrical rods, each having one hemispherical tip, with SAM2X5 deposited on the outer diameters of the rods, as well as over the entire surface of the hemispherical tip. The nominal length and diameter of each rod were 8 and 5/8 inches, respectively. The coating thickness was approximately 17 ± 2 mils. Test environments were: (1) natural seawater at 90°C; (2) 3.5-molal NaCl solution at 30°C; (3) 3.5-molal NaCl solution at 90°C; (4) 3.5-molal NaCl and 0.525-molal KNO_3 solution at 90°C; (5) simulated dilute water, referred to as SDW, at 90°C; (6) simulated concentrated water, referred to as SCW, at 90°C; and (7) simulated acidic water, referred to as SAW, at 90°C. After more than four months exposure, the LPCR values for these coatings in the seven test solutions were: (1) 12.3 μm/yr; (2) 2.91 μm/yr; (3) 176 μm/yr; (4) 2.83 μm/yr; (5) 2.61 μm/yr; (6) 12.4 μm/yr; and (7) 81.1 μm/yr, respectively. Clearly, the greatest electrochemical activities, which were quantified in terms of the measured LPCR values, were observed in 3.5-molal NaCl solution and SAW, both at 90°C, with the SAW having an acidic pH. The next highest LPCR values were observed in natural seawater and SCW, both at 90°C with near-neutral pH. Not surprisingly, the lowest LPCR values were observed in 3.5-molal NaCl solution and SDW, both at 30°C with near-neutral pH, as well as in 3.5-molal NaCl and 0.525-molal KNO_3 solution at 90°C. The nitrate inhibitor reduced the LPCR value observed in 3.5-molal NaCl solution from 176 to 2.83 μm/yr, nearly two orders-of-magnitude. The bar chart shown in the following figure summarizes these trends in corrosion rate graphically.

Figure 19 shows values of the OCP for SAM2X5 coating samples during immersion in seven different brines over period of approximately 135 days. These samples were produced by depositing Lot #06-015 powder on Ni-based Alloy C-22 substrates with a hydrogen-fueled high-velocity oxy-fuel (HVOF) process. In the case of the OCP and LPCR measurements, the Alloy C-22 substrates were cylindrical rods, each having one hemispherical tip, with SAM2X5 deposited on the outer diameters of the rods, as well as over the entire surface of the hemispherical tip. The nominal length and diameter of each rod were 8 and 5/8 inches, respectively. The coating thickness was approximately 17 ± 2 mils. Test environments were: (1) natural seawater at 90°C; (2) 3.5-molal NaCl solution at 30°C; (3) 3.5-molal NaCl solution at 90°C; (4) 3.5-molal NaCl and 0.525-molal KNO_3 solution at 90°C; (5) simulated dilute water, referred to as SDW, at 90°C; (6) simulated concentrated water, referred to as SAW, at 90°C; and (7) simulated acidic water, referred to as SAW, at 90°C.Corrosion Rates – Weight-Loss & Dimensional Measurements

Weight-loss and dimensional measurements were used to determine the corrosion rates of SAM2X5 coatings (Lot # 06-015 powder) on Alloy C-22 weight-loss samples, as shown in Figure 20. Depending upon the assumed coating density, these rates were determined to be: (1)

14.3-15.9 μm/yr in natural seawater at 90°C; (2) 8.4-9.3 μm/yr in 3.5-molal NaCl solution at 30°C; (3) 26.1-29.7 μm/yr in 3.5-molal NaCl solution at 90°C; (4) 4.6-5.1 μm/yr in 3.5-molal NaCl and 0.525-molal KNO_3 solution at 90°C; (5) 8.3-9.4 μm/yr in SDW at 90°C; (6) 2.8-3.0 μm/yr in SCW at 90°C; and (7) 16.5-18.1 μm/yr in SAW at 90°C. In the case of 3.5-molal NaCl solution at 90°C, the electrochemical measurement over predicted the actual corrosion rate determined with weight loss and dimensional measurements by a factor of about six (×6). In the case of SAW at 90°C, the electrochemical measurement also over predicted the actual corrosion rate determined with weight loss and dimensional measurements, this time by a factor of about five (×5). While electrochemical measurements such as linear polarization could be used to determine qualitative trends in corrosion rates during these long-term immersion tests, absolute values in the most aggressive electrolytes were over predicted by a factor of five-to-six (×5 to ×6). In contrast, the corrosion rates determined with linear polarization proved to be non-conservative in the more benign electrolytes, and under predicted the actual corrosion rates by a factor of about two-to-three (×2 to ×3). Linear polarization is a beneficial method for determining qualitative trends in corrosion rate in real time, but cannot measure corrosion rates accurately enough for reliable long-term prediction.

Weight-loss and dimensional measurements were used to determine the corrosion rates of SAM2X5 coatings (Lot # 06-015 powder) on Alloy C-22 crevice-corrosion samples after 135 days immersion, as shown in Figure 21. Depending upon the assumed coating density, these rates were determined to be: (1) 14.7-17.3 μm/yr in natural seawater at 90°C; (2) 8.8-9.9 μm/yr in 3.5-molal NaCl solution at 30°C; (3) 28.8-32.5 μm/yr in 3.5-molal NaCl solution at 90°C; (4) 4.2-4.3 μm/yr in 3.5-molal NaCl and 0.525-molal KNO_3 solution at 90°C; (5) 8.2-9.5 μm/yr in SDW at 90°C; (6) 2.7-3.2 μm/yr in SCW at 90°C; and (7) 19.7-22.5 μm/yr in SAW at 90°C. In the case of 3.5-molal NaCl solution at 90°C, the electrochemical measurement over predicted the actual corrosion rate determined with weight loss and dimensional measurements by a factor of about six (×6). In the case of SAW at 90°C, the electrochemical measurement also over predicted the actual corrosion rate determined with weight loss and dimensional measurements, this time by a factor of about five (×5). While electrochemical measurements such as linear polarization could be used to determine qualitative trends in corrosion rates during these long-term immersion tests, absolute values in the most aggressive electrolytes were over predicted by a factor of five-to-six (×5 to ×6). In contrast, the corrosion rates determined with linear polarization proved to be non-conservative in the more benign electrolytes, and under predicted the actual corrosion rates by a factor of about two-to-three (×2 to ×3). Linear polarization is a beneficial method for determining qualitative trends in corrosion rate in real time, but cannot measure corrosion rates accurately enough for reliable long-term prediction.

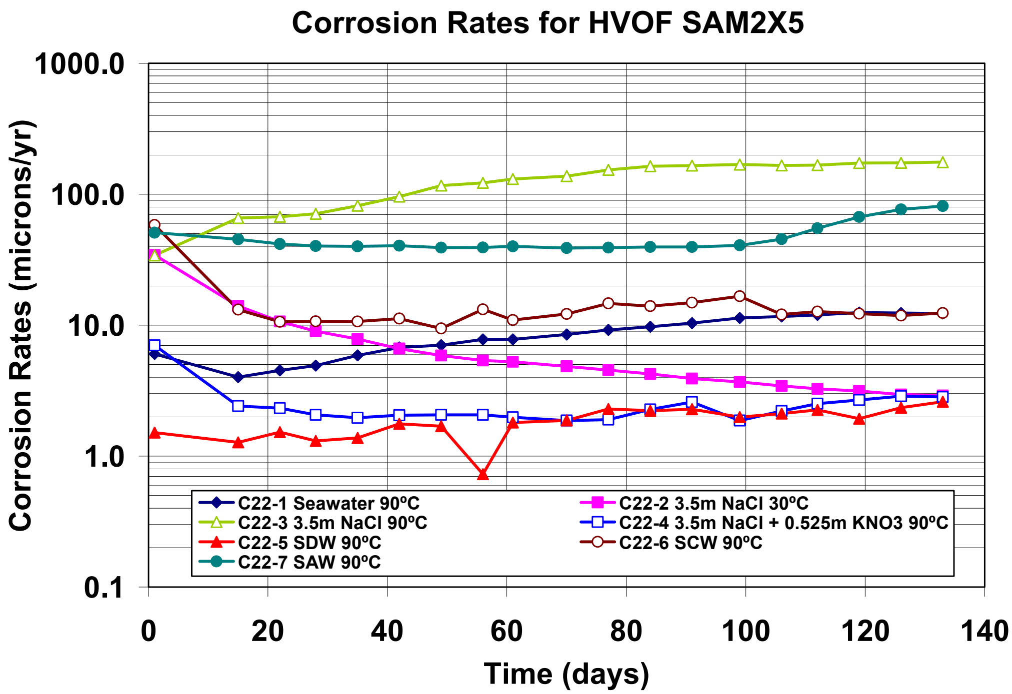

Figure 18 – Apparent corrosion rates of SAM2X5 coatings (powder lot # 06-015 powder) on Alloy C-22 rods during immersion in seven different brines over period of approximately 135 days, as determined with linear polarization.

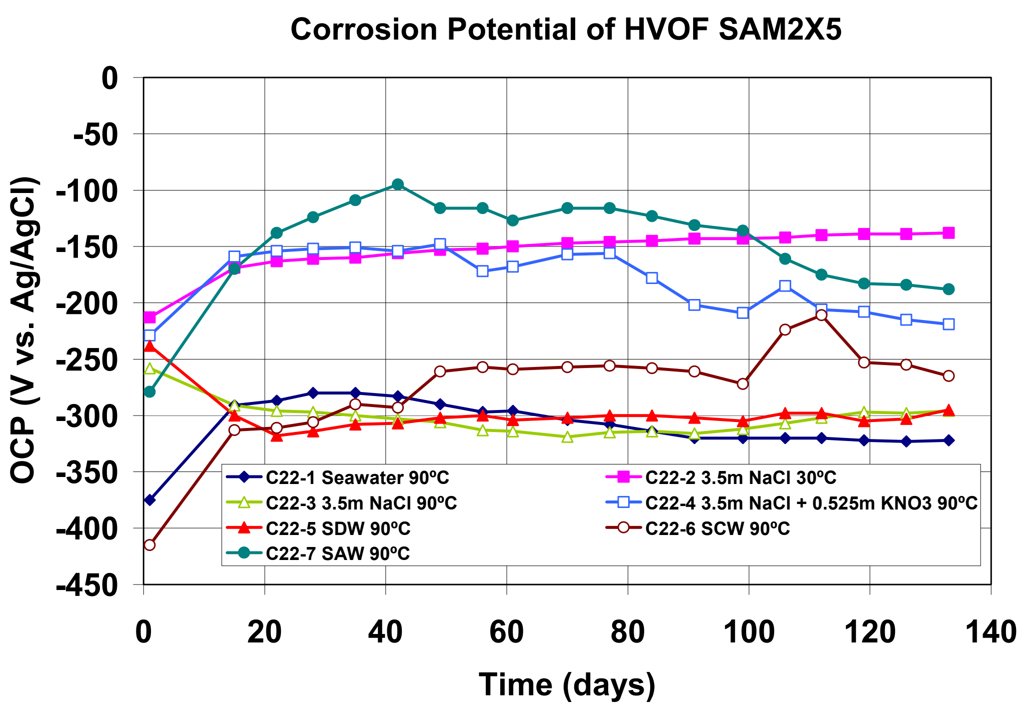

Figure 19 – OCP values of SAM2X5 coatings (powder lot # 06-015 powder) on Alloy C-22 rods during immersion in seven different brines over period of approximately 133 days.

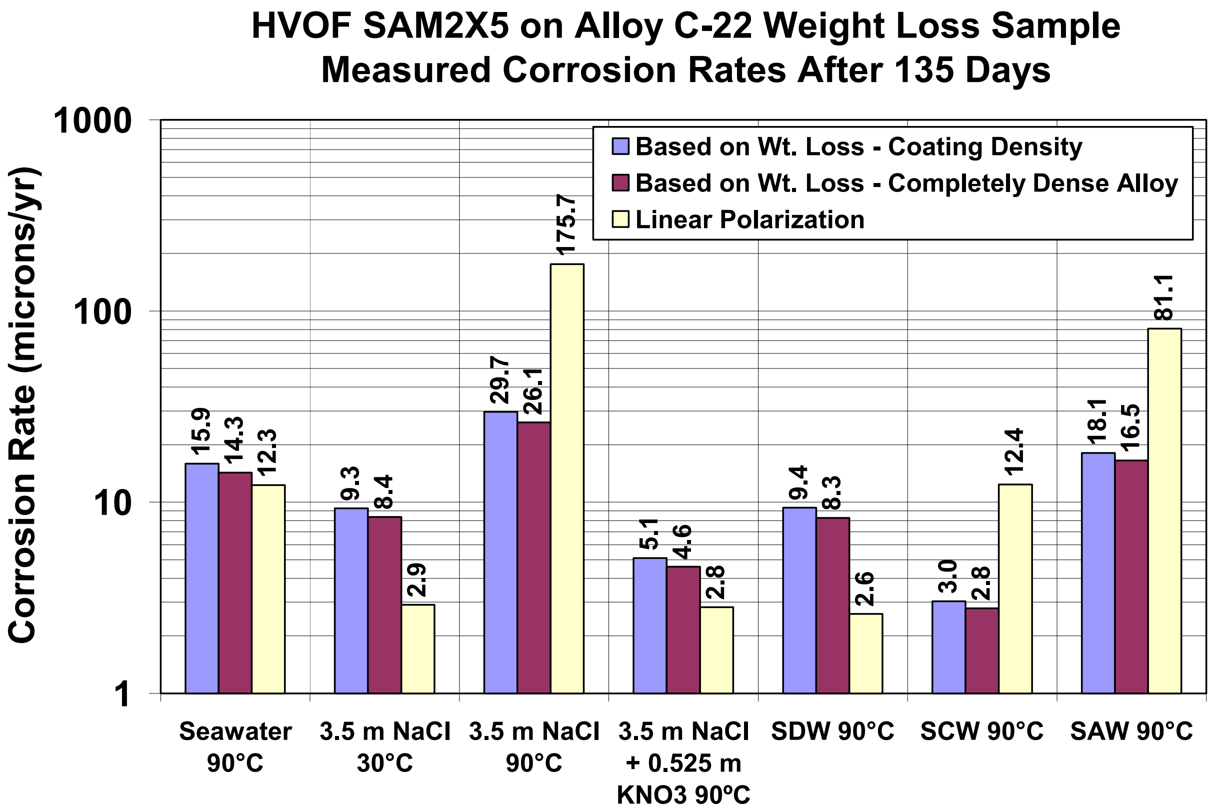

Figure 20 – After 135 days immersion, weight loss and dimensional measurements were used to determine the corrosion rates of SAM2X5 coatings on Alloy C-22 weight-loss samples. Depending upon the assumed coating density, these rates were determined to be: (1) 14.3-15.9 μm/yr in natural seawater at 90°C; (2) 8.4-9.3 μm/yr in 3.5-molal NaCl solution at 30°C; (3) 26.1-29.7 μm/yr in 3.5-molal NaCl solution at 90°C; (4) 4.6-5.1 μm/yr in 3.5-molal NaCl and 0.525-molal KNO_3 solution at 90°C; (5) 8.3-9.4 μm/yr in SDW at 90°C; (6) 2.8-3.0 μm/yr in SCW at 90°C; and (7) 16.5-18.1 μm/yr in SAW at 90°C.

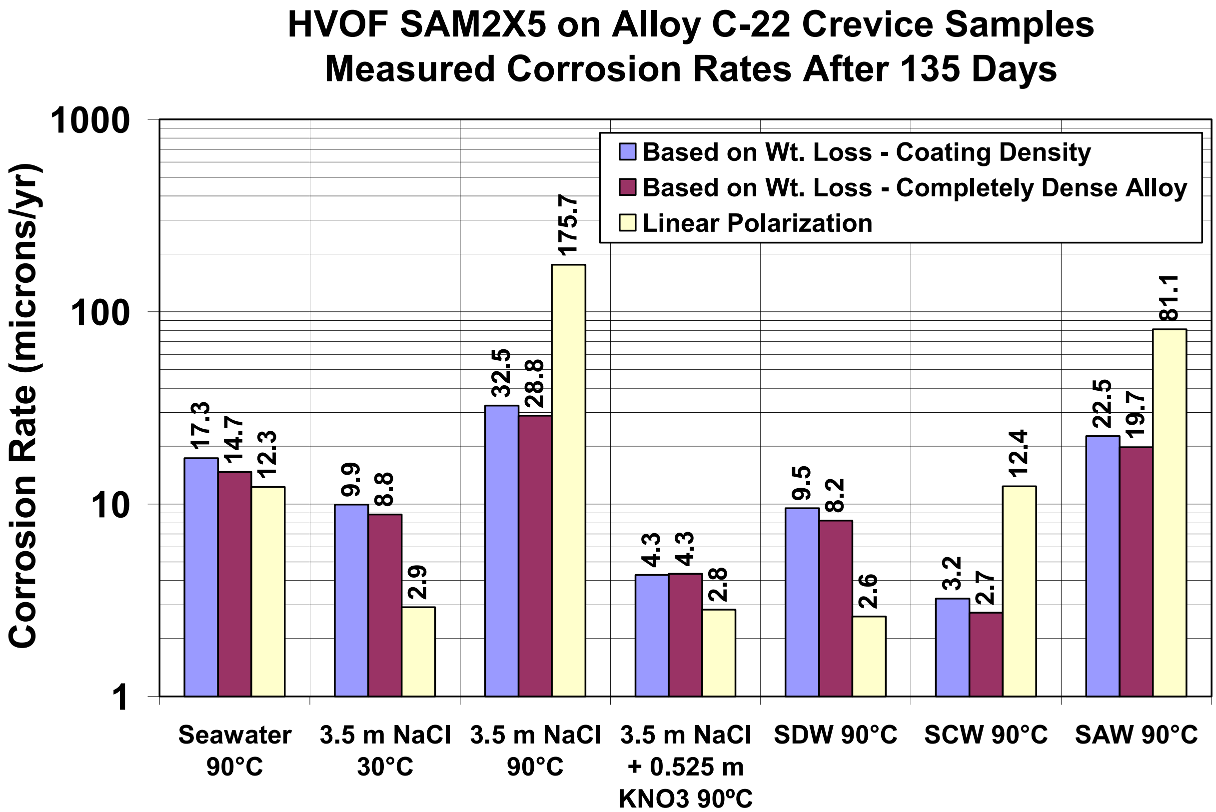

Figure 21 – After 135 days immersion, weight loss and dimensional measurements were used to determine the corrosion rates of SAM2X5 coatings on Alloy C-22 crevice-corrosion samples. Depending upon the assumed coating density, these rates were determined to be: (1) 14.7-17.3 µm/yr in natural seawater at 90°C; (2) 8.8-9.9 µm/yr in 3.5-molal NaCl solution at 30°C; (3) 28.8-32.5 µm/yr in 3.5-molal NaCl solution at 90°C; (4) 4.2-4.3 µm/yr in 3.5-molal NaCl and 0.525-molal KNO_3 solution at 90°C; (5) 8.2-9.5 µm/yr in SDW at 90°C; (6) 2.7-3.2 µm/yr in SCW at 90°C; and (7) 19.7-22.5 µm/yr in SAW at 90°C.

Corrosive attack of the SAM2X5 coating after immersion for 135 days in SDW, SCW and SAW at 90°C is characterized as non-existent to light, with the possibility of hydrogen absorption and cracking at very low pH. SAM2X5-coated weight-loss and crevice samples immersed in SDW showed no evidence of corrosion, and only slight discoloration. Identical samples immersed in SCW and SAW showed no significant corrosion, and only slight discoloration. However, in the low-pH SAW environment, an array of fine cracks was observed in the center of all weight-loss samples, with corrosion products inside the crack. Since this type of cracking was only observed with acidic solutions, it is believed that the cracking may be due to the coating's absorption of hydrogen near the cracks. The galvanic coupling of the anodic oxidation of metal within the crack could drive cathodic hydrogen reduction near the cracks. The cracking observed in low-pH weight loss samples could therefore be due to hydrogen-induced cracking. SAM2X5-coated cylinders used for LPCR and OCP determination in SDW and SAW 90°C showed no discoloration or rust spots on the outer diameter (barrel), and no corrosion products at the interface between the coating and the insulating sheath. An identical cylinder used for LPCR and OCP determination in SCW 90°C showed no discoloration or rust spots on the outer diameter (barrel), but the formation of patches of rust at the interface between the coating and the insulating sheath, and a white film of salt precipitates from the rapid drying of the electrolyte during removal of the sample from the test solution.

Corrosive attack of the SAM2X5 coating after immersion for 135 days in natural seawater at 90°C is characterized as light-to-moderate. Weight-loss and crevice samples had only slight stain, with some sparse pits around the perimeter of the sample, and with the inhibitory effects of nitrate in near-boiling concentrated chloride solutions clearly evident. In this case, the SAM2X5-coated cylinder used for LPCR and OCP determination showed slight discoloration and some small rust spots on the outer diameter, but no corrosion products at the interface between the coating and the insulating sheath.

Corrosive attack of the SAM2X5 coating after immersion for 135 days in pure 3.5-molal NaCl solution without nitrate inhibitor or other ions is characterized as light-to-moderate at 30°C and moderate-to-heavy at 90°C. After immersion in 3.5-molal NaCl solution at 30°C for 135 days, SAM2X5-coated weight-loss and crevice samples had stain on the surface, with some sparse rust spots. In 3.5-molal NaCl solution at 90°C, identical samples developed heavier stain and rust spots, as would be expected at higher temperature. The SAM2X5-coated cylinder used for LPCR and OCP determination in 3.5-molal NaCl solution at 30°C showed a few sparse rust spots on the outer diameter, but no corrosion products at the interface between the coating and the insulating sheath. An identical cylinder used for LPCR and OCP determination in 3.5-molal NaCl solution at 90°C showed a dense rust spots on the outer diameter, but preferential formation of corrosion products at the interface between the coating and the insulating sheath.

Corrosive attack of the SAM2X5 coating after immersion for 135 days in 3.5-molal NaCl and 0.525-molal KNO_3 solution at 90°C is characterized as very light, due to the beneficial inhibitor-effect of nitrate. Weight-loss and crevice samples had only slight stain, with some sparse pits around the perimeter of the sample, and with the inhibitory effects of nitrate in near-boiling concentrated chloride solutions clearly evident. In this case, the SAM2X5-coated cylinder used for LPCR and OCP determination showed slight discoloration (some very small rust spots) on the outer diameter, but no corrosion products at the interface between the coating and the insulating sheath. These trends are illustrated with Figure 22.

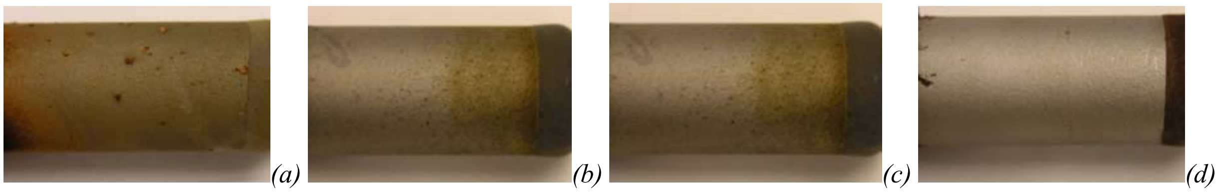

Figure 22 – Corrosive attack of barrel section of SAM2X5-coated rods after 135 days at 90°C in range of representative environments: (a) natural seawater; (b) 3.5-molal NaCl + 0.525-molal KNO3; (c) neutral SDW; and (d) acidic SAW.

Salt-Fog Performance

Early salt fog testing confirmed the corrosion resistance of the corrosion resistance of thermal spray coatings of SAM2X5 relative to other alloys with less molybdenum. As previously discussed, these coatings were deposited with the high-velocity oxy-fuel (HVOF) process, using amorphous metal powders. HVOF coatings of Type 316L stainless steel and the parent alloy, SAM40, showed significant rusting after only 13 cycles in the GM salt fog test. In contrast, HVOF coatings on nickel-based Alloy C-22 and amorphous SAM2X5 showed no obvious corrosion or rusting after more than 60 cycles.

Figure 23 shows a sample coated with SAM2X5, prepared with Lot # 06-015 powder and thermally sprayed with the JK2000 gun using hydrogen fuel, and a 1018 carbon steel control (reference) samples, after eight full cycles in the GM salt fog test. No rust was seen on these thermally sprayed amorphous metal coatings, though slight discoloration of was observed on some. In sharp contrast, severe attack of 1018 carbon steel reference samples was observed.

Figure 24 shows half-scale prototypical spent-nuclear fuel (SNF) containers, fabricated from Type 316L stainless steel, being coated with SAM1651 and SAM2X5. These prototypes were then subjected to the standard General Motors salt-fog test identified as GM9540P [11]. After eight cycles in this salt-fog test, SAM1651 and SAM2X5 coatings on the prototypical containers proved to be corrosion resistant, whereas the steel reference samples underwent aggressive attack (Figures 25 and 26). In the case of the SAM1651 coated container, some running rust was observed on one bottom of the container, which may be due to surface preparation prior to coating. Based upon these tests, it has been concluded that these new amorphous metal coatings, prepared with powders have a particle size distribution suitable for HVOF, can protect a less corrosion resistant substrate, such as steel reinforcement bars, from corrosion.

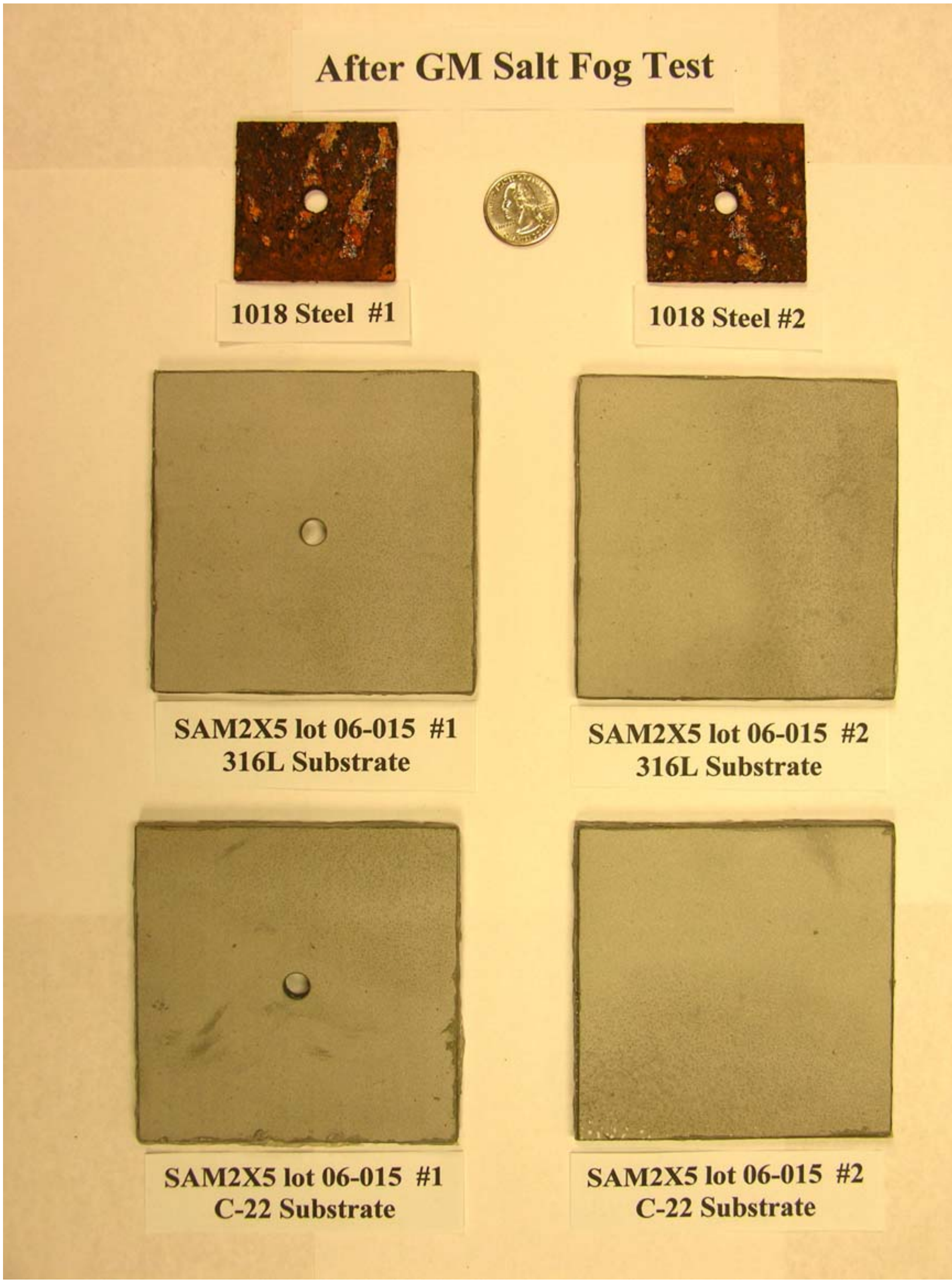

Figure 23 – {FX15} Results of salt-fog testing of SAM2X5 thermal-spray coatings and 1018 carbon steel control samples. No corrosion of the SAM2X5 coatings was observed after eight cycles, while the 1018 carbon steel samples experienced severe attack.

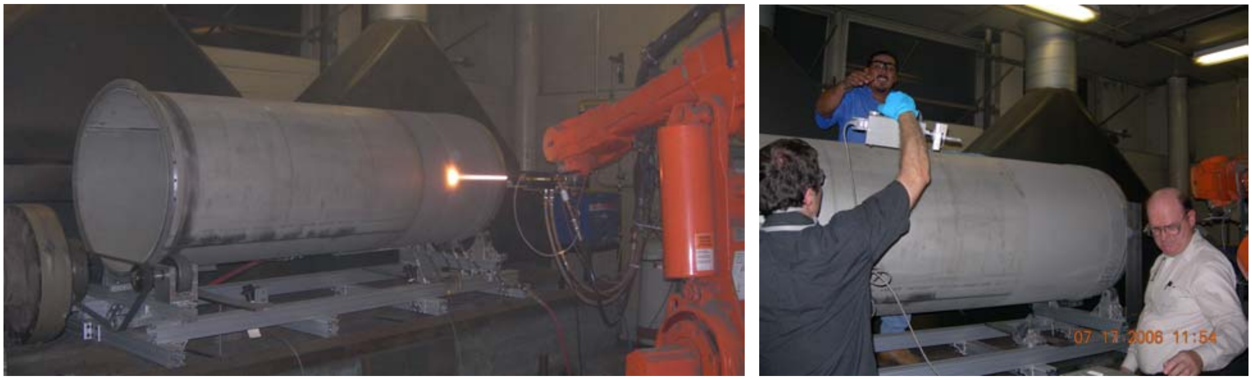

Figure 24 – High-velocity oxy-fuel process at Caterpillar used to coat half-scale containers with SAM1651 amorphous metal. The torch is shown in the left frame, and quality assurance checks of the coating thickness and roughness are shown in the right frame.

Figure 25 – Effect of GM9540P salt-fog test on HVOF coating of SAM1651 amorphous metal on half-scale SNF prototypical container (bottom center).

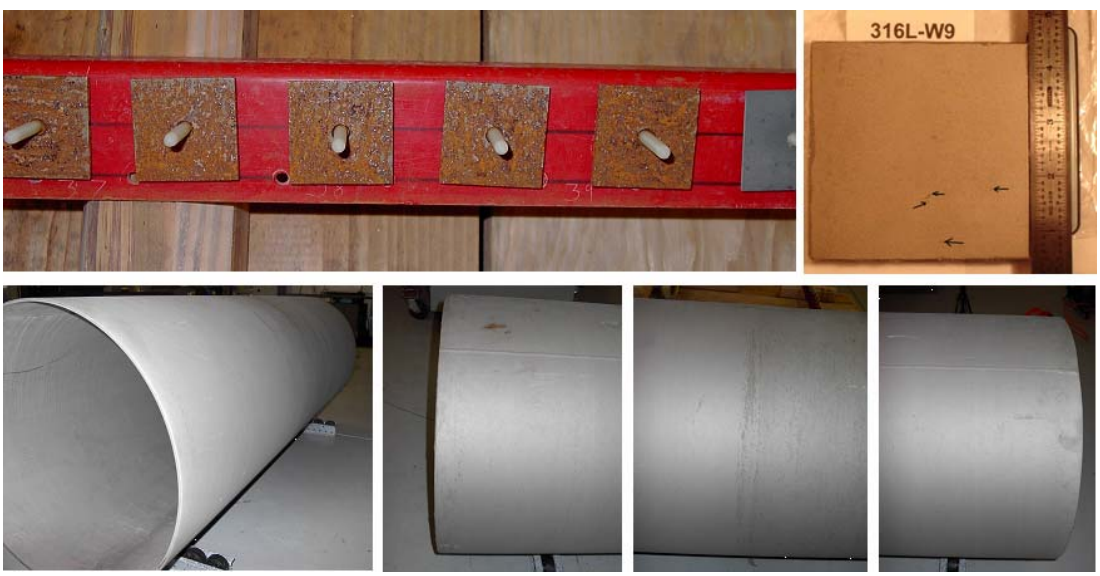

Figure 26 – Samples and prototypes after eight (8) full cycles in the GM salt fog test: [upper left] reference samples of 1018 carbon steel; [upper right] Type 316L stainless steel plate coated with Lot # 06-015 SAM2X5 powder; [lower photographs] half-scale model of spent-nuclear-fuel (SNF) container fabricated from Type 316L stainless steel pipe (Schedule 10s) coated with Lot # 06-015 SAM2X5 powder.

Formulations Exist with Potentially Better Corrosion Resistance

Other amorphous alloys may be more corrosion resistant than the SAM1651 and SAM2X5 discussed here. In addition to synthesizing these alloys, melt-spun ribbon (MSR) samples of $Fe_{43}Cr_{16}Mo_{16}B_5C_{10}P_{10}$ (SAM6) were also prepared [8]. As shown in Figure 27, while MSR samples of Alloy 22 were completed dissolved in hydrochloric acid after several-days exposure (left), MSR samples with SAM6 composition did not dissolve (right).

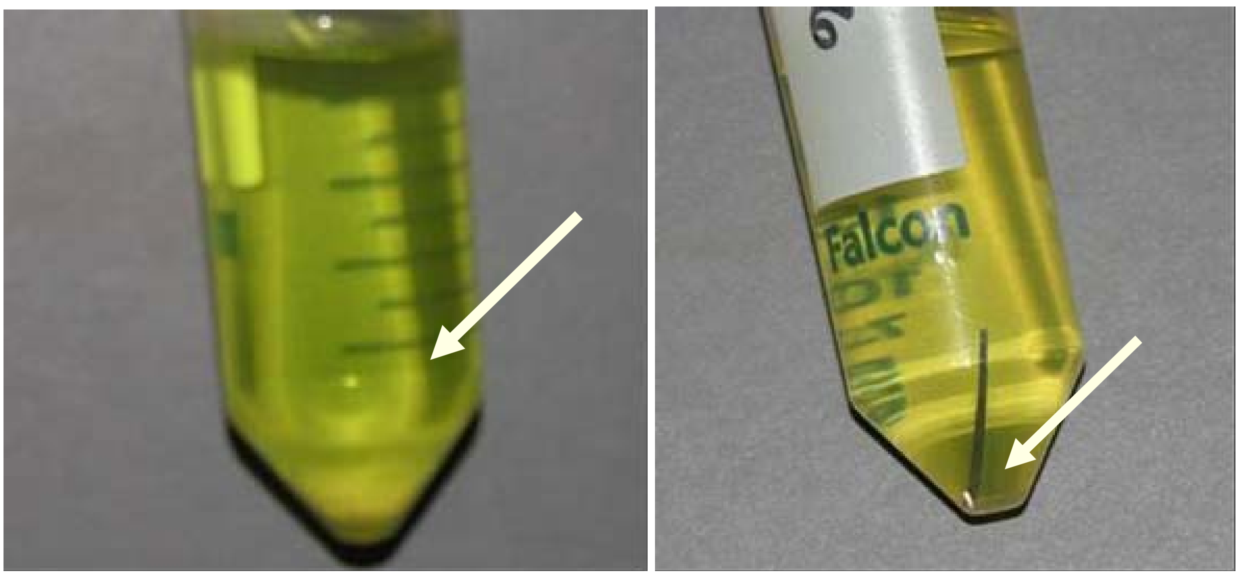

Figure 27 – Alloy C-22 dissolved in concentrated HCl (left), while a melt-spun ribbon of SAM6 remained intact for an exposure lasting several months (right). Extreme corrosion resistance is possible with iron-based amorphous metals.

Discussion

It has been recognized that the corrosion resistance of both iron- and nickel based crystalline alloys can be enhanced through the additions of Cr, Mo and W for many years [35-36]. These alloying elements also enhance the corrosion resistance of iron-based amorphous metals. While the pitting resistance equivalence number (PREN) was developed for crystalline alloys, it was used for guidance in determining maximum beneficial elemental concentrations of Cr, Mo and W used in the materials studied here. Initial calculations of the PREN for these amorphous alloys were done using formulae from the published literature.

As pointed out in the literature, an estimate of the relative pitting resistance of alloys can be made using the pitting resistance equivalence number (PREN), which is calculated using the elemental composition of the alloy [37-41]. PREN values for the Fe-based amorphous metals of interest here, and the crystalline reference materials, which include Type 316L stainless steel and Ni-based Alloy C-22, have been calculated using the following equations. Equation 8 has been used for estimating the PREN for nickel-based alloys, and accounts for the beneficial effects of Cr, Mo, W and N on corrosion resistance [37].

$$PREN = [\%Cr] + 3.3 \times [\%Mo + \%W] + 30 \times [\%N] \tag{6}$$

However, this equation was used to predict comparable corrosion resistance for Alloys C-276 and Alloy C-22, while Alloy C-22 was known to be more corrosion resistant. An equation that has been used to make reasonable predictions of the relative corrosion resistance of austenitic stainless steels and nickel-based alloys such as Alloy C-22 is [38].

$$PREN = [\%Cr] + 3.3 \times \left([\%Mo] + 0.5 \times [\%W]\right) + k \times [\%N] \tag{7}$$

The factor k is an adjustable parameter used to account for the beneficial effects of nitrogen. Reasonable values of the factor k range from 12.8 to 30, with 16 being accepted as a reasonable value [39]. Estimates presented here are based on the assumption that the value of k is 16.

PREN values calculated with Equation 7 indicated that the resistance of the SAM2X5 and SAM1651 amorphous metal formulations should be more resistant to localized corrosion than Type 316L stainless steel or nickel-based Alloy C-22. As in the case of crystalline Fe-based and Ni-based alloys, it was found experimentally that the addition of Cr, Mo, and W substantially increased the corrosion resistance of these amorphous alloys. Additional passive film stability may have been observed, which cannot be attributed to composition alone, and may be attributable to the glassy structure. Additional work is required to further understand the relative roles of composition and crystalline structure in high-performance amorphous metal coatings, such as the ones discussed here.

An obvious deficiency associated with the use of a parameter based on chemical composition alone to assess the relative corrosion resistance of both crystalline and amorphous alloys is that microstructural effects on passive film breakdown are ignored. The lack of crystalline structure is believed to be a key attribute of corrosion resistant amorphous metals.

The effect of powder size on the corrosion performance of Fe-based amorphous metal coatings was studied. Coatings prepared with coarse (-53/+30 μm) powders may have surface features more like fully dense, melt spun ribbons than did coatings prepared with relatively fine (+30/+15 μm) powders. In potential-step experiments with the application of 900, 1000, 1100, 1200, 1300 and 1400 mV vs. OCP, the passive film on coatings prepared with fine (+30/+15 μm) powders exhibited current density transients, which indicated periodic losses of passivity, with intervening periods of repassivation. Such transient were not observed with coatings prepared with coarser (-53/+30 μm) powders. The passive film on nickel-based Alloy C-22 started to destabilize at 900 mV vs. OCP, whereas passive film stability of melt-spun ribbons of SAM2X5 was maintained at an applied potential of 1500 mV and lost at 1600 mV. In the case of the thermal spray coatings of SAM2X5 prepared with relatively coarse powder, the passive film maintained stability at 1400 mV vs. OCP, but lost stability at 1500 mV. In the case of the thermal spray coatings of SAM2X5 prepared with the relatively fine powder, the onset of passive film de-stabilization was observed at 900 mV vs. OCP.

The passive film stability observed with coatings prepared with finer particles could be due to any number of phenomena, and deserves further investigation in the future. For example, any residual porosity in the coatings may have behaved like the occluded regions found within a pit or crevice, with lowered pH due to the combined effects of differential aeration, anion transport into the pores, and hydrolysis reactions involving dissolved metal species within the pores, with the production of hydrogen ions. Furthermore, the oxide film covering these occluded surfaces could be more highly defected.

The linear polarization method is widely used by the corrosion science community, and was taken directly from standardized ASTM procedures and a NACE Corrosion Engineer's Reference Book. Even so, this method is limited in that it deduces the apparent corrosion rate from a measurement of current density across the entire surface of the sample, and cannot be used to separate general and localized corrosion.

Conclusions

Several amorphous alloys with very good corrosion resistance were developoed, including SAM2X5 ($Fe_{49.7}Cr_{17.7}Mn_{1.9}Mo_{7.4}W_{1.6}B_{15.2}C_{3.8}Si_{2.4}$), SAM1651 ($Fe_{48}Mo_{14}Cr_{15}Y_{2}C_{15}B_{6}$) and SAM6 ($Fe_{43}Cr_{16}Mo_{16}B_{5}C_{10}P_{10}$). These materials were produced as melt-spun ribbons, as well as gas atomized powders and thermal-spray coatings. Chromium (Cr), molybdenum (Mo) and tungsten (W) provided corrosion resistance, and boron (B) enabled glass formation. The high boron content of this particular amorphous metal made it an effective neutron absorber, and suitable for criticality control applications. Earlier studies have shown that ingots and melt-spun ribbons of these materials have good passive film stability in these environments. Thermal spray coatings of these materials have now been produced, and have undergone a variety of corrosion testing, including both atmospheric and long-term immersion testing. The modes and rates of corrosion have been determined in the various environments, and are reported here.

The hypothesis that the corrosion resistance of iron-based amorphous metals can be enhanced through application of heuristic principles related to the additions of chromium, molybdenum, tungsten has been tested with $Fe_{49.7}Cr_{17.7}Mn_{1.9}Mo_{7.4}W_{1.6}B_{15.2}C_{3.8}Si_{2.4}$ (SAM2X5) and found to have merit. Electrochemical tests show that passive film stability superior to that of Type 316L stainless steel and comparable to that of Alloy C-22 can be achieved iron-based amorphous metals in natural seawater at 30 and 90°C. The passive film on nickel-based Alloy C-22 started to destabilize at approximately 900 mV vs. OCP. The passive films on melt-spun ribbons of SAM2X5 maintained stability at applied potentials greater than 1500 mV vs. OCP, with destabilization observed at 1600 mV.

In general, the corrosion resistance of such iron-based amorphous metals is maintained at operating temperatures up to the glass transition temperature. Thus, the upper operating temperature for such materials was concluded to be about 570°C ($T_g \approx 579$°C). Above the crystallization temperature ($T_x \approx 628$°C), deleterious crystalline phases formed, and the corrosion resistance was lost.

The passive film stability and corrosion resistance found with iron-based amorphous metals depends upon the form being tested. For example, melt-spun ribbons and ingots have been found to have better passive film stability and corrosion resistance than thermal spray coatings. No significant level of Cr_2B, WC, $M_{23}C_6$ and bcc ferrite was detected in the melt spun ribbons, whereas distinct peaks representing these crystalline phases were observed in the XRD of thermal spray coatings.

The effect of powder size on the corrosion performance of Fe-based amorphous metal coatings was studied. The volume fraction of Cr_2B, WC, $M_{23}C_6$ and bcc ferrite in the thermal spray coating depended upon the particle size distribution of the feed powder, but was not the sole determining factor in the relative corrosion resistance of the coatings. In potential-step experiments with the application of 900, 1000, 1100, 1200, 1300 and 1400 mV vs. OCP, the passive film on coatings prepared with relatively fine (+30/+15 μm) powder exhibited current density transients, which indicated periodic losses of passivity, with intervening periods of repassivation. Such transients were not observed with coatings prepared with coarser (-53/+30 μm) powder. Coatings produced with coarse (-53/+30 μm) powder behaved more like the fully dense melt spun ribbon than did the coating produced with relatively fine (+30/+15 μm) powder. Surprisingly, the coatings produced with the coarse powder, with slightly more Cr_2B, WC, $M_{23}C_6$ and bcc ferrite, had better passive film stability than the coatings produced with relatively fine powder. However, complete devitrification with the formation of much larger concentrations of these precipitates substantially diminishes corrosion resistance.

Thermal spray coatings prepared with early Type 316L stainless steel and the amorphous parent alloy, SAM40, were aggressively attacked during standardized salt fog testing. However, coatings of SAM2X5 prepared with completely amorphous powder showed no corrosion after as many as 60 cycles in standard salt fog tests.

Melt-spun ribbons of SAM2X5, and other similar iron-based amorphous metals, have better passive film stability and corrosion resistance than thermal-spray coatings, in a broad range of aggressive environments. However, the coating process for these amorphous alloys has no progressed to the point where thermal-spray coatings can be produced with corrosion resistance comparable to or better than other neutron absorbing steels, including but not limited to borated stainless steel.

Type 316L stainless-steel cylinders were coated with SAM2X5, and served as half-scale models of containers for the storage of spent nuclear fuel. SAM2X5-coated cylinders and plates were subjected to eight (8) full cycles in the GM salt fog test. No rust was observed with this thermally sprayed amorphous metal coating, while substantial attack of the 1018 carbon steel was observed. A single spot showed rust, which is an area where the coating appears to have been accidentally removed by gouging during handling. Slight discoloration was observed in a band of coating near the center of the container, and on a spot on the bottom edge of the container. Such amorphous metal coatings may therefore provide a good means for protecting less corrosion resistant surfaces.

After 133 days immersion, open-circuit potential (OCP) values for SAM2X5 coatings were determined to be (1) −322 mV in natural seawater at 90°C; (2) −138 mV in 3.5-molal NaCl solution at 30°C; (3) −296 mV in 3.5-molal NaCl solution at 90°C; (4) −219 mV in 3.5-molal NaCl and 0.525-molal KNO_3 solution at 90°C; (5) −295 mV in SDW at 90°C; (6) −265 mV in SCW at 90°C; and (7) −188 mV in SAW at 90°C. All values were measured relative to a standard Ag/AgCl reference electrode.

After 133 days immersion, linear-polarization corrosion rate (LPCR) values for SAM2X5 coatings were determined to be (1) 12.3 μm/yr in natural seawater at 90°C; (2) 2.91 μm/yr in 3.5-

molal NaCl solution at 30°C; (3) 176 μm/yr in 3.5-molal NaCl solution at 90°C; (4) 2.83 μm/yr in 3.5-molal NaCl and 0.525-molal KNO_3 solution at 90°C; (5) 2.61 μm/yr in SDW at 90°C; (6) 12.4 μm/yr in SCW at 90°C; and (7) 81.1 μm/yr in SAW at 90°C. In general, trends in LPCR values were consistent with trends in corrosion rates based upon weight-loss and dimensional change. In seawater at 90C, the LPCR values were accurate predictors of corrosion rates based upon weight-loss and dimensional change. However, the highest LPCR values, which were measured in 3.5-molal NaCl solution, SCW and SAW at 90°C, were found to be overly conservative. The lowest LPCR values, which were measured in 3.5-molal NaCl solution at 30°C, 3.5-molal NaCl solution with nitrate inhibitor at 90°C, and SDW at 90°C, were not conservative enough.

After 135 days immersion, weight loss and dimensional measurements were used to determine the corrosion rates of SAM2X5 coatings on Alloy C-22 weight-loss samples. Depending upon the assumed coating density, these rates were determined to be: (1) 14.3-15.9 μm/yr in natural seawater at 90°C; (2) 8.4-9.3 μm/yr in 3.5-molal NaCl solution at 30°C; (3) 26.1-29.7 μm/yr in 3.5-molal NaCl solution at 90°C; (4) 4.6-5.1 μm/yr in 3.5-molal NaCl and 0.525-molal KNO_3 solution at 90°C; (5) 8.3-9.4 μm/yr in SDW at 90°C; (6) 2.8-3.0 μm/yr in SCW at 90°C; and (7) 16.5-18.1 μm/yr in SAW at 90°C.

After 135 days immersion, weight loss and dimensional measurements were used to determine the corrosion rates of SAM2X5 coatings on Alloy C-22 crevice-corrosion samples. Depending upon the assumed coating density, these rates were determined to be: (1) 14.7-17.3 μm/yr in natural seawater at 90°C; (2) 8.8-9.9 μm/yr in 3.5-molal NaCl solution at 30°C; (3) 28.8-32.5 μm/yr in 3.5-molal NaCl solution at 90°C; (4) 4.2-4.3 μm/yr in 3.5-molal NaCl and 0.525-molal KNO_3 solution at 90°C; (5) 8.2-9.5 μm/yr in SDW at 90°C; (6) 2.7-3.2 μm/yr in SCW at 90°C; and (7) 19.7-22.5 μm/yr in SAW at 90°C.

Acknowledgments

This work was performed by Lawrence Livermore National Laboratory under Contract Number W-7405-Eng-48 and under the auspices of the United States Department of Energy. Work was co-sponsored by the Office of Civilian and Radioactive Waste Management (OCRWM) of the United States Department of Energy (DOE), and the Defense Science Office (DSO) of the Defense Advanced Research Projects Agency (DARPA). The guidance of Jeffrey Walker at DOE OCRWM and Leo Christodoulou at DARPA DSO is gratefully acknowledged. Recent salt-fog testing has been conducted by E-Labs in Fredericksburg, Virginia by Ken Maloy and co-workers. Several substantive scientific comments were provided by Thomas Wolery at LLNL, and served to improve this work.

Table IV – Thermal analysis data (DTA or DSC) for Fe-based glass forming alloys, including SAM2X5 ($Fe_{49.7}Cr_{17.7}Mn_{1.9}Mo_{7.4}W_{1.6}B_{15.2}C_{3.8}Si_{2.4}$), suitable for thermal spray deposition.

Alloy	T_g (°C)	T_x (°C)	T_m (°C)	T_L (°C)	T_{rg}
SAM40	568-574	623	1110	1338	0.53
SAM2X1	575	620	1124	1190-1210	0.57
SAM2X3	578	626	1131	1190-1210	0.57
SAM2X5	579	628	1133	1190-1210	0.57
SAM2X7	573	630	1137	1190-1210	0.57

PART F: STATEMENT OF WORK

1. Use of gas atomization process for the production of additional iron-based amorphous-metal powder
2. Coating of steel reinforcement bar with iron-based amorphous metal coatings
    a. SAM40 – parent alloy
    b. SAM2X5 – Mo-enhancement of parent alloy (HPCRM Program)
    c. SAM6 – P-containing formulation (inspired by work of Inoue et al.)
    d. SAM1651 – Y-containing formulation (inspired by work of Poon et al.)
    e. SAM8 – W- and Y-containing formulation
    f. Thermally sprayed rebar with epoxy coating over amorphous metal
3. Coating of steel reinforcement bar with control materials
    a. Ceramic coatings (Al_2O_3, TiO_2, ZrO_2, etc.)
    b. Type 304 and 316 Stainless Steel
    c. Ni-based Alloy C-276 or C-22
4. Embedding coated and uncoated steel reinforcement bar in concrete
5. Corrosion testing of coated and uncoated steel reinforcement bar
    a. Salt fog testing
        i. Air exposure – control sample
        ii. Spraying with salt solution representative of sea mist
    b. Immersion without encapsulation in concrete
        i. Fresh water
        ii. Fresh water equilibrated with concrete
        iii. Seawater
        iv. Seawater equilibrated with concrete
    c. Immersion after embedding in concrete
        i. Fresh water
        ii. Fresh water equilibrated with concrete
        iii. Seawater
        iv. Seawater equilibrated with concrete
6. Environmental cracking of coated and uncoated steel reinforcement bar
    a. Salt fog exposure
        i. Control samples in air
        ii. Spraying with salt solution representative of sea mist
    b. Immersion without encapsulation in concrete
        i. Fresh water
        ii. Fresh water equilibrated with concrete
        iii. Seawater
        iv. Seawater equilibrated with concrete
    c. Immersion after embedding in concrete
        i. Fresh water
        ii. Fresh water equilibrated with concrete
        iii. Seawater
        iv. Seawater equilibrated with concrete

7. Pullout test with coated and uncoated steel reinforcement bar embedded in concrete
    a. Salt fog exposure
        i. Control samples in air
        ii. Spraying with salt solution representative of sea mist
    b. Immersion after embedding in concrete
        i. Air exposure – control samples
        ii. Fresh water
        iii. Fresh water equilibrated with concrete
        iv. Seawater
        v. Seawater equilibrated with concrete
8. Burn tests
    a. Temperature profile experienced by amorphous metals
    b. Assess performance of ceramic coatings as thermal barriers
9. Documentation of results from laboratory tests
10. Establishment of standards for production and use
    a. ASME
    b. ASTM
    c. Other
11. Productization with steel reinforcement bar company
    a. Explore options
        i. Onsite coating capability
        ii. Offsite coating by sub-contractor
        iii. Selection of best options
    b. Establish production capability
    c. Pilot production of coated steel reinforcement bar
12. Design of prototypical steel reinforced concrete structures
13. Construction and testing of prototypical steel reinforced concrete structures
    a. Construction of prototypical concrete structures with coated and uncoated rebar
    b. Exposure of prototypical concrete structure to marine environment
    c. Destructive testing of structures
    d. Characterization of debris from destructive tests
14. Documentation of results from pilot-scale testing

PART G: SCHEDULE, MILESTONES & EVALUATION METRICS

1.	Powder Production – Prototypical	FY08	Month 1 to 2
2.	Thermal Spray Coating of Rebar – Prototypical	FY08	Month 2 to 4
	a. SAM40		
	b. SAM2X5		
	c. SAM6		
	d. SAM1651		
	e. SAM8		
	f. Epoxy Over Each Amorphous Metal		
3.	Coating of Rebar Control Samples	FY08	Month 4 to 6
	a. Ceramic		
	b. Stainless Steel		
	c. Ni-Cr-Mo Alloy		
4.	Embedding Coated Rebar in Concrete	FY08	Month 6 to 7
5.	Corrosion Test	FY08	Month 7 to 12
	a. Salt Fog		
	b. Immersion – No Concrete		
	c. Immersion – Embedded in Concrete		
	d. UCRL Report Documenting Corrosion Test		
6.	Environmental Cracking	FY08	Month 7 to 12
	a. Salt Fog		
	b. Immersion – No Concrete		
	c. Immersion – Embedded in Concrete		
7.	Pullout Testing	FY08	Month 7 to 12
	a. Salt Fog		
	b. Immersion – Embedded in Concrete		
8.	Fire Tests	FY09	Month 1 to 3
	a. Amorphous Metal Coatings		
	b. Ceramic Coating		
9.	Final Report with All Laboratory Test Results	FY09	Month 1 to 3
10.	Standards for Production & Use	FY09	Month 3 to 6
11.	Initial Commercialization of Rebar Coating Process	FY09	Month 3 to 6
12.	Design of Prototypical Structures	FY09	Month 3 to 6
13.	Construction and Testing of Prototypical Structures	FY09	Month 6 to 10
14.	Detailed Forensic Analysis of All Results	FY10	Month 10 to 11
15.	Final Report with All Pilot-Scale Test Results	FY10	Month 11 to 12

PART H: DELIVERABLES AND METRICS

1. Fabrication of appropriate test samples for evaluation of concept.
2. Collect production and test data for coated steel reinforcement bars to enable systematic comparison of various coating options, based on corrosion performance and economics.
   a. No coating
   b. Epoxy coating
   c. Thermal-spray coatings
      i. Ceramics
      ii. Stainless Steels
      iii. Fe-Based Amorphous Metals
      iv. Ni-Cr-Mo Alloys
      v. Ni-Based Amorphous Metals
   d. Thermal-spray coatings with epoxy coating
3. Construction and testing of concrete structures with coated steel reinforcement bars, thereby demonstrating the value of amorphous-metal coatings.

PART I: PROPRIETARTY CLAIMS

It is believed that the U.S. Government maintains intellectual property rights to inventions made during the expenditure of federal funding. All materials technology that will be employed during this proposal appear to have been developed with federal funding. Commercial entities and individuals with relevant intellectual property will be invited to participate in the proposed research, and will benefit commercially from any large-scale production of coated steel reinforcement bars. Such intellectual property does not preclude materials research and development, but could require licenses for commercialization.

An intellectual property portfolio evolved during execution of DARPA-DOE sponsored HPCRM Program. The following invention disclosures, provisional patents, and patent applications serve as a partial list of the intellectual property portfolio, and would be leveraged for the proposed work.

1. New Composities Consisteing of Amorphous Metals and Ceramic Nano-Particles, Farmer (LLNL) et al., IL-11529; Provisional Patent 60/736958, Filed November 14, 2005.
2. High-Performance Corrosion Resistant Material for Making Full-Density Pore-Free Corrosion-Resistant Thermal-Spray Amorphous-Metal Coatings with Materials with Relatively High Critical Cooling Rates, Farmer (LLNL) et al. IL-11557, S-106,896, Notification September 2, 2005; Provisional Patent 60/736793, Filed November 14, 2005.
3. High-Performance Corrosion Resistant Material: New Compositions of Corrosion-Resistant Fe-Based Amorphous Metal Suitable for Producing Thermal Spray Coatings, Farmer (LLNL) et al. IL-11558, S-106,897, Notification April 24, 2006; Provisional Patent 60/737,029, Filed November 14, 2005.
4. High-Performance Corrosion Resistant Material: Metal Ceramic Composite Coatings and Materials, Formed from Corrosion-Resistant Amorphous Metals and Ceramic Particles, Using Thermal or Cold spray Processes for Application, Farmer (LLNL) et al. IL-11559, S-106,898, Notification September 2, 2005; Provisional Patent 60/736792, Filed November 14, 2005.
5. Corrosion Resistant Neutron Absorbing Coatings, Choi (LLNL) et al., IL-11,584, S-108,232, Notification November 23, 2005; Provisional Patent 60/737026, Filed November 14, 2005.
6. Novel Amorphous Metal Formulations, Composites and Structure Coating for Corrosion and Wear Resistance, and Criticality Control in Nuclear Systems, IL-11628, S-108,274, Farmer (LLNL) et al., Notification January 19, 2006.
7. Physical and Chemical Vapor Deposition Processes for High-Performance Corrosion-Resistant Amorphous Metals, Farmer (LLNL) et al. IL-11631, S-108,282, Notification February 7, 2006.
8. The Computational Design of a High-Performance Corrosion Resistant Material (HPCRM) with Combinatorial Approaches Relying on Information from Thermochemical and Kinetic Modeling, and Expert Knowledge, Ji (LLNL) et al. IL-11632, S-108,283, Notification February 7, 2006.
9. Magnetic Separation of Devitrified Particles from Corrosion-Resistant Iron-Based Amorphous Metal Powders; Associated Magnetic-Based Methaods for QA/QC of Iron-Based Amorphous Metal Powders and Thermal Spray Coatings, Hailey (LLNL) et al. IL-11654, S-110,006, Notification April 10, 2006; Provisional Patent Submitted.
10. Enhanced Powder Flow Characteristics (of SAM1651) Through Milling, Lavernia (UCD) et al. UC Case No. 2006-172-1, Notification October 5, 2005; IL-11880, Filed September 28, 2005.

Parent alloys such as SAM27, SAM35, SAM40 and others used to make the corrosion-resistant formulations during the HPCRM Project appear to have been developed at the U.S. Department of Energy Idaho National Laboratory (INL) with federal funding.

1. U. S. Pat. 6,125,912, October 3, 2000
2. U. S. Pat. 6,767,419, November 9, 2000
3. U. S. Pat. 6,258,185, July 10, 2001
4. U. S. Pat. Appl. 20030051781, Filed March 20, 2003
5. U. S. Pat. Appl. 20050013723, Filed February 11, 2004
6. U. S. Pat. Appl. 20040141868, Filed July 22, 2004
7. U. S. Pat. Appl. 20040140021, Filed July 22, 2004
8. U. S. Pat. Appl. 20040140017, Filed July 27, 2004
9. U. S. Pat. Appl. 20040253381, Filed December 16, 2004
10. U. S. Pat. Appl. 20040250929, Filed December 16, 2004
11. U.S. Pat. Appl. 20040250926, Filed December 16, 2004

Researchers at the University of Virginia are attributed with discovering that rare earths such as yttrium lower the critical cooling rate of iron based amorphous metals. These discoveries were made with funding from DARPA DSO, and conducted as part of the Structural Amorphous Metals (SAM) Program. Prior to the HPCRM Project, no work was done on rendering these materials as thermal spray coatings, and developing an understanding of their corrosion resistance.

1. S. Joseph Poon, Gary J. Shiflet, Vijayabarathi Ponnabalam, Bulk-Solidifying High-Manganese Non-Ferromagnetic Amorphous Steel Alloys and Related Method of Using and Making the Same (University of Virginia), United States Patent 2003/0164209 A1, Filed February 11, 2003, Published September 4, 2003.
2. Z. P. Lu, C. T. Liu, W. D. Porter, Role of Yttrium in Glass Formation of Fe-Based Bulk Metallic Glasses (Oak Ridge National Laboratory), Applied Physics Letters, Volume 83, Number 13, Received May 9, 2003, Accepted August 1, 2003, Published September 29, 2003.
3. F. Guo, S. Joseph Poon, Metallic Glass Ingots Based on Yttrium, Applied Physics Letters, 83 (13) 2575-2577, September 29, 2003.
4. V. Ponnambalam, S. Joseph Poon and Gary J. Shiflet, Fe-Mn-Cr-Mo-(Y,Ln)-C-B (Ln = Lanthanides) Bulk Metallic Glasses as Formable Amorphous Steel Alloys, Journal of Materials Research, Volume 19, Number 5, p. 1320, 2004.

PART J: MANAGEMENT PLAN

This program will be managed in a manner similar to that used to manage the DARPA-DOE HPCRM Program. The work scope and deliverables will be established by the federal sponsor and the prime contractor (LLNL). Key sub-contractors (team members) will be funded through contracts issued by the procurement department at LLNL. The work of the prime contractor and key sub-contractors will be coordinated during weekly teleconferences. Brief weekly progress reports, more detailed monthly reports, and comprehensive annual reports will be required of each program participant. The budget and scheduled will be tracked, and documented with Microsoft Excel spreadsheets, and Microsoft Project Gantt charts. There will be a kick-off meeting at LLNL for all project participants, and an annual program review in either Washington, DC (close proximity to the FHWA) or in Livermore, CA (close proximity to LLNL).

PART K: TECHNOLOGY TRANSITION PLAN

The HPCRM Project was led by LLNL, and involved several industrial sub-contractors as project participants. This involvement enabled process scale-up and the production of several large-scale prototypes. Sub-contractors who may be involved in this project, based upon need, include: The NanoSteel Company (TNC), Carpenter Powder Products (CPP), Plasma Technology Incorporated (PTI); Caterpillar (CAT); and E-labs. Powder production with gas atomization may be done by TNC and CPP. Thermal spray coatings may be produced by PTI and CAT. Alloy and process design, materials characterization and testing, and project management will be done by LLNL. Any advanced deposition processes will also be done by LLNL. Salt-fog testing of large-scale prototype structures may be done in the chambers of E-Labs, located in Fredericksburg, Virginia.

PART L: FACILITIES

Facilities at LLNL that will be used for this program include:

1. Corrosion testing laboratories, with numerous potentiostats, temperature controlled electrochemical cells, long-term immersion test stations, environmental chambers, drip tests. Potentiostats are capable of performing cyclic polarization (CP), linear polarization (LP), potential-step testing (PST), and electrochemical impedance spectroscopy (EIS).
2. Environmental scanning electron-microscope, with energy dispersive analysis by X-rays (EDAX), as well as conventional and dynamic transmission electron microscope
3. X-ray diffraction
4. Various surface analytical tools including: Auger electron spectroscopy (AES, X-ray photoelectron spectroscopy (XPS), time-of-flight secondary-ion mass spectrometry (TOF-SIMS), Rutherford backscattering (RBS), and others.
5. Advanced deposition laboratories, including multi-magnetron sputter deposition, electron-beam evaporation, and others.
6. Sub-contractors have gas atomization and thermal spray capabilities, including high-velocity oxy-fuel (HVOF) deposition.

PART M: EXPERIENCE

1. Leadership of multi-institutional HPCRM Program for DOE RW and DARPA DSO, with successful development of amorphous metal coatings for DOE and DARPA sponsors.
2. Commercial-scale production of iron-based amorphous-metal powders, coatings and coated prototypes Gas atomized powders were produced by both Carpenter Powder Products and The NanoSteel Company. Coated prototypes were produced at Cateripillar Technical Center in Peoria, Illinois, Sandia Laboratories in Albuquerque, New Mexico, and Plasma Technology Incorporated in Torrance, California.
    a. Six half-scale spent nuclear fuel containers were coated, three with SAM2X5 formulation, and three with SAM1651 formulation.
    b. Two half-scale criticality control assemblies for the inside of half-scale spent nuclear fuel assemblies were als coated.
    c. Corrosion testing of half-scale prototypes and coated plates was conducted in large salt-fog chambers at E-Labs in Virginia, a laboratory involved in testing military hardware for the Navy and Marine Corps. The prototypes successfully passed the standard GM salt-fog test, whereas reference samples made of conventional steels failed.
    d. Completion of long-term immersion testing of SAM2X5 in seven relevant environments, with continuous in situ measurements of open circuit potential, linear-polarization corrosion rates, in situ characterization of the passive film with electrochemical impedance spectroscopy, followed by post-exposure rate determination with weight loss and dimensional change, as well as sample characterization.
    e. Neutron radiography and transmission measurements with coated prototypes and plates were conducted with a 1.5 megawatt TRIGA reactor at the McClellan Nuclear Radiation Center. Values of the neutron absorption cross-section in transmission (Σ_t) for several materials of interest were determined, including SAM2X5 HVOF coatings. Average values for 316L, C-22, borated stainless steel, Ni-Cr-Mo-Gd, and SAM2X5 are 1.1, 1.3, 2.3, 3.8 and 7.1 respectively. The relatively high value for SAM2X5 provides clear insight into the potential importance of this new material to the nuclear industry. Given this potential application, it should be noted that this material and its parent alloy have also been shown to remain in the amorphous state after receiving relatively high neutron dose, and after annealing at temperatures up to the glass transition temperature.
    f. As a result, DOE has told us that they plan to carry high-boron SAM2X5 as a backup criticality control material for the repository. Eventually, it could become the primary material, following the initial license application. While DOE have been given no funding for any of the projects being funded as part of this national program in FY08, we have been told by Russ Dyer, the Chief Scientist for RW, that they have every intention of re-starting the work in FY09, following the license application.
    g. DARPA has directed the Naval Research Laboratory (NRL) to continue work on the deployment of HPCRM's SAM1651 formulation as anti-skid decking for the littoral combat ships. Originally, two ships were scheduled to be built. I have recently been told that the number has been temporarily reduced to one.

PART N: KEY PERSONNEL

Joseph Farmer, Ph.D. – Chemical Engineering & Materials Science
Jeffrey Haslam, Ph.D. & P.E. – Mechanical Engineering & Materials Science
Jor-Shan Choi, Ph.D. – Nuclear Engineering
Cheng Saw, Ph.D. – Materials Science
Tiangan Lian, Ph.D. – Materials Science

PART O: QUALIFICATIONS

Joseph Collin Farmer

Lawrence Livermore National Laboratory
7000 East Avenue, Livermore, California 94550
Office 925-423-6575, Cell 925-337-1188
Email farmer4@llnl.gov

See addendum for details.

PART P: OTHER PROPOSALS

The amorphous metal coatings proposed for application to steel reinforcement bars were developed during execution of the DARPA-DSO and DOE-RW HPCRM Project, which was funded during FY03, FY04, FY05, FY06 and FY07. No further funding is anticipated, and there is no research similar to that discussed in this proposal has been submitted elsewhere. This would be the first and only funded research directed at using these novel materials for transportation infrastructure applications. While no proposal has been prepared or submitted on future research directed at the use of boron-containing amorphous metals for criticality control applications associated with the transportation and storage of the Nation's spent nuclear fuel, such research has been contemplated. However, that nuclear-related research is entirely different from that discussed here.

PART Q: BIBLIOGRAPHY

1. P. Virmani: Corrosion Costs and Preventative Strategies in the United States, Technical Brief: FHWA-RD-01-157 (Federal Highway Administration, U.S. Department of Transportation, March 2002) 17p.
2. W. H. Hartt, R. G. Powers, D. K. Lysogorski, M. Paredes, Y. P. Virmani: Job Site Evaluation of Corrosion-Resistant Alloys for Use as Reinforcement in Concrete: FHWA-HRT-06-078 (Federal Highway Administration, U.S. Department of Transportation, March 2002), 78 p.
3. M. Telford: The case for bulk metallic glass. *Materials Today*, **3,** 36-43 (2004).
4. N. R. Sorensen and R. B. Diegle: Corrosion of amorphous metals. In *Corrosion, Metals Handbook*, 9th Ed., Vol. 13, edited by J. R. Davis and J. D. Destefani (ASM Intl., Metals Park, OH, 1987), pp. 864-870.
5. D. E. Polk and B. C. Giessen: Overview of principles and applications. Chapter 1, in *Metallic Glasses*, edited by J. J. Gilman and H. J. Leamy (ASM Intl., Metals Park, OH, 1978), pp. 2-35.
6. K. Kishitake, H. Era, and F. Otsubo: Characterization of plasma sprayed Fe-10Cr-10Mo-(C,B) amorphous coatings. *J. Thermal Spray Technology*, **5** (2), 145-153 (1996).
7. S. Pang, T. Zhang, K. Asami, and A. Inoue: Effects of chromium on the glass formation and corrosion behavior of bulk glassy Fe-Cr-Mo-C-B alloys. *Materials Transactions*, **43** (8), 2137-2142 (2002).
8. S. J. Pang, T. Zhang, K. Asami, and A. Inoue: Synthesis of Fe-Cr-Mo-C-B-P bulk metallic glasses with high corrosion resistance. *Acta Materialia*, **50**, 489-497 (2002).
9. F. Guo, S. J. Poon, and G. J. Shiflet: Metallic glass ingots based on yttrium. *Metallic Applied Physics Letters*, **83** (13), 2575-2577 (2003).
10. Z. P. Lu, C. T. Liu, and W. D. Porter: Role of yttrium in glass formation of Fe-based bulk metallic glasses. *Metallic Applied Physics Letters*, **83** (13), 2581-2583 (2003).
11. V. Ponnambalam, S. J. Poon, and G. Shiflet: Fe-Mn-Cr-Mo-(Y,Ln)-C-B (Ln=Lanthanides) bulk metallic glasses as formable amorphous steel alloys. *J. Materials Research*, **19** (5), 1320, 2004.
12. D. Chidambaram, C. R. Clayton, and M. R. Dorfman: Evaluation of the electrochemical behavior of HVOF-sprayed alloy coatings. *Surface and Coatings Technology*, **176**, 307-317 (2004).
13. J. C. Farmer, J. J. Haslam, S. D. Day, D. J. Branagan, C. A. Blue, J. D. K. Rivard, L. F. Aprigliano, N. Yang, J. H. Perepezko, and M. B. Beardsley: Paper PVP2005-71664, Pressure Vessels and Piping Division Conference, Denver, CO, July 17-21, 2005 (ASME, Three Park Avenue, New York, NY, 2005).
14. J. C. Farmer, J. J. Haslam, S. D. Day, T. Lian, R. Rebak, N. Yang, and L. Aprigliano: Corrosion resistance of iron-based amorphous metal coatings. Paper PVP2006-ICPVT11-

93835, *Pressure Vessels and Piping Division Conference*, Vancouver, BC, July 23-27, 2006 (ASME, Three Park Avenue, New York, NY, 2006).
15. J. Farmer, J. Haslam, S. Day, T. Lian, C. Saw, P. Hailey, J-S. Choi, R. Rebak, N. Yang, R. Bayles, L. Aprigliano, J. Payer, J. Perepezko, K. Hildal, E. Lavernia, L. Ajdelsztajn, D. J. Branagan, and M. B. Beardsely: A high-performance corrosion-resistant iron-based amorphous metal – the effects of composition, structure and environment on corrosion resistance. Proc. Scientific Basis for Nuclear Waste Management XXX, Materials Research Society Symposium Series, Vol. 985 (MRS, Warrendale, PA, 2006).
16. T. Lian, D. Day, P. Hailey, J-S. Choi, and J. Farmer: Comparative study on the corrosion resistance of Fe-based amorphous metal, borated stainless steel and Ni-Cr-Mo-Gd alloy. Proc. Scientific Basis for Nuclear Waste Management XXX, Materials Research Society Symposium Series, Vol. 985 (MRS, Warrendale, PA, 2006).
17. D. J. Branagan, Method of modifying iron-based glasses to increase crystallization temperature without changing melting temperature. U.S. Patent Application No. 20040250929, Filed December 16, 2004 (Published by U.S. Patent and Trademark Office).
18. D. J. Branagan: Properties of amorphous/partially crystalline coatings. U.S. Patent Application No. 20040253381, Filed December 16, 2004 (Published by U.S. Patent and Trademark Office).
19. J-S. Choi, C. Lee, J. Farmer, D. Day, M. Wall, C. Saw, M. Boussoufi, B. Liu, H. Egbert, D. Branagan, and A. D'Amato: Application of neutron-absorbing structural amorphous metal coatings for spent nuclear fuel container to enhance criticality safety controls. Proc. Scientific Basis for Nuclear Waste Management XXX, Materials Research Society Symposium Series, Vol. 985 (MRS, Warrendale, PA, 2006).
20. C. K. Saw: In *X-ray Scattering Techniques for Characterization Tools in the Life Sciences, Nanotechnologies for the Life Science*, edited by Challa Kumar (Wiley-VCH Verlag GmbH and Company, KGaA, Weinheim, 2006).
21. C. K. Saw and R. B. Schwarz: Chemical short-range order in dense random-packed models. *J. Less-Common Metals*, **140**, 385-393 (1988).
22. J. Farmer, S. Lu, D. McCright, G. Gdowski, F. Wang, T. Summers, P. Bedrossian, J. Horn, T. Lian, J. Estill, A. Lingenfelter, and W. Halsey: General and localized corrosion of high-level waste container in Yucca Mountain. Pressure Vessel and Piping Conference, Seattle, WA, July 23-27, 2000, In *Transportation, Storage, and Disposal of Radioactive Materials*, PVP Vol. 408 (ASME, Three Park Avenue, New York, NY, 2000), pp. 53-70.
23. K. A. Gruss, G. A. Cragnolino, D. S. Dunn, and N. Sridar: Repassivation potential for localized corrosion of alloys 625 and C22 in simulated repository environments. Paper 149, *Corrosion 98* (NACE Intl., Houston, TX, 1998).
24. Standard reference test method for making potentiostatic and potentiodynamic anodic polarization measurements. Designation G 5-94, In *1997 Annual Book of American Society for Testing and Materials Standards,* Section 3, Vol. 3.02 (ASTM, 1997), pp. 54–57.
25. Standard reference test method for making potentiostatic and potentiodynamic anodic polarization measurements. Designation G 5-87, In *1989 Annual Book of American Society for Testing and Materials Standards*, Section 3, Vol. 3.02 (ASTM, 1989), pp. 79–85.
26. Standard practice for conventions applicable to electrochemical measurements in corrosion testing. Designation G 3-89, In *1997 Annual Book of American Society for Testing and Materials Standards*, Section 3, Vol. 3.02, (ASTM, 1997), pp. 36–44.
27. Standard test method for conducting cyclic potentiodynamic polarization measurements for localized corrosion susceptibility of iron-, nickel-, or cobalt-based alloys. Designation G 61-

86, In 1997 Annual Book of American Society for Testing and Materials Standards, Section 3, Vol. 3.02 (ASTM, 1997), pp. 231–235.
28. R. S. Treseder, R. Baboian, and C. G. Munger: Polarization resistance method for determining corrosion rates. In *Corrosion Engineer's Reference Book*, 2nd Ed. (NACE Intl., Houston, TX, 1991), pp. 65-66.
29. D. A. Jones: Electrochemical kinetics of corrosion – Faraday's law. Chapter 3, in *Principles and Prevention of Corrosion*, 2nd Ed., Section 3.1.1, Equations 3-5 (Prentice Hall, Upper Saddle River, NJ, 1996), pp. 75–76.
30. A. J. Bard and L. R. Faulkner: Potentials and thermodynamics of cells – liquid junction potentials. Chapter 2, in *Electrochemical Methods, Fundamentals and Applications*, Section 2.3, Table 2.3.2, Equation 2.3.39 (John Wiley and Sons, New York, NY, 1980), p. 67, 71.
31. J. E. Harrar, J. F. Carley, W. F. Isherwood, and E. Raber: Report of the committee to review the use of J-13 well water in Nevada Nuclear Waste Storage Investigations, *UCID-21867* (LLNL, Livermore, CA, 1990).
32. G. E. Gdowski: Formulation and make-up of simulated dilute water (SDW), Low Ionic Content Aqueous Solution, *YMP TIP-CM-06, Rev. CN TIP-CM-06-0-2* (LLNL, Livermore, CA, 1997).
33. G. E. Gdowski: Formulation and Make-up of simulated concentrated water (SCW), high ionic content aqueous solution, *YMP TIP-CM-07, Rev. CN TIP-CM-07-0-2* (LLNL, Livermore, CA, 1997).
34. G. E. Gdowski: Formulation and make-up of simulated acidic concentrated water (SAW), high ionic content aqueous solution, *YMP TIP-CM-08, Rev. CN TIP-CM-08-0-2* (LLNL, Livermore, CA, 1997).
35. H. P. Hack: Crevice corrosion behavior of molybdenum-containing stainless steel in seawater. *Materials Performance*, **22** (6) 24–30 (1983).
36. A. I. Asphahani: Corrosion resistance of high performance alloys. *Materials Performance*, **19** (12) 33–43 (1980).
37. R. B. Rebak and P. Crook: Improved pitting and crevice corrosion resistance of nickel and cobalt based alloys. In *Proc. Symposium on Critical Factors in Localized Corrosion III*, 194th Meeting of the Electrochemical Society, Boston, Massachusetts, November 1-6, 1998, Vol. 98-17 (ECS, Pennington, NJ, 1999), pp. 289-302.
38. Z. Szklarska-Smialowska: Pitting resistance equivalence number, effect of alloying elements on stainless steels and Ni-base alloys. Chapter 13, in *Pitting and Crevice Corrosion* (NACE Intl., Houston, TX, 2005), p. 318-321.
39. 4. A. J. Sedriks: Introduction, pitting. Chapter 4, in *Corrosion of Stainless Steels* (J. Wiley & Sons, Inc., New York, NY, 1996), p. 111-113.
40. D. C. Agarwal and M. Kohler: Alloy 33, a new material resisting marine environment. Paper 424, *Corrosion 97* (NACE Intl., Houston, TX 1997).

C. Thornton and C. Cooper: Overmatching superalloy consumable Inco-weld, 686CPT broadens its applications to include welding super austenitic and super duplex stainless steels. In *Stainless Steel World* (KCI Publishing BV 1, 2004).

ADDENDUM: QUALIFICATIONS

Joseph Collin Farmer

Lawrence Livermore National Laboratory
7000 East Avenue, Livermore, California 94550
Office 925-423-6575, Cell 925-337-1188
Email farmer4@llnl.gov

Education

Ph.D. Chemical Engineering, University of California, Berkeley, 1979-83
B.S. Chemical Engineering, Virginia Tech, 1973-77

Work Experience

Development of new research and development programs, including conception new ideas, marketing and identification of funding, successful scientific and technical execution, management of laboratory staff and facilities, and deployment of technologies. Over the past twenty years, projects have involved management of research funding ranging from $1 million to over $20 million, with a typical responsibility being $3-5 million. Management of materials testing program with implementation of nuclear quality assurance program. Extensive data analysis, technical writing, publication & presentation.

Lawrence Livermore National Laboratory, Livermore, CA [1987-2000; 2001-2007].

- Directorate Senior Scientist, Materials & Life Sciences (CMLS), Reporting to Associate Director [2001-Present].
  - Government-sponsored battery project.
- Associate Program Leader (APL), Nuclear Science & Systems Engineering Program (NSSEP), Energy & Environment Directorate (EED) [2006-Present]
  - High Performance Corrosion Resistant Materials (HPCRM) Project [2003-2007]. Principal Investigator & Project Manager responsible for the successful development of high-performance corrosion-resistant neutron-absorbing amorphous-metal coatings that can be applied with various thermal spray processes. Leadership of multi-institutional research team which included: Sandia National Laboratory; Oak Ridge National Laboratory; Naval Research Laboratory; Naval Surface Warfare Center Carderock; University of Wisconsin Madison; Case Western Reserve University; University of California Davis; University of Nevada Reno; Caterpillar; Nanosteel; Plasma Technology; and Carpernter Powder Products. Co-Sponsored by Defense Advanced Research Projects Agency (DARPA) Defense Science Office (DSO), and Department of Energy (DOE) Office of Civilian and Radioactive Waste Management (OCRWM) Office of Chief Scientist (OCS).
  - Smart Surface Projrect [2005-2006]. Principal Investigator responsible for the successful development of multifunctional coatings with special sensing capabilities. Sponsored by DARPA DSO.
- Repository Science Program, Energy & Environment Directorate (EED) [1997-2003].
  - Chief Scientist & Acting Program Leader [2001-2004].
  - Senior Scientist & Acting Technical Area Leader [1997-2000]. Author of initial Waste Package Degradation Process Model Report (PMR – TDR-WIS-MD-000002 Rev. 0) and several of the original Analysis & Model Reports (AMRs – ANL-EBS-MD-000003 Rev. 0

and others) for proposed deep geological repository. Selection of engineering materials for spent nuclear fuel containers through testing and modeling. Defense of waste package design at national level, including numerous briefings to the Under Secretary of Energy, the Nuclear Waste Technical Review Board (NWTRB), and the Advisory Committee on Nuclear Waste (ACNW).

- Fissile Materials Disposition Program (FMDP) [1996-97].
  - Principal Investigator & Team Leader, Process Development Team.
  - Responsible for process development supporting synthesis of new glass & ceramic waste forms. Creation of ceramics processing laboratory (B241) for pressing and sintering ceramic waste forms, as well as the adaptation of induction-heated bottom-pour and tilt-pour furnaces (B231 & B332) for the production of prototypical glass waste forms.
- National Ignition Facility (NIF) Program [1996-97].
  - LDRD investigator responsible for initially fielding experiments for the selection of protective optical coatings to prevent corrosion of silver flashlamp reflectors in large laser system.
- Electrochemical Processing Group, Materials Science & Technology Division (MSTD) [1992-1999].
  - Group Leader & Principal Investigator. Responsible for organization and management of the Electrochemical Processing Group. Author of several successful proposals for DOE Office of Basic Energy Science (OBES), DoD Strategic Environmental Research and Development Program (SERDP), United States Air Force (USAF), and DARPA DSO.
  - Development and evaluation of large-scale electrochemical processes for the treatment of aqueous waste streams and water, novel thermoelectric thin-films, and models to predict the time-dependent reflectivity of large plated mirrors, accounting for atmospheric corrosion and protective optical coatings. Development of novel multi-layer thermoelectric thin films and devices for direct energy conversion and cooling (work by research team received Award for Best Paper, International Thermoelectrics Conference, 1996). Initially sponsored by DOE OBES, subsequently Sponsored by DARPA DSO.
  - Development of electrochemical process for removing ionic impurities from water, with minimal secondary wastes, using LLNL's carbon aerogel. Initially sponsored by SERDP, with subsequent sponsorship by USAF.
- Special Isotope Separation (SIS) Program & Environmental Technology Program (ETP) [1990-92].
  - Principal Investigator & Deputy Group Leader, Aqueous Processing Group.
  - Research and development of electrochemical, photochemical, and thermochemical processes for the processing and treatment of mixed wastes.
- Deep Geological Repository Program [1987-1990]. Principal Investigator. Initial materials selection for spent nuclear fuel and high-level waste containers to be placed in deep geological repository at Yucca Mountain.

PolyStor Corporation, Livermore, California [2000-2001].

- Director of Research and Development, direct reporting to the Chief Techical Officer (CTO).
- PolyStor was a spin-off of LLNL involved in the high-volume manufacture of lithium ion batteries for the wireless communications industry.
- Established advanced Li Ion Battery Materials Program. Responsible for winning, management and execution of NIST-sponsored ATP Project. Development of electrode materials with high energy density; separators, electrolytes, and additive systems for

inherently safe operation; and light, soft packaging for advanced polymer-gel lithium ion batteries. Transitioned materials concepts to production. Lead team that included Argonne National Laboratory (ANL), Illinois Institute of Technology (IIT), Minnesota Mining and Metals Corporation (3M), and others. Sponsored by National Institute of Standards and Technology (NIST) Advanced Technology Program (ATP).

- Establishment and operation of the new Analytical Services Laboratory (SEM, EDS, FTIR, HPLC, GC, UV-Visible, TGA, DSC, BET, SSRT, CV, EIS), recruitment and training of technical staff, investigation of new battery materials, and resolution of technical problems facing productization. Assisted CTO and attorneys in the legal defense of intellectual property.

Betz Corporation, Trevose, Pennsylvania, Senior Scientist [1992].

- LLNL leave-of-absence. Research in high-temperature high-pressure boiler environment. Modeling chemical additives and associated control systems used to control boiler water chemistry.

Sandia National Laboratory, Livermore, California [1983-87].

- Member of Technical Staff. Development of electroplating and electroforming processes; establishment of state-of-the-art electroanalytical laboratory. In situ studies of the electrode-electrolyte interface using AC-impedance, Raman spectroscopy and optical second harmonic generation.

Lawrence Berkeley National Laboratory & University of California, Berkeley, California 1979-83].

- Graduate Student Research & Teaching Assistant, Acting Instructor, Part-Time Staff. In situ studies of organic adsorbates on electrode surfaces (coverage, identification, orientation), determination of structure of electrodeposited films (submonolayer to 1000 Angstroms thick). Development of fast-scanning spectroscopic ellipsometer and software. Assisted in teaching separations, unit operations laboratory & optical methods for chemical engineers. Leave of absence from Union Carbide Corporation.

R&D Department, Union Carbide Technical Center, South Charleston, West Virginia [1976-78].

- Synthesis Gas (PSG) Project. Pilot Plant Engineer 1977-78. Research and development of high-pressure homogeneous catalysis as a means for the direct conversion of synthesis gas to ethylene glycol at 15-20,000 psi. Separation process development, residence time distribution studies with tracers, experimental design (design of experiment), statistical data analysis, kinetic modeling.
- Amines Project. Summer Hire 1976. Catalyst leaching studies.

Department of Chemical Engineering, Virginia Tech, Blacksburg, Virginia [1975]

- National Science Foundation Summer Fellowship. Construction of tunable dye laser for isotope separation project.

Texaco Sales and Manufacturing, Norfolk, Virginia [1974].

- Operations Trainee. Detailed training in the operations of a sales and manufacturing terminal; practical aspects of chemical engineering.

Examples of Service

- Symposium Organizer, Iron-Based Amrophous Metals – An Important Family of High-Performance Corrosion-Resistant Materials, Mateials Science & Technology 2007 Conference and Exhibition, September 16-20, 2007, COBO Center, Detroit, Michigan, Sponsored by The Minerals, Metals & Materials Society (TMS), The American Ceramic Society (ACerS), Association for Iron & Steel Technology (AIST), and ASM International.
- Defense Science Board (DSB), Task Force on Corrosion Control, Office of Secretary of Defense (2003-2004)
- Project Oversight Board, Yucca Mountain Project, Management & Operating Contractor (2002-2004)
- Expert Elicitation Panel, Yucca Mountain Project, Department of Energy (1998)
- Red Team Member, Waste Isolation Pilot Plant, Department of Energy (1992)

Honors

- 2006 Energy & Environmnent Directorate Award – Highly Successful Amorphous Metals Program
- 2000 Invited Speaker, Gordon Conference on Corrosion, Colby Sawyer College
- 2000 Energy & Environment Directorate Award – Completion of Initial PMR and AMR Reports
- 1999 Task Achievement Award – U. S. DOE CRWMS Management & Operating Contractor
- 1998 Plenary Speaker, Symposium on Electrochemical and Photochemical Methods for Chemical Recycling & Pollution Abatement, 193rd Meeting of The Electrochemical Society
- 1996 Award for Best Paper, International Thermoelectrics Conference
- 1995 R&D 100 Award
- 1990 Silver Medal Award for Outstanding Paper in Plating Surface Finish – AESF
- 1986 Norman J. Hackerman (Young Author) Award – Electrochemical Society
- 1985 Gold Medal Award Plating Surface Finish – AESF
- 1984 Boris and Renee Joffee Award for Best Paper, Interfinish '84, Jerusalem, Israel
- 1976 Sigma Xi Award for Outstanding Undergraduate Research
- 1975 NSF Summer Fellowship

Professional Memberships

- American Society of Mechanical Engineers
- Materials Research Society
- Electrochemical Society
- American Chemical Society
- American Society of Testing & Materials
  - Member of Sub-Committee C26.13
- American Electroplaters & Surface Finishers Society
  - Research Board Member, Vice-Chairman of Finances, Project Supervisor, 1986-1994

Patents

1. B. B. Ebbinghaus, R. A. Van Konynenburg, E. R. Vance, M. W. Steward, P. A. Walls, W. A. Brummond, G. A. Armantrout, C. C. Herman, B. F. Hobsohn, D. T. Herman, P. G. Curtis, J. C. Farmer, *Process for Making a Ceramic Composition for Immobilization of Actinides*, U. S. Pat. No. 6,320,091, November 20, 2001.
2. T. Tran, J. C. Farmer, L. Murguia, *Method and Apparatus for Capacitive Deionization and Electrochemical Purification, and Regeneration of Electrodes*, October 30, 2001.
3. J. C. Farmer, *Method and Apparatus for Capacitive Deionization, Electrochemical Purification, and Regeneration of Electrodes*, U. S. Pat. No. 5,954,937, September 21, 1999.
4. J. C. Farmer, R. A. Van Konynenburg, *Means for Limiting and Ameliorating Electrode Shorting*, U. S. Pat. No. 5,980,718, November 9, 1999.
5. J. C. Farmer, F. T. Wang, R. G. Hickman, P. R. Lewis, *Mediated Electrochemical Oxidation without Electrode Separators*, U.S. Pat. No. 5,516,972, May 14, 1996.
6. J. C. Farmer, *Method and Apparatus for Capacitive Deionization, Electrochemical Purification, and Regeneration of Electrodes*, U. S. Pat. No. 5,428,858, June 20, 1995.
7. W. D. Bonivert, J. C. Farmer (principal inventor), Hachman, H. T., *Measuring Surfactant Concentrations in Plating Solutions*, U.S. Pat. No. 4,812,210, Oct. 16, 1987.

Recent Provisional Patents

1. New Composities Consisteing of Amorphous Metals and Ceramic Nano-Particles, J. Farmer et al., IL-11529; Provisional Patent 60/736958, Filed November 14, 2005.
2. High-Performance Corrosion Resistant Material for Making Full-Density Pore-Free Corrosion-Resistant Thermal-Spray Amorphous-Metal Coatings with Materials with Relatively High Critical Cooling Rates, J. C. Farmer, C. A. Blue, E. J. Lavernia, J. H. Schoenung, J. J. Haslam, J. H. Perepezko, J. L. Ajdelsztajn, L. Kaufman, N. Y. Yang, IL-11557, S-106,896, Notification September 2, 2005; Provisional Patent 60/736793, Filed November 14, 2005.
3. High-Performance Corrosion Resistant Material: New Compositions of Corrosion-Resistant Fe-Based Amorphous Metal Suitable for Producing Thermal Spray Coatings, J. C. Farmer, A. Heuer, M. B. Beardsley, C. A. Blue, D. J. Branagan, E. J. Lemieux, E. J. Lavernia, F. Wong, J. J. Haslam, J. D. K. Rivard, J. H. Perepezko, L. Kaufman, L. K. Kohler, L. F. Aprigliano, N. Y. Yang, R. Bayles, IL-11558, S-106,897, Notification April 24, 2006; Provisional Patent 60/737,029, Filed November 14, 2005.
4. High-Performance Corrosion Resistant Material: Metal Ceramic Composite Coatings and Materials, Formed from Corrosion-Resistant Amorphous Metals and Ceramic Particles, Using Thermal or Cold spray Processes for Application, J. C. Farmer, C. A. Blue, E. J. Lavernia, F. Wong, J. H. Schoenung, J. L. Ajdelsztajn, J. J. Haslam, J. H. Perepezko, L. Kaufman, N. Y. Yang, O. A. Graeve, R. Bayles, IL-11559, S-106,898, Notification September 2, 2005; Provisional Patent 60/736792, Filed November 14, 2005.
5. Neutron Absorbing Coatings for Spent Nuclear Fuel (SNF) Support Structures Inside Transportation and Storage Containers – Use of Novel Coating Materials to Enhance Criticality Safety, J-S. Choi, C. K. Lee, J. Walker, J. Kirkwood, J. C. Farmer, N. Y. Yang, P. Russell, V. Champaign, IL-11584, S-108,232, Notification November 23, 2005; Provisional Patent 60/737026, Filed November 14, 2005.
6. Novel Amorphous Metal Formulations, Composites and Structure Coating for Corrosion and Wear Resistance, and Criticality Control in Nuclear Systems, J. C. Farmer, IL-11628, S-108,274, Notification January 19, 2006.

7. Physical and Chemical Vapor Deposition Processes for High-Performance Corrosion-Resistant Amorphous Metals, J. C. Farmer, C. A. Blue, J. H. Perepezko, IL-11631, S-108,282, Notification February 7, 2006.
8. The Computational Design of a High-Performance Corrosion Resistant Material (HPCRM) with Combinatorial Approaches Relying on Information from Thermochemical and Kinetic Modeling, and Expert Knowledge, X. Ji, J. J. Haslam, J. H. Perepezko, J. C. Farmer, L. Kaufman, R. B. Rebak, IL-11632, S-108,283, Notification February 7, 2006.
9. Enhanced Powder Flow Characteristics Through Milling, J. Dannenberg, E. J. Lavernia, J. C. Farmer, J. H. Schoenung, J. L. Ajdelsztajn, N. Y. Yang, IL-11660, U.C. Davis.
10. Magnetic Separation of Devitrified Particles from Corrosion-Resistant Iron-Based Amorphous Metal Powders; Associated Magnetic-Based Methaods for QA/QC of Iron-Based Amorphous Metal Powders and Thermal Spray Coatings, P. D. Hailey, J. C. Farmer, L. Kaufman, N. Y. Yang, S. D. Day, T. Devine, IL-11654, S-110,006, Notification April 10, 2006; Provisional Patent Submitted.
11. Indirect Detection of Radiation Sources via Direct Detection of Radiolysis Productts – Sensors Based Upon Redox Potential and Optical Detection, J. C. Farmer, L. E. Fischer, T. E. Felter, IL-11042, Director's Office.
12. Smart Surface & Intellicoat Coatings for Detection of Hidden Corrosion-Cracking Damage & Warning of Chemical and Radiological Attack, J. C. Farmer, IL-11524, EED.
13. Smart Surface & Intellicoat – Coatings for Detection of Radiation – Differential & Integrating Coatings, J. C. Farmer, J. L. Brunk, S. D. Day, IL-11567, EED.
14. Solid-State Rechargeable Lithium-Ion Battery with Lithium-Based Alloy Anodes, Fast-Ion Conductor Electrolyte, and Compatible Intercalation Compound (or Other) Cathodes for Unmanned and Autonomous Underwater Vehicles, J. Farmer, K. Wolf, IL-11522, CMLS.
15. Multi-Functional Armor with Energy Storage Capabilities – Capacitors with Ceramic Conduction Layer, J. Farmer & M. Finger, IL-11523.
16. Advanced Energy Conversion and Storage for Underwater Vehicles – Multifunctional Materials for Structure, Fuel Cells, Semi-Fuel Cells, Metal Air Batteries, Rechargeable Secondary Batteries, and Capacitors, J. Farmer, A. Halter, F. van Mierlo, K. Wolf, R. Brown, IL-11534, CMLS.

Publications – Electrochemical Processing

1. J. C. Farmer, R. G. Hickman, F. T. Wang, P. R. Lewis, *Mediated Electrochemical Oxidation of Ethylene Glycol*, UCRL-JC-105357 (1990); 179th Electrochem. Soc. Meeting, Washington, DC, May 5-10, 1991, Ext. Abs., Vol. 91-1, pp. 799-800, Electrochem. Soc., Pennington, NJ (1991).
2. J. C. Farmer, R. G. Hickman, F. T. Wang, P. R. Lewis, L. J. Summers, *Initial Study of the Complete Mediated Electrochemical Oxidation of Ethylene Glycol*, UCRL-LR-106479 (1991).
3. J. C. Farmer, R. G. Hickman, F. T. Wang, P. R. Lewis, L. J. Summers, *Electrochemical Treatment of Mixed and Hazardous Wastes: Oxidation of Ethylene Glycol by Ag(II)*, UCRL-JC-106947 Rev. 2 (1991).
4. J. C. Farmer, F. T. Wang, R. A. Hawley-Fedder, P. R. Lewis, L. J. Summers, L. Foils, *Electrochemical Treatment of Mixed and Hazardous Wastes: Oxidation of Benzene by Ag(II)*, UCRL-JC-107043 Rev. 2 (1991).
5. J. C. Farmer, F. T. Wang, R. A. Hawley-Fedder, P. R. Lewis, L. J. Summers, L. Foils, *Initial Study of Halide-Tolerant Mediators for the Electrochemical Treatment of Mixed and Hazardous Wastes*, UCRL-LR-107781 (1991).

6. J. C. Farmer, F. T. Wang, R. G. Hickman, R. A. Hawley-Fedder, P. R. Lewis, L. J. Summers, Foiles, L., *Mediated Electrochemical Oxidation of Hazardous and Mixed Waste*s, Section 8, Waste Processing and Management, in 1990-1991 Chemistry and Materials Science, UCRL-53943-91, 137-140 (1991).
7. J. C. Farmer, *Electrochemical Oxidation of Hazardous and Radioactive Wastes at Ambient Temperature*, in Energy and Technology Review, State of the Laboratory, July-August (1991).
8. J. F. Cooper, W. A. Brummond, J. R. Celeste, J. C. Farmer, Hoenig, C. L., Krikorian, O. H., Upadhye, R. S., Gay, R., Stewart, A., Yosim, S., *Molten Salt Processing of Mixed Wastes with Offgas Condensation*, Proc. 1991 Incineration Conf., Knoxville, TN, May 13-17, 1991 (1991).
9. R. M. Yamamoto et al., *The Design of an Electrochemical Waste Treatment System*, 179th Electrochem. Soc. Meeting, Washington, DC, May 5-10, 1991, Ext. Abs., Vol. 91-1, p. 792, Electrochem. Soc., Pennington, NJ (1991).
10. R. G. Hickman, J. C. Farmer, F. T. Wang, *Mediated Electrochemical Hazardous Waste Destruction*, Emerging Technologies for Hazardous Waste Management: 1991 Book of Abstracts for the Special Symposium, Atlanta, GA, Oct. 1-3, 1991, pp. 349-351, Indust. Eng. Chem. Div., Am. Chem. Soc., Washington, DC (1991).
11. J. C. Farmer, F. T. Wang, R. A. Hawley-Fedder, P. R. Lewis, L. J. Summers, L. Foils, *Electrochemical Treatment of Mixed and Hazardous Wastes: Oxidation of Ethylene Glycol and Benzene by Silver(II)*, J. Electrochem. Soc., Vol. 139, No. 3, pp. 654-662 (1992).
12. J. C. Farmer, F. T. Wang, P. R. Lewis, L. J. Summers, *Electrochemical Treatment of Mixed and Hazardous Wastes: Oxidation of Ethylene Glycol by Cobalt(III) and Iron(III)*, Transactions of the Institute of Chemical Engineering, Vol. 70 B, pp. 158-164 (1992).
13. J. C. Farmer, F. T. Wang, P. R. Lewis, L. J. Summers, *Destruction of Chloriinated Organics by Cobalt(III)-Mediated Electrochemical Oxidation*, J. Electrochem. Soc., Vol. 139, No. 11, pp. 3025-3029 (1992).
14. R. G. Hickman, J. C. Farmer, F. T. Wang, *Mediated Electrochemical Process for Hazardous Waste Destruction*, Chapt. 21, in Emerging Technologies in Hazardous Waste Management III, D. William Tedder, Frederick G. Pohland, Eds., ACS Symposium Series 518, American Chemical Society, Washington, DC, pp. 430-438 (1993).
15. J. C. Farmer, *Electrochemical Treatment of Mixed and Hazardous Wastes*, Environmental Oriented Electrochemistry, C. A. C. Sequeira, Ed., Elsevier Science Publishers B. V., Amsterdam, The Netherlands, Studies in Environmental Science, Series 59, pp. 565-598 (1994).
16. J. C. Farmer, Z. Chiba, *Fundamental Studies of the Mediated Electrochemical Oxidation of Wastes*, Proc. Symposium on Water Purification by Photocatalytic, Photoelectrochemical, and Electrochemical Processes, 185th Electrochem. Soc. Meeting, San Francisco, CA, May 22-27, 1994, T. L. Rose, O. Murphy, E. Rudd, B. E. Conway, Eds., Electrochem. Soc., Pennington, NJ, Vol. 94-19, pp. 144-151 (1994).
17. J. C. Farmer, D. V. Fix, R. G. Hickman, V. M. Oversby, M. G. Adamson, *Regeneration of Acids and Bases by Electrodialysis,* Proc. Symposium on Water Purification by Photocatalytic, Photoelectrochemical, and Electrochemical Processes, 185th Electrochem. Soc. Meeting, San Francisco, CA, May 22-27, 1994, T. L. Rose, O. Murphy, E. Rudd, B. E. Conway, Eds., Electrochem. Soc., Pennington, NJ, Vol. 94-19, pp. 184-190 (1994).
18. J. C. Farmer, Z. Chiba, *Fundamental Studies of the Mediated Electrochemical Oxidation of Wastes*, 185th Electrochem. Soc. Meeting, San Francisco, CA, May 22-27, 1994, Ext. Abs., Vol. 94-1, pp. 1708-09, Electrochem. Soc., Pennington, NJ (1994).

19. J. C. Farmer, D. V. Fix, R. G. Hickman, V. M. Oversby, M. G. Adamson, *Regeneration of Acids and Bases by Electrodialysis,* 185th Electrochem. Soc. Meeting, San Francisco, CA, May 22-27, 1994, Ext. Abs., Vol. 94-1, p. 1717, Electrochem. Soc., Pennington, NJ (1994).
20. J. C. Farmer, R. W. Pekala, D. V. Fix, J. Phillips, J. F. Poco, C. T. Alviso, *Capacitive Deionization: New Water Treatment Technology*, Chemistry and Materials Science, 1992-94, C. Gatrousis, Ed., UCRL-53943-93, pp. 134-135 (1994).
21. G. V. Mack, J. C. Farmer, D. V. Fix, G. W. Johnson, D. W. O'Brien, *Design of the Control System for the Continuous-Flow Potential-Swing Capacitive Deionization Process*, UCRL-ID-117626, September 30 (1994).
22. J. C. Farmer, D. V. Fix, G. V. Mack, R. W. Pekala, J. F. Poco, *The Use of Capacitive Deionization with Carbon Aerogel Electrodes to Remove Inorganic Contaminants from Water*, Proceedings of the 1995 International Low Level Conference, Advanced Wet Waste Processing and Technology, Orlando, Florida, July 10-12, 1995, Electric Power Research Institute (EPRI) Rept. TR-105569, EPRI, Palo Alto, CA, pp. 42 1-23 (1995).
23. J. C. Farmer, D. V. Fix, G. V. Mack, R. W. Pekala, J. F. Poco, *Capacitive Deionization of Water: An Innovative New Process*, Proceedings of the Fifth International Conference on Radioactive Waste Management and Environmental Remediation, ICEM 95, Berlin, Germany, September 3-9, 1995, American Society of Mechanical Engineers (ASME), New York, NY, Vol. 2, pp. 1215-1220 (1995).
24. J. C. Farmer, D. V. Fix, G. V. Mack, R. W. Pekala, J. F. Poco, *Capacitive Deionization with Carbon Aerogel Electrodes: Carbonate, Sulfate, and Phosphate*, Proceedings of the 1995 International SAMPE Technical Conference, Albuquerque, NM, October 9-12, 1995, Society for the Advancement of Material and Process Engineering (SAMPE), Covina, CA, Vol. 27, pp. 294-304 (1995).
25. J. F. Cooper, F. T. Wang, J. C. Farmer, R. J. Foreman, T. E. Shell, K. J. King, *Direct Chemical Oxidation of Hazardous and Mixed Wastes*, American Society of Mechanical Engineers, Proc. Third Biennial Mixed Waste Symposium, Baltimore, Maryland, August 7-11 (1995).
26. F. T. Wang, J. F. Cooper, J. C. Farmer, M. G. Adamson, Shell, T., *Destruction of Ion Exchange Resins by Wet Oxidation and by Direct Chemical Oxidation--A Comparison Study*, Proc. World Environmental Congress, International Conference and Trade Fair, London, Ontario, September 17-22 (1995).
27. J. C. Farmer, D. V. Fix, G. V. Mack, R. W. Pekala, J. F. Poco, *Capacitive Deionization of NaCl and $NaNO_3$ Solutions with Carbon Aerogel Electrodes*, J. Electrochem. Soc., Vol. 143, No. 1, pp. 159-169, 1996.
28. J. F. Cooper, F. T. Wang, R. L. Krueger, K. J. King, J. C. Farmer, M. G. Adamson, *Destruction of Organic Wastes by Ammonium Peroxydisulfate with Electrolytic Regeneration of the Oxidant*, J. Electrochem. Soc., submitted for publication.
29. J. C. Farmer, D. V. Fix, G. V. Mack, R. W. Pekala, J. F. Poco, *Capacitive Deionization of NH_4ClO_4 Solutions with Carbon Aerogel Electrodes*, Journal of Applied Electrochemistry, Vol. 26, pp. 1007-1018 (1996).
30. J. C. Farmer, S. M. Bahowick, J. E. Harrar, D. V. Fix, R. E. Martinelli, A. K. Vu, K. L. Carrol, *Electrosorption of Chromium Ions on Carbon Aerogel Electrodes as a Means of Remediating Ground Water*, Journal of Energy and Fuels, American Chemical Society, Vol. 11, No. 2, pp. 337-347 (1996).
31. J. C. Farmer, D. V. Fix, R. W. Pekala, Nielsen, J. K., Volpe, A. M., Dietrich, D. D., *The Use of Carbon Aerogel Electrodes for Environmental Cleanup*, Proc. Symposium on the Production and Use of Carbon-Based Materials for Environental Cleanup, 1996 Spring

Meeting of the American Chemical Society, New Orleans, Louisiana, March 24-29, 1996, Vol. 41, p. 484 (1996).

32. J. C. Farmer, R. W. Pekala, F. T. Wang, D. V. Fix, Volpe, A. M., Dietrich, D. D., Siegel, W. H., *Electrochemical and Photochemical Treatment of Aqueous Waste Streams*, Proc. Spectrum 96, Nuclear and Hazardous Waste Management International Topical, American Nuclear Society, Seattle, Washington, August 18-23, 1996, Am. Nucl. Soc., La Grange Park, IL, Vol. 1, pp. 435-440 (1996).
33. J. C. Farmer, D. V. Fix, R. W. Pekala, J. K. Nielsen, A. M. Volpe, D. D. Dietrich, *The Use of Carbon Aerogel Electrodes for Environmental Cleanup*, Symposium on the Production and Use of Carbon-Based Materials for Environental Cleanup, 1996 Spring Meeting of the American Chemical Society, New Orleans, LA, March 24-29 (1996).
34. J. C. Farmer, D. V. Fix, R. W. Pekala, J. K. Nielsen, A. M. Volpe, D. D. Dietrich, *Carbon Aerogel Electrodes for Removing Impurities from Aqueous Solutions*, 70th Colloid and Surface Science Symposium, Division of Colloid and Surface Chemistry, American Chemical Society, Clarkson University, Potsdam, NY, June 16-19 (1996).
35. J. H. Richardson, J. C. Farmer, D. V. Fix, J. A. H. De Pruneda, G. V. Mack, J. F. Poco, J. K. Nielsen, R. W. Pekala, *Desalting in Wastewater Reclamation Using Capacitive Deionization with Carbon Aerogel Electrodes,* The American Desalting Association Conference, Monterey, CA, August 4-8 (1996).
36. J. C. Farmer, R. W. Pekala, F. T. Wang, D. V. Fix, A. M. Volpe, D. D. Dietrich, W. H. Siegel, *Electrochemical and Photochemical Treatment of Aqueous Waste Streams*, Proc. Spectrum 96, Nuclear and Hazardous Waste Management International Topical, American Nuclear Society, Seattle, Washington, August 18-23 (1996).
37. J. C. Farmer, *The Design of Electrochemical Processes for Treatment of Unusual Waste Streams*, Plenary Speaker, Symposium on Electrochemical and Photochemical Methods for Chemical Recycling and Pollution Abatement, 193rd Meeting of The Electrochemical Society, San Diego, California, May 3-8, 1998, Ext. Abs., Vol. 98-1, Abs. No. 577, Electrochemical Society, Pennington, NJ (1998).
38. J. C. Farmer, *Treatment of Aqueous Wastes for the United States Air Force: First Progress Report*, submitted to Lt. Ray Anthony Smith, Program Manager, Environmental Compliance Division, Armstrong Laboratory, AL/EQS, 139 Barnes Drive, Tyndall Air Force Base, Florida 32403-5323, May 4 (1995).
39. J. C. Farmer, LDRD Midyear Report on Mixed Waste Treatment Technologies, 94-ERP-032, submitted to Dr. John Holzrichter, Manager, LLNL LDRD Program, April 7 (1995).
40. 1995 R&D 100 Award Winners, R&D 100 Awards Recognize Five Laboratory Inventions, Science & Technology Review, Lawrence Livermore National Laboratory, Livermore, CA, November/December Issue, pp. 20-33 (1995).
41. J. C. Farmer, S. M. Bahowick, J. E. Harrar, D. V. Fix, Martinelli, R. E., Vu, A. K., Carroll, K. L., *Electrosorption of Chromium Ions on Carbon-Aerogel Electrodes: Treatment of Contaminated Groundwater*, Laboratory Directed Research and Development, Annual Report, FY 1996, R. A. Al-Ayat, G. L. Struble, Eds., UCRL-LR-113717, Project No. 96-ERD-067, p. 97 (1996).
42. J. C. Farmer, J. H. Richardson, D. V. Fix, S. L. Thomson, S. C. May*, Desalination with Carbon Aerogel Electrodes*, UCRL-ID-125298 Rev. 1, December 4 (1996).
43. T. D. Tran, J. C. Farmer, R. W. Pekala, *Carbon Aerogels and Their Applications in Supercapacitors and Electrosorption Processes*, Proc. Second VACETS Technical International Conference, San Jose State University, Session 7, Energy and Environmental Technology, July 17-19 (1997).

44. T. D. Tran, J. C. Farmer, J. H. De Pruneda, J. H. Richardson, *Electrosorption on Carbon Aerogel Electrodes as a Means of Treating Low-Level Radioactive Wastes and Remediating Contaminated Ground Water*, Proceedings of the Sixth International Conference on Radioactive Waste Management and Environmental Remediation, Session L-7 on Hazardous & Radioactive Waste, ICEM 97, Singapore, October 12-16, 1997, American Society of Mechanical Engineers (ASME), New York, NY, 16 p. (1997)
45. J. C. Farmer, T. D. Tran, J. H. Richardson, D. V. Fix, S. C. May, S. L. Thomson, *The Application of Carbon Aerogel Electrodes to Desalination and Waste Treatment*, Annual Meeting of the American Institute of Chemical Engineers (AIChE), Los Angeles, CA, November 16-21, 1997, Preprints of Topical Conference on Separation Science and Technologies, Part I, November 17-19, 1997, W.S. Winstonito, Chair, AIChE Separations Division, R. G. Luo, Preprint Volume Coordinator, American Institute of Chemical Engineers, 345 East 47th Street, New York, NY 10017, pp. 577-585 (1997).
46. J. C. Farmer, G. V. Mack, D. V. Fix, *The Use of Carbon Aerogel Electrodes for Deionizing Water and Treating Aqueous Process Wastes*, International Journal of Environmentally Conscious Design & Manufacturing, Vol. 6, No. 2, pp. 43-48 (1997).
47. J. F. Cooper, G. B. Balazs, P. L. Lewis, J. C. Farmer, *Direct Chemical Oxidation of Mixed or Toxic Wastes*, Proceedings of the Advanced Research Workshop: Environmental Aspects of Converting CW Facilities to Peaceful Purpose, March 10, 1999, Spiez, Switzerland, March 1999, 15 pages (this paper written in reponse to an invitation to J. C. Farmer).

Publications – Electrochemistry & Electrodeposition

48. R. H. Muller, J. C. Farmer, *Fast, Self-Nulling Spectroscopic Ellipsometer Instrumentation and Application*, J. Physique, Vol. 44, No. 12, pp. C10-57 (1983).
49. R. H. Muller, J. C. Farmer, *Macroscopic Optical Model for the Ellipsometry of Underpotential Deposits: Lead on Copper and Silver*, Surf. Sci., Vol. 135, pp. 521-531 (1983).
50. R. H. Muller, J. C. Farmer, *Fast, Self-Compensating Spectral Scanning Ellipsometer*, Rev. Sci. Instruments, Vol. 55, No. 3, pp. 371-374 (1984).
51. J. C. Farmer, R. H. Muller, *Effect of Rhodamine-B on Pb Electrodeposition on Ag and Cu*, 163rd Electrochem. Soc. Meeting, San Francisco, CA, May 8-13, 1983, Ext. Abs., Vol. 83, No. 1, pp. 1218-1219, Electrochem. Soc., Pennington, NJ (1983).
52. J. C. Farmer, R. H. Muller, *Nucleation of Pb Electrodeposits on Ag and Cu*, 163rd Electrochem. Soc. Meeting, San Francisco, CA, May 8-13, 1983, Ext. Abs., Vol. 83, No. 1, pp. 1220-1221, Electrochem. Soc., Pennington, NJ (1983).
53. R. H. Muller, J. C. Farmer, *Effect of Organic Adsorbates on the Initial Stage of Electrolytic Metal Deposition: Development and Use of a Spectroscopic Ellipsometer*, Ph.D. Dissertation, LBL-15607 (1983).
54. R. H. Muller, J. C. Farmer, *Automatic, Self-Nulling, Spectral Scanning Ellipsometer: Software for the LSI-11 Data Acquisition System*, LBL-15525 (1983).
55. J. C. Farmer, *Effect of Saccharin on Nickel Electrodeposition on Platinum Studied by AC-Cyclic Voltammetry: Experimental*, 165th Electrochem. Soc. Meeting, Cincinnati, OH, May 6-11, 1984, Ext. Abs., Vol. 84, No. 1, pp. 580-581, Electrochem. Soc., Pennington, NJ (1984).
56. J. C. Farmer, R. H. Muller, *Spectroscopic Ellipsometry of Rhodamine-B Adsorbed on Platinum, Silver, and Copper*, 35th Intl. Soc. Electrochem. Meeting, Berkeley, CA, Aug. 5-10, 1984, Ext. Abs., pp. 463-466, U.S. DOE, Washington, DC (1984).

57. J. C. Farmer, R. H. Muller, *Nucleation of Pb Electrodeposits on Ag and Cu*, J. Electrochem. Soc., Vol. 132, No. 1, pp. 39-45 (1985).
58. J. C. Farmer, R. H. Muller, *Effect of Rhodamine-B on the Electrodeposition of Lead on Copper*, J. Electrochem. Soc., Vol. 132, No. 2, pp. 313-319 (1985).
59. R. J. Anderson, J. C. Farmer, G. W. Foltz, *Detection of Monolayer Adsorbates Using Surface Second Harmonic Generation*, 169^{th} Electrochem. Soc. Meeting, Boston, MA, May 4-9, 1986, Ext. Abs., Vol. 86, No. 1, pp. 814-815, Electrochem. Soc., Pennington, NJ (1986).
60. J. C. Farmer, H. R. Johnson, *Effect of Rhodamine-B and Saccharin on the Electric Double Layer During Ni Electrodeposition on Pt Studied by AC-Cyclic Voltammetry*, Proc. 11^{th} World Congress Met. Fin., Intl. Un. Surf. Fin. Interfinish 84, Oct. 21-26, 1984, Jerusalem, Israel, pp. 343-356, International, Ltd., Tel Aviv, Israel (1984).
61. J. C. Farmer, *Underpotential Deposition of Copper on Gold and the Effects of Thiourea Studied by AC Impedance*, J. Electrochem. Soc., Vol. 132, No. 11, pp. 2640-2648 (1985).
62. J. C. Farmer, H. R. Johnson, *Application of Dynamic Impedance Measurements for Adsorbed Plating Additives*, Plating and Surface Finish, Vol. 172, No. 8, pp. 60-66 (1985).
63. J. C. Farmer, *Underpotential Deposition on Gold and the Effects of Thiourea Studied by AC-Impedance*, 168^{th} Electrochem. Soc. Meeting, Las Vegas, NV, Ext. Abs., Vol. 85, No. 2, pp. 359-360, Electrochem. Soc., Pennington, NJ (1985).
64. J. C. Farmer, W. D. Bonivert, J. T. Hachman, *Tuned-Frequency Reversible Impedance Probe for the Measurement of Dilute Organic Additivesin Electroplating Baths*, 172^{nd} Electrochem. Soc. Meeting, Honolulu, HI, Oct. 18-23, 1987, Ext. Abs., Vol. 87, No. 2, , pp. 809-810, Electrochem. Soc., Pennington, NJ (1987).
65. D. B. Hopkins et al., *Electroforming Process Development for the High Gradient Test Structure*, Proc. Particle Accelerator Conf., Washington, DC (1987).
66. J. C. Farmer et al., *Electroforming Process Development for the Two-Beam Accelerator*, Plating and Surface Finish, Vol. 75, No. 3, pp. 48-52 (1988).
67. D. B. Hopkins et al., *Design and Fabrication of 33 GHz High-Gradient Accelerator Sections*, LBL-25368; 1988 European Particle Accelerator Conference, Rome, Italy, Jun. 7-11 (1988).
68. J. C. Farmer, W. D. Bonivert, *Impedance Probe for Monitoring Organic Plating Additives*, Plating and Surface Finish, Vol. 76, No. 8, pp. 56-61 (1989).
69. W. D. Bonivert, J. S. Krafcik, J. T. Hachman, J. C. Farmer, Development Report: An In-Situ Sensor for Monitoring Organic Additives in Copper Plating Solutions, Sandia Natl. Lab. Rept. (1991).

Publications – Corrosion Science & Engineering

70. J. C. Farmer, J. C. Hamilton, C. Boney, *Anodic Films on the Eutectic Alloy of Silver and Copper in Sodium Hydroxide: An In Situ Raman Spectroscopic Investigation*, 167^{th} Electrochem. Soc. Meeting, Toronto, Canada, May 12-17, 1985, Ext. Abs., Vol. 85, No. 1, pp. 32-33 Electrochem. Soc., Pennington, NJ (1985).
71. J. C. Hamilton, J. C. Farmer, C. Boney, *Formation of Anodic Films on Copper and Silver in Sodium Hydroxide: An In Situ Raman Spectroscopic Investigation*, 167^{th} Electrochem. Soc. Meeting, Toronto, Canada, May 12-17, 1985, Ext. Abs., Vol. 85, No. 1, pp. 34-35 Electrochem. Soc., Pennington, NJ (1985).
72. J. C. Hamilton, J. C. Farmer, R. J. Anderson, *In Situ Raman Spectroscopy of Anodic Films Formed on Copper and Silver in Sodium Hydroxide Solution*, J. Electrochem. Soc., Vol. 85, No. 4, pp. 739-745 (1986).

73. J. C. Farmer, R. D. McCright, J. N. Kass, *Overview,* in Survey of Degradation Modes of Candidate Materials for High-Level Radioactive-Waste Disposal Containers, UCID-21362 (1988).
74. J. C. Farmer, R. A. Van Konynenburg, R. D. McCright, D. B. Bullen, *Localized Corrosion and Stress Corrosion Cracking of Austenitic Steels*, in Survey of Degradation Modes of Candidate Materials for High-Level Radioactive-Waste Disposal Containers, UCID-21362, Vol. 3 (1988).
75. J. C. Farmer, R. A. Van Konynenburg, R. D. McCright, G. E. Gdowski, *Stress Corrosion Cracking in Copper-Based Materials*, in Survey of Degradation Modes of Candidate Materials for High-Level Radioactive-Waste Disposal Containers, UCID-21362, Vol. 4 (1988).
76. J. C. Farmer, R. A. Van Konynenburg, R. D. McCright, G. E. Gdowski, *Localized Corrosion of Copper-Based Alloys*, in Survey of Degradation Modes of Candidate Materials for High-Level Radioactive Waste Disposal Containers, UCID-21362, Vol. 5 (1988).
77. W. G. Halsey, J. C. Farmer, R. D. McCright, R. A. Van Konynenburg, D. B. Bullen, *Localized Corrosion and Stress Corrosion Cracking of Austenitic Candidate Materials for High-Level Radioactive Waste Disposal Containers: Analysis of Data*, 174th Electrochem. Soc. Meeting, Chicago, IL, Oct. 9-14, 1988, Ext. Abs., Vol. 88, No. 2, p. 212, Electrochem. Soc., Pennington, NJ (1988).
78. J. C. Farmer, G. E. Gdowski, R. D. McCright, H. S. Ahluwalia, *Corrosion Models for Performance Assessment of High-Level Radioactive Waste Containers*, UCID-21756 (1989) & UCRL-JC-103517 (1989).
79. J. C. Farmer, R. D. McCright, *Localized Corrosion and Stress Corrosion Cracking of Candidate Materials for High-Level Radioactive Waste Disposal Containers in U.S.: A Critical Literature Review*, Proc. Scientific Basis for Nucl. Waste Mgmt. Symp., Berlin, West Germany, Oct. 10-13, 1988, Vol. 127, pp. 359-371, Matls. Res. Soc. (1989).
80. J. C. Farmer, R. D. McCright, *A Review of Models Relevant to the Prediction of Performance of High-Level Radioactive Waste Disposal Containers*, Corrosion/89, Apr. 17-21, 1989, New Orleans, LA, Paper No. 519, Natl. Assoc. Corr. Engrs., Houston, TX (1989).
81. W. L. Clarke, J. C. Farmer, W. G. Halsey, R. D. McCright, *Container Material Selection, Modeling and Testing*, Proc. Intl. Topical Meeting, High-Level Rad. Waste Mgmt., Las Vegas, NV, Apr. 8-12, 1990, Vol. 1, pp. 437-442, Amer. Nucl. Soc. and Amer. Soc. of Civil Engrs. (1990).
82. S. L. Robinson, N. R. Moody, S. M. Myers, J. C. Farmer, F. A. Greulich, *The Effects of Current Density and Recombination Poisons on Electrochemical Charging of Deuterium into an Iron-Base Superalloy*, J. Electrochem. Soc., Vol. 137, No. 5, p. 1391 (1990).
83. J. C. Farmer, G. E. Gdowski, R. D. McCright, H. S. Ahluwalia, *Corrosion Models for Performance Assessment of High-Level Radioactive Waste Containers*, Nuclear Engineering Design, Vol. 129, pp. 57-88 (1991).
84. R. D. McCright, J. C. Farmer, D. L. Fleming, *An Electrochemical Approach to Predicting Corrosion Performance of Container Materials*, Proc. 2nd Ann. Intl. High-Level Rad. Waste Mgmt. Conf. Expo., Las Vegas, NV, Apr. 28 - May 3, 1991, Vol. 2, pp. 940-944, Amer. Nucl. Soc. and Amer. Soc. of Civil Engrs. (1991).
85. J. C. Farmer, Crevice Corrosion and Pitting of High-Level Waste Containers: A First Step Towards the Integration of Deterministic and Probabilistic Models, UCRL-ID-117626, 84 p, August 14 (1997).

86. J. C. Farmer, Crevice Corrosion and Pitting of High-Level Waste Containers: The Integration of Deterministic and Probabilistic Models II, UCRL-ID-127980, Part 2, October 8 (1997).
87. J. C. Farmer, *Elicitation Summary*, in *Waste Package Degradation Expert Elicitation Project*, JF-1 through JF-74, Rev. 1, K. J. Coppersmith, R. C. Perman, R. R. Youngs, Eds., Civilian Radioactive Waste Management System Management and Operating Contractor, Geomatrix Consultants, Inc., 100 Pine Street, San Francisco, CA, June 15 (1998).
88. J. C. Farmer et al., *Protective Ceramic Coatings for High-Level Radioactive Waste Containers*, UCRL-MI-131293, Presented to Ceramic Peer Review Panel, SRI International, Palo Alto, CA, August 17 (1998).
89. J. C. Farmer, *Predictioin of Penetration Rates for Ti Gr 7 Inner Barrier*, UCRL-ID-131915 Rev. 1, October 9 (1998).
90. J. C. Farmer, K. R. Wilfinger, *Process Level Model for Ceramic Coating*, UCRL-ID-131899 Rev. 2, November 14 (1998).
91. J. C. Farmer, R. D. McCright, *Crevice Corrosion and Pitting of High-Level Waste Containers: Integration of Deterministic and Probabilistic Models*, Paper No. 98160, Symposium 98-T-2A, Annual Meeting of the National Association of Corrosion Engineers (NACE), Corrosion 98, San Diego, CA March 22-27 (1998).
92. J. C. Farmer, R. D. McCright, A. K. Roy, G. E. Gdowski, F. T. Wang, J. C. Estill, K. J. King, S. R. Gordon, D. L. Fleming, B. Y. Lum, *Development of Corrosion Models for High-Level Waste Containers,* Session on Environment – Induced Degradation of Nuclear Waste Package Materials, 1998 ASME/JSME/SFEN ICONE-6, Proceedings of the 6th International Conference on Nuclear Engineering (CD ROM), May 10-15, 1998, Paper No. 6290, Track 9, Session 9.02, American Society of Mechanical Engineers, American Socieity of Nuclear, 345 East 47th Street, New York, NY 10017 (1998).
93. J. C. Farmer, P. J. Bedrossian, R. D. McCright, *Modeling the Corrosion of High-Level Waste Containers: CAM-CRM Interface*, Proceedings of the International Conference on Decommissioning and Decontamination and on Nuclear and Hazardous Waste Management, Denver, Colorado, September 13-18, 1998, American Nuclear Society, 555 N. Kensington Avenue, LaGrange Park, IL 60526, p. 610-623 (1998).
94. Norman Thomas, Jesse Wolfe, Joseph Farmer, *Protected Silver Coating for Astronomical Mirrors*, Part of the SPIE Conference on Advanced Technology Optical/IR Telescopes VI, Kona, Hawaii, March 1998, SPIE Vol. 3352, pp. 580-586 (1998).
95. J. C. Farmer, R. D. McCright, J-S. Huang, A. K. Roy, K. R. Wilfinger, F. T. Wang, P. J. Bedrossian, J. C. Estill, J. M. Horn, *Development of Integrated Mechanistically-Based Degradation-Mode Models for Performance Assessment of High-Level Waste Containers*, UCRL-ID-130811 Rev. 1, February (1999).
96. J. C. Farmer et al., *General and Localized Corrosion of Waste Package Outer Barrier*, UCRL-ID-134993, YMP M&O ANL-EBS-MD-000003 Rev. 00D, December (1999).
97. J. C. Farmer et al., *General and Localized Corrosion of the Drip Shield*, YMP M&O ANL-EBS-MD-000004 Rev. 00D, December (1999).
98. J. C. Farmer et al., *Degradation of Stainless Steel Structural Support for Waste Package*, YMP M&O ANL-EBS-MD-000007 Rev. 00B, December (1999).
99. J. C. Farmer, R. D. McCright, J. C. Estill, S. R. Gordon, *Development of Integrated Mechanistically-Based Degradation-Mode Models for Performance Assessment of High-Level Containers*, Proceedings of the Symposium on the Scientific Basis for Nuclear Waste Manatement XXII, D. J. Wronkiewicz, J. H. Lee, Eds., Materials Research Society Symposium Series, Warrendale, PA, Vol. 556, pp. 855-862 (1999).

100. P. J. Bedrossian, J. C. Farmer, R. D. McCright, D. L. Phinney, J. C. Estill, *Passive Films and Blistering of Titanium*, Proceedings of the Symposium on the Scientific Basis for Nuclear Waste Manatement XXII, D. J. Wronkiewicz, J. H. Lee, Eds., Materials Research Society Symposium Series, Warrendale, PA, Vol. 556, pp. 863-869 (1999).
101. K. R. Wilfinger, J. C. Farmer, R. W. Hopper, T. E. Shell, *Corrosion Protection of Metallic Waste Packages Using Thermal Sprayed Ceramic Coatings*, Proceedings of the Symposium on the Scientific Basis for Nuclear Waste Manatement XXII, D. J. Wronkiewicz, J. H. Lee, Eds., Materials Research Society Symposium Series, Warrendale, PA, Vol. 556, pp. 927-934 (1999).
102. J. C. Farmer, *The Safe Storage of Hazardous and Radioactive Materials: Development of Integrated Process-Level Corrosion Models*, General Corrosion Session, 195th Meeting of the Electrochemical Society, Seattle, Washington, May 2-6, 1999, Ext. Abs., Vol. 99-1, Abs. No. 109, Electrochemical Society, Pennington, NJ (1999).
103. J. C. Farmer, *Process-Level Deterministic and Probabilistic Corrosion Models for High-Level Waste Containers*, Research in Progress Symposium, Session 1, Probabilistic and Deterministic Modeling of Corrosion Processes, NACE Corrosion 99, Henry B. Gonzalez Convention Center, San Antonio, Texas, April 25-30 (1999).
104. J. Farmer, S. Lu, D. McCright, G. Gdowski, F. Wang, T. Summers, P. Bedrossian, J. Horn, T. Lian, J. Estill, A. Lingenfelter, W. Halsey, *General and Localized Corrosion of High-Level Waste Container in Yucca Mountain*, The 2000 ASME Pressure Vessel and Piping Conference, Seattle, Washington, July 23-27, 2000, Transportation, Storage, and Disposal of Radioactive Materials, PVP Vol. 408, pp. 53-70 (2000).
105. J. Farmer, S. Lu, T. Summers, D. McCright, A. Lingenfelter, F. Wang, J. Estill, L. Hackel, H-L. Chen, G. Gordon, V. Pasupathi, P. Andresen, S. Tang, M. Herrera, Modeling and Mitigation of Stress Corrosion Cracking in Closure Welds of High-Level Waste Containers for Yucca Mountain, The 2000 ASME Pressure Vessel and Piping Conference, Seattle, Washington, July 23-27, 2000, Transportation, Storage, and Disposal of Radioactive Materials, PVP Vol. 408, pp. 71-81 (2000).
106. G. O. Ilvebare, T. Lian, J. C. Farmer, Environmental Considerations in the Studies of Corrosion Resistant Alloys for High-Level Radioactive Waste Containers, Paper No. 02539, NACE Corrosion 2002, Denver, Colorado, April 7-11 (2002).
107. J. C. Farmer et al., High-Performance Corrosion-Resistant Amorphous Metals, Proc. Global 2003, New Orleans, Louisiana, American Nuclear Society (2003).
108. J. C. Farmer, J. J. Haslam, S. D. Day, D. J. Branagan, M. C. Marshall, B. E. Mecham, E. J. Buffa, C. A. Bue, J. D. K. Rivard, D. C. Harper, M. B. Beardsley, D. T. Weaver, L. F. Aprigliano, L. Kohler, R. Bayles, E. J. Lemieux, T. M. Wolejsza, N. Yang, G. Lucadamo, J. H. Perepezko, K. Hildal, L. Kaufman, A. H. Heuere, F. Ernst, G. M. Michal, H. Kahn, E. J. Lavernia, High-Performance Corrosion-Resistant Materials: Iron-Based Amorphous-Metal Thermal-Spray Coatings, High-Performance Corrosion-Resistant Materials (HPCRM) Annual Report, UCRL-TR-206717, Lawrence Livermore National Laboratory, Livermore, California, 178 pages, September 28 (2004).
109. J. J. Haslam, J. C. Farmer, R. W. Hopper, K. R. Wilfinger, Ceramic Coatings for Corrosion Resistant Nuclear Waste Container Evaluated in Simulated Ground Water at 90°C, UCRL-JRNL-206107, Lawrence Livermore National Laboratory, Livermore, California, August 17, 2004 (34 p.); Metallurgical and Materials Transactions A, Volume 36A, May 2005, p. 1085-1095 (2004).
110. J. Farmer, C. Earl, C. Doty, D. Spence, J. Walker, F. Wong, J. Payer, G-Q. Lu, D. E. Clark, D. C. Folz, A. Heuer, O. Graeve, D. Branagan, C. Blue, J. Rivard, J. Perepezko, L. Kaufman,

N. Yang, E. Lavernia, J. Haslam, E. Lemieux, L. Aprigliano, B. Beardsley, T. Weaver, B. Edwards, B. Brown, Ar. Halter, B Bayles, J. Lewandowski, DARPA-DOE High Performance Corrosion-Resistant Materials (HCPRM) Principal Investigator's Meeting, Turtle Bay Resort, Oahu, Hawaii, January 10-13, 2005, UCRL-PRES-214672, Lawrence Livermore National Laboratory, Livermore, California, 407 pages (2005).

111. J. C. Farmer, J. J. Haslam, S. D. Day, D. J. Branagan, C. A. Blue, J. D. K. Rivard, L. F. Aprigliano, N. Yang, J. H. Perepezko, M. B. Beardsley, Corrosion Characterization of Iron-Based High-Performance Amorphous-Metal Thermal-Spray Coatings, PVP2005-71664, Proceedings of ASME PVP: Pressure Vessels & Piping Division Conference, Grand Hyatt, Denver, Colorado, July 17-21, 2005, American Society of Mechanical Engineers, Three Park Avenue, New York, New York, 7 pages (2005).
112. Defense Science Board Report on Corrosion Control, Office of the Under Secretary of Defense for Acquisition, Technology & Logistics, Washington, D. C. 20301-3140, October 14, 2004, 87 pages (2004).
113. J. C. Farmer, J. J. Haslam, S. D. Day, T. Lian, R. Rebak, N. Yang, L. Aprigliano, Corrosion Resistance of Iron-Based Amorphous Metal Coatings, Proceedings of ASME PVP: Pressure Vessels & Piping (PVP) Division Conference, July 23-27, 2006 Vancouver, British Colombia, American Society of Mechanical Engineers, PVP2006-ICPVT11-93835, New York, NY 7 p. (2006).
114. J. C. Farmer, The Development of Next-Generation Materials for Nuclear Energy, UCRL-PRES-219330, Energy and Environment Directorate Review Committee, March 7-9, 2006, Lawrence Livermore National Laboratory, Livermore California, 17 pages (2006).
115. J. C. Farmer, Team FY05 HPCRM Annual Report: High-Performance Corrosion-Resistant Iron-Based Amorphous Metal Coatings, UCRL-SR-219257, January 2006, Contributions by J. C. Farmer, J-S. Choi, J. J. Haslam, S. D. Day, N. Yang, T. Headley, G. Lucadamo, J. L Yio, J. Chames, A. Gardea, M. Clift, C. A. Blue, W. H. Peters, J. D. K. Rivard, D. C. Harper, D. Swank, R. Bayles & E. J. Lemieux, Robert Brown & Theresa M. Wolejsza, L. F. Aprigliano, D. J. Branagan, M. C. Marshall, Brian E. Meacham, E. Joseph Buffa, M. Brad Beardsley, E. J. Lavernia, J. Schoenung, L. Ajdelsztajn, J. Dannenberg, O. A. Graeve, J. J. Lewandowski, John H. Perepezko, Kjetil Hildal, L. P. Kaufman, J. Boudreau, Lawrence Livermore National Laboratory, Livermore, California, 138 pages (2006).
116. J. C. Farmer, J. J. Haslam, S. D. Day, HPCRM Annual Report: High-Performance Corrosion-Resistant Iron-Based Amorphous-Metal coatings: Evaluation of Corrosion Resistance, UCRL-SR-218144, January 2006, Lawrence Livermore National Laboratory, Livermore, California, 68 pages (2006).
117. J. Farmer, J. Haslam, S. Day, T. Lian, C. Saw, P. Hailey, J-S. Choi, N. Yang, C. Blue, W. Peter, R. Bayles, R. Brown, J. Payer, J. Perepezko, K. Hildal, E. Lavernia, L. Ajdelsztajn, D. J. Branagan, J. Buffa, M. Beardsley, L. Aprigliano and J. Boudreau, Corrosion Resistance of Iron-Based Amorphous Metals in Hot Concentrated Calcium Chloride and Seawater: $Fe_{48}Mo_{714}Cr_{15}Y_2C_{15}B_6$, UCRL-TM-224159, Lawrence Livermore National Laboratory, Livermore, CA, 47 pages, August 30th (2006).
118. J. Farmer, J. Haslam, S. Day, T. Lian, C. Saw, P. Hailey, J-S. Choi, N. Yang, C. Blue, W. Peter, J. Payer and D. Branagan, Corrosion Resistances of Iron-Based Amorphous Metals with Yttrium and Tungsten Additions in Hot Calcium Chloride Brine and Natural Seawater, $Fe_{48}Mo_{14}Cr_{15}Y_2C_{15}B_6$ and W-containing Variants, *Critical Factors in Localized Corrosion 5, A Symposiun in Honor of Hugh Issacs*, 210th Meeting of the ECS, Cancun, Mexico, 2006, edited by N. Missert, Electrochemical Society Transations, Vol. 3, Electrochemical Society, Pennington, NJ (2006).

119. J-S. Choi, J. Farmer, C. Lee, Application of Neutron-Absorbing Structural-Amorphous Metal (SAM) Coatings for Spent Nuclear Fuel (SNF) Container: Use of Novel Coating Materials to Enhance Criticality Safety Controls, UCRL-MI-220385, April 5, 2006, Lawrence Livermore National Laboratory, Livermore, California, 32 pages (2006); Proceedings of CALPHAD Meeting, Haifa, Israel, May 11th (2006).
120. J. Farmer, J. Haslam, S. Day, T. Lian, C. Saw, P. Hailey, J-S. Choi, R. Rebak, N. Yang, R. Bayles, L. Aprigliano, J. Payer, J. Perepezko, K. Hildal, E. Lavernia, L. Ajdelsztajn, D. J. Branagan, and M. B. Beardsely, A High-Performance Corrosion-Resistant Iron-Based Amorphous Metal – The Effects of Composition, Structure and Environment on Corrosion Resistance, *Scientific Basis for Nuclear Waste Management XXX*, Symposium NN, Boston, MA, November 27th through December 1st 2006, Materials Research Society Symposium Series, Warrendale, PA, Vol. 985 (2006).
121. T. Lian, D. Day, P. Hailey, J-S. Choi, and J. Farmer, Comparative Study on the Corrosion Resistance of Fe-Based Amorphous Metal, Borated Stainless Steel and Ni-Cr-Mo-Gd Alloy, *Scientific Basis for Nuclear Waste Management XXX*, Symposium NN, Boston, MA, November 27th through December 1st 2006, Materials Research Society Symposium Series, Warrendale, PA, Vol. 985 (2006).
122. J-S. Choi, C. Lee, J. Farmer, D. Day, M. Wall, C. Saw, M. Boussoufi, B. Liu, H. Egbert, D. Branagan, and A. D'Amato, Application of Neutron-Absorbing Structural Amorphous Metal Coatings for Spent Nuclear Fuel Container to Enhance Criticality Safety Controls, *Scientific Basis for Nuclear Waste Management XXX*, Symposium NN, Boston, MA, November 27th through December 1st 2006, Materials Research Society Symposium Series, Warrendale, PA, Vol. 985 (2006).
123. C. C. Scheffing, K. Jagannadham, M-S. Yim, M. A. Bourham, J. C. Farmer, J. J. Haslam, S. D. Day, D. V. Fix, Properties of Titanium-Nitride for High-Level Waste Packaging Enhancement, Nuclear Technology, American Nuclear Society, La Grange Park, Illinois, Vol. 156, pp. 213-221 (2006).
124. J. C. Farmer, J. J. Haslam, S. D. Day, T. Lian, C. K. Saw, P. D. Hailey, J-S. Choi, R. B. Rebak, N. Yang, J. H. Payer, J. H. Perepezko, K. Hildal, E. J. Lavernia, L. Ajdelsztajn, D. J. Branagan, Corrosion Resistance of Thermally Sprayed High-Boron Iron-Based Amorphous-Metal Coatings: $Fe_{49.7}Cr_{17.7}Mn_{1.9}Mo_{7.4}W_{1.6}B_{15.2}C_{3.8}Si_{2.4}$, UCRL-TR-227111 Rev. 1, Lawrence Livermore National Laboratory, Livermore, CA, January 22nd 2007; submitted to Journal of Materials Research, Materials Research Society, Warrendale, PA.

Publications – Energy Conversion & Storage

125. J. C. Farmer, T. W. Barbee, R. J. Foreman, L. J. Summers, *Deposition and Evaluation of Multilayer Thermoelectric Films*, Proc. Symposium on Microstructures and Microfabricated Systems, 185th Electrochem. Soc. Meeting, San Francisco, CA, May 22-27, 1994, Vol. 94-14, pp. 231-242, Electrochem. Soc., Pennington, NJ (1994).
126. J. C. Farmer, T. W. Barbee, G. F. Chapline, Jr., R. J. Foreman, L. J. Summers, M. S. Dresselhaus, L. D. Hicks, *Sputter Deposition of Multilayer Thermoelectric Films: An Approach to the Fabrication of Two-Dimensional Quantum Wells*, Thirteenth International Conference on Thermoelectrics, Kansas City, Missouri, August 30 to September 1, 1994, American Institute of Physics Proceedings 316, Eds. Mathiprakasam, B., Heenan, P., American Institute of Physics Press, New York, NY, pp. 217-225 (1994).
127. J. C. Farmer, T. W. Barbee, R. J. Foreman, L. J. Summers, *Deposition and Evaluation of Multilayer Thermoelectric Films*, Proc. Symposium on Microstructures and Microfabricated

Systems, 185th Electrochem. Soc. Meeting, San Francisco, CA, May 22-27, 1994, Electrochem. Soc., Pennington, NJ, Vol. 94-14, pp. 231-242 (1994).

128. J. C. Farmer, S. Ghamaty, N. Elsner, *Synthesis and Evaluation of Novel Thermoelectric Thin Films*, Paper No. 74, Symposium on Materials Synthesis and Characterization, Division of Industrial and Engineering Chemistry, 207th Meeting of the American Chemical Society, San Diego, CA, March 13-17, 1994, Abstracts, American Chemical Society (1994).
129. J. C. Farmer, T. W. Barbee, R. J. Foreman, L. J. Summers, *Deposition and Evaluation of Multilayer Thermoelectric Films*, 185th Electrochem. Soc. Meeting, San Francisco, CA, May 22-27, 1994, Ext. Abs., Vol. 94-1, pp. 1661-62, Electrochem. Soc., Pennington, NJ (1994).
130. A. V. Wagner, R. J. Foreman, L. J. Summers, T. W. Barbee, J. C. Farmer, *Multilayer Thermoelectric Films: A Strategy for the Enhancement of ZT*, Proc. 30th Intersociety Energy Conversion Engineering Conference, Orlando, Florida, July 31 through August 4, 1995, Vol. 3, pp. 87-92 (1995).
131. A. V. Wagner, R. J. Foreman, L. J. Summers, T. W. Barbee, J. C. Farmer, *Multilayer Thin Film Thermoelectrics Produced by Sputtering*, Proc. XIV International Conference onThermoelectrics, St. Petersburg, Russia, June 27-30, 1995, Vedernikov, M. V., Fedorov, M. I., Kaliazin, A. E., Ed., A. F. Ioffe Physical-Technical Institute, St. Petersburg, Russia, pp. 283-287 (1995).
132. A. V. Wagner, R. J. Foreman, L. J. Summers, T. W. Barbee, J. C. Farmer, *Synthesis and Evaluation of Thermoelectric Multilayer Film*, Proc. XV International Conference on Thermoelectrics, Pasadena, California, March 26-29 (1996).
133. A. V. Wagner, R. J. Foreman, L. J. Summers, T. W. Barbee, J. C. Farmer, *Fabrication and Testing of Thermoelectric Thin Film Devices*, Proc. XV International Conference on Thermoelectrics, Pasadena, California, March 26-29 (1996).
134. J. C. Farmer et al., *Thermoelectric Materials with Exceptional Figures of Merit*, Chemistry and Materials Science Progress Report, Weapons-Supporting Research and Laboratory Directed Research and Development, First Half, FY 1993, UCID-20622-93-1, July, 1993, pp. 51-52 (1993).
135. J. C. Farmer, T. W. Barbee, R. J. Foreman, L. J. Summers, *Multilayer Thermoelectric Films: A Novel Approach for Achieving Exceptional Figures of Merit*, Chemistry and Materials Science, 1992-94, C. Gatrousis, Ed., UCRL-53943-93, pp. 130-133 (1994).
136. J. Farmer, P. Hailey, K. Wolf, A Comparative Study of Polymer-Gel Lithium Ion Battery Chemistry, Materials and Architecture, UCRLR-TR-218097 Revision 5, June 22, 2006, Official Use Only, Lawrence Livermore National Laboratory, Livermore, California, 100 pages (2006).

Publications – Reaction Engineering & Catalysis

137. J. C. Farmer, J. M. Hurt, S. C. Winans, *The Production of Ethylene Glycol from Synthesis Gas in the Continuous Experimental Unit (CEU): The First Crown Solvent Attempt Using Cesium as the Cation*, Union Carbide Corp., Proj. No. 136E10, File No. 24025, Aug. 18 (1977).
138. J. C. Farmer, C. E. Lawson, *Feasibility of 18-Crown-6 Recovery in the CEU by Batch Vacuum Distillation: Experimental Determination of the Glycerine/18-Crown-6 Heterogeneous Azeotrope*, Union Carbide Corp., Proj. No. 136E10, File No. 24124, Sept. 15 (1977).
139. J. C. Farmer, J. M. Hurt, S. C. Winans, *Synthesis Gas to Ethylene Glycol, An Evaluation of the K/18-Crown-6/ N-Methylmorpholine Formulation of the PSG Catalyst*, Union Carbide Corp., Proj. No. 136E10, File No. 25174, Feb. 27 (1978).

140. J. C. Farmer, J. M. Hurt, S. C. Winans, *The Effect of Pressure on Rates in a $KHCO_3$/18-Crown-6/N-Methylmorpholine PSG Formulation*, Union Carbide Corp., Proj. No. 136E10, File No. 25174, Jun. 13 (1978).
141. J. C. Farmer, J. M. Hurt, S. C. Winans, *CEU Evaluation of the TPPO-18-Crown-Ether Cosolvent Formulation of the PSG Catalyst*, Union Carbide Corp., Proj. No. 136E10, File No. 25578, Jun. 29 (1978).
142. A. R. Doumaux, J. C. Farmer, J. M. Hurt, W. E. Walker, *Synthesis Gas to Glycol Superior Process, Stripping Reactor Startup*, Union Carbide Corp., Proj. No. 136E10, File No. 25421, Aug. 22 (1978).
143. J. C. Farmer, *Ethylene Glycol from Synthesis Gas PSG Single Pass Stripping Reactor*, Data Reduction Computer Program, Union Carbide Corp., Proj. No. 136E10, File No. 25578, Oct. 5 (1978).
144. L. M. Bruger, J. C. Farmer, J. M. Hurt, S. C. Winans, *CEU Single Pass Stripping Reactor, Study of the Effect of Cation, Temperature, Pressure, and Hydrogen Concentration on Catalyst Stability and Volatility*, Union Carbide Corp., Proj. No. 136E10, File No. 25747, Dec. 1 (1978).

Publications – Sensor Technology

145. J. C. Farmer, J. L. Brunk, S. D. Day, M. Steward, P. D. Hailey, Smart Surfaces – Part 1: Special Formulations for Alpha and Gamm Radiation – Part 2: Special Paint Formulations for Detection of Gamma Dose Over Prolonged Periods of Time, UCRL-TR-220528, Lawrence Livermore National Laboratory, Livermore, CA 94550, 37 pages, April 9th (2005).
146. J. C. Farmer, J. L. Brunk, S. D. Day, M. Steward, P. D. Hailey, Smart Surfaces – Part. 1: Novel Paint Formulations for the Detection of Alpha-Particles from Pu-239 and Gamma-Rays from Ra-226, Progress Report – First Quarter, UCRL-AR-214603, Lawrence Livermore National Laboratory, Livermore, CA 94550, 22 pages, August 5th (2005).
147. J. C. Farmer, J. L. Brunk, S. D. Day, M. Steward, P. D. Hailey, Smart Surfaces – Special Paint Formulations for Instantaneious Detection of Alpha and Gamma Radiation and Measurement of Intgegral Dose for Prolonged Periods of Time, UCRL-TR-221189, Lawrence Livermore National Laboratory, Livermore, CA 94550, 37 pages, May 7th (2006).